

A screen for proteins involved in parasitism from *Meloidogyne hapla*
identifies an amphid localized transthyretin-like protein as a potential
effector

Dissertation

for the award of the degree

“Doctor rerum naturalium”

of the Georg-August-Universität Göttingen

within the doctoral program Microbiology and Biochemistry

of the Georg-August University School of Science (GAUSS)

submitted by

Frederik Gunnar Polzin

from Frankfurt am Main, Germany

Göttingen 2015

Thesis Committee

Jun. Prof. Dr. Cynthia Gleason

(Department of Molecular Plant Sciences, Georg-August-Universität, Göttingen)

Prof. Dr. Christiane Gatz

(Department of Plant Molecular Biology and Physiology, Georg-August-Universität, Göttingen)

Prof. Dr. Volker Lipka

(Department of Plant Cell Biology, Georg-August-Universität, Göttingen)

Members of the Examination Board

Referee: **Jun. Prof. Dr. Cynthia Gleason**

(Department of Molecular Plant Sciences, Georg-August-Universität, Göttingen)

2nd Referee: **Prof. Dr. Christiane Gatz**

(Department of Plant Molecular Biology and Physiology, Georg-August-Universität, Göttingen)

Further members of the Examination Board

Prof. Dr. Volker Lipka

(Department of Plant Cell Biology, Georg-August-Universität, Göttingen)

Prof. Dr. Ivo Feußner

(Department of Plant Biochemistry, Georg-August-Universität, Göttingen)

PD Dr. Thomas Teichmann

(Department of Plant Cell Biology, Georg-August-Universität, Göttingen)

Prof. Dr. Jörg Stülke

(Department General Microbiology, Georg-August-Universität, Göttingen)

Date of oral examination: 14.10.2015

Declaration

Hereby, I declare that this dissertation was undertaken independently and without any unauthorized aid.

I declare that this Ph.D. dissertation has not been presented to any other examining body either in its present or similar form.

Furthermore, I also affirm that I have not applied for a Ph.D. or Dr.rer.nat. at any other higher school of education.

Göttingen 19.08.15

Frederik Polzin

I. Table of contents

1. Introduction	1
1.1 The importance of root-knot nematodes – <i>Meloidogyne sp.</i>	1
1.2 <i>Meloidogyne sp.</i> biology	3
1.3 The plant defense system and pathogen effectors	7
1.4 Goal of this thesis	13
2. Materials and Methods	14
2.1 Materials	14
2.1.1 Devices	14
2.1.2 Consumables	16
2.1.3 Chemicals	16
2.1.4 Media	19
2.1.5 Buffers	24
2.1.6 Primers	27
2.1.7 Organisms	31
2.1.8 Plasmids	32
2.1.9 Kits	32
2.2 Methods	33
2.2.1 General molecular methods	33
2.2.3 Pathogen assays	36
2.2.4 RNA extraction and gene expression analysis	38
2.2.5 PAMP associated assays	40
2.2.6 <i>In situ</i> hybridization on <i>Meloidogyne sp.</i>	41
2.2.7 Subcellular localization of fluorescence tagged proteins	43
2.2.8 Protein analysis using Western blot	43
2.2.9 Protein interaction assays using yeast	44
3. Results	46
3.1 Bioinformatic screen reveals seven potential effector proteins in <i>M. hapla</i>	46
3.3 Mh265 and Mh270 exhibit enhanced gene expression in the pre- and early infection stages of <i>Meloidogyne hapla</i>	52
3.4 <i>In situ</i> localization of candidate effector <i>Mh270</i> shows labelling of the amphid region	53
3.5 <i>Mh270</i> expression in plants does not affect flg22-induced PTI responses	54

3.5.1	The early PAMP response ROS-burst is not altered in Mh270 transgenic plants	55
3.5.2	Expression of <i>Mh270</i> in planta does not have an influence of flg22 responsive genes..	56
3.6	The susceptibility of <i>Mh270</i> transgenic lines to diverse pathogens is similar to that of wildtype plants.....	58
3.6.1	Penetration assays reveal no difference in number of nematodes entering the root between transgenic and Col-0 wild type plants.....	58
3.6.2	Mh270 transgenic lines are not altered in nematode susceptibility	59
3.6.3	Susceptibility to <i>M. hapla</i> is not altered in lines expressing a RNAi hairpin construct specifically targeting <i>Mh270</i>	60
3.6.4	<i>Mh270</i> expressing plants have no altered susceptibility to <i>Pst-LUX</i>	61
3.6.5	Transgenic <i>Mh270</i> lines were not more susceptible to less virulent strains of <i>Pseudomonas syringae</i>	62
3.7	Expression of <i>Mh270</i> in less virulent <i>Pseudomonas syringae</i> strains does not enhance bacterial growth	63
3.8	Fluorescently-tagged Mh270 stable transgenic Arabidopsis lines were generated	65
3.8.1	Western blot analysis of fluorescently-tagged Mh270 expressed in Arabidopsis reveals instability of the N-terminal construct	65
3.8.2	Mh270-GFP localizes to the chloroplast of Arabidopsis leaves.....	66
3.9	A yeast-two-hybrid screen reveals a potential plant interaction partner for Mh270	68
4.	Discussion.....	71
4.1	The pros and cons of the “effector detector vector” screen for identifying nematode effectors	71
4.2	Transgenic lines expressing <i>Mh270</i> do not show an altered infection phenotype for <i>M. hapla</i> and <i>Pseudomonas syringae</i> strains	76
4.3	Expression of an RNAi construct in plants did not affect nematode susceptibility.	77
4.4	<i>Mh270</i> expression has no effect on flg22 triggered responses	78
4.5	<i>Mh270</i> did not enhance the virulence of <i>Pst</i> Δ <i>CEL</i> and <i>Pst</i> Δ <i>AvrPto</i> / Δ <i>AvrPtoB</i>	80
4.6	A GFP-tagged Mh270 shows different sub-cellular location in roots versus leaves.	81
4.6	<i>Mh270</i> interacts with AtVDAC3 in a yeast-two-hybrid assay	82
5.	Appendix.....	86
	References	92
	Acknowledgements.....	103
	Curriculum vitae	104

II. List of tables

Table 2.1 : Equipment used during the experiments of this thesis.....	14
Table 2.2 : Disposable materials used.....	16
Table 2.3 : Chemical compounds that were used in the different experiments.....	16
Table 2.4 : Composition Murashige and Skoog plant media.	19
Table 2.5 : Composition KNOPs media..	19
Table 2.6 : Composition of the 10x salt stock for KNOPs.	19
Table 2.7 : Composition of the 2000x micronutrient stock for KNOPs.	19
Table 2.8 : Composition of the Arabidopsis thaliana culture medium..	20
Table 2.9 : Composition of ATM micronutrient stock.	20
Table 2.10 : Composition of Kings B medium.	20
Table 2.11 : Composition of LB medium..	21
Table 2.12 : Composition of YEB medium.	21
Table 2.13 : Composition of YPAD medium.....	21
Table 2.14 : Composition of the yeast transformation medium.....	21
Table 2.15 : Semi-solid SC media composition.....	22
Table 2.16 : Composition SC dropout media for yeast.....	23
Table 2.17 : Composition of alkaline phosphatase buffer used for <i>in situ hybridization</i>	24
Table 2.18 : Composition of Böhlinger blocking reagent mix used for <i>in situ hybridization</i>	24
Table 2.19 : Composition of Denhardtts (50x) buffer mix used for <i>in situ hybridization</i>	24
Table 2.20 : Composition of hybridization buffer used for <i>in situ hybridization</i> . I.....	24
Table 2.21 : Composition of the maleic acid buffer used for <i>in situ hybridization</i>	25
Table 2.22 : Composition of the callose staining buffer.....	25
Table 2.23 : Composition of the immunoprecipitation extraction buffer.	25
Table 2.24 : Acrylamide gel composition used to run SDS-PAGE.	25
Table 2.25 : Composition of the blocking buffer for Western blot.....	26
Table 2.26 : Composition of the transfer buffer used for Western blot.....	26
Table 2.27 : Composition of concentrated running buffer for SDS-PAGE.....	26
Table 2.28 : Composition of concentrated 10xTBS buffer.	27
Table 2.29 : Composition of TBS working solution.	27
Table 2.30 : Sequence list of used qRT-PCR primers in the direction 5`-3`.....	27
Table 2.31 : List of primers used for cloning.....	28
Table 2.32 : Organisms used during the experiments of this thesis.	31

Table 2.33 : Plasmids that were used for cloning or experimental procedures.....	32
Table 2.34 : List of kits used during this thesis..	32
Table 2.35 : Contents of a standard phusion taq amplification mix.	33
Table 2.36 : Standard PCR cyler program to amplify a fragment of 500b.	33
Table 2.37 : Standard reaction mix for qRT-PCR using biolione taq polymerase.	39
Table 2.38 : Program of qRT-PCR cyler using bioline taq polymerase.....	39
Table 2.39 : Reactive oxygen species detection mix.	40
Table 2.40 : Phusion polymerase mix to amplify DIG-labeled DNA probes.....	41
Table 2.41 : Excitation and detection values in nm for YFP, GFP and autoflourescence for fluorescence microscopy.	43
Table 3.1 : List of remaining candidates after all bioinformatic analyses were performed.....	48
Table 3.2 : List of positive candidates derived from both root and cell line library.....	68

II. List of figures

Figure 1.1: Tomato roots heavily infected with <i>M. incognita</i>	1
Figure 1.2 : Worldwide distribution of <i>M. hapla</i>	2
Figure 1.3 : The life cycle of <i>Meloidogyne sp.</i>	3
Figure 1.4: Schematic of a root-knot nematode manipulating a plant cell.....	5
Figure 1.5 : Zig-Zag model – coevolution of defense mechanism with pathogen derived effectors.	9
Figure 3.1 : Pipeline for the identification of potential <i>M. hapla</i> candidates for subsequent testing	46
Figure 3.2 : ATR13 and some nematode effector candidates can promote <i>Pst-LUX</i> growth <i>in planta</i>	50
Figure 3.3 : Mh265 and Mh270 can increase <i>Pst-LUX</i> bioluminescence and this correlates with enhanced bacterial populations in planta.....	51
Figure 3.4 : qRT-PCR expression analysis of Mh265 and Mh270 over different life stages of <i>M. hapla</i>	52
Figure 3.5: <i>In situ</i> hybridization shows localization of <i>Mh270</i> and <i>Mi-PG1</i> in pre-parasitic juveniles.	53
Figure 3.6 : Homozygous, stable transgenic Arabidopsis lines express Mh270.	54
Figure 3.7 Flg22-induced ROS production is not affected in <i>Mh270</i> transgenic lines.....	55
Figure 3.8 : Flg22 responsive genes were expressed at similar levels in Col-0 and transgenic M270 lines.....	56
Figure 3.9: Flg22-induced root growth inhibition is the same in Col-0 and Mh270 transgenic lines.	57
Figure 3.10: Nematode attraction and penetration were not affected in the Mh270 lines.	58
Figure 3.11: Mh270 transgenic lines were not affected in nematode susceptibility.	59
Figure 3.12 Expressing an RNAi-Mh270 construct in Arabidopsis had no effect on plant susceptibility.	60
Figure 3.13: Arabidopsis plants expressing <i>Mh270</i> did not exhibit enhanced <i>Pst-LUX</i> growth.....	61
Figure 3.14 : Arabidopsis plants expressing Mh270 did not exhibit enhanced growth of either <i>Pst</i> Δ CEL or <i>Pst</i> Δ AvrPto/ Δ AvrPtoB	62
Figure 3.15 : Transgenic <i>Pst</i> Δ CEL and <i>Pst</i> Δ AvrPto/ Δ AvrPtoB expressing Mh270 or ATR13 did not have altered growth on Col-0 leaves.	63

Figure 3.16 : The enhanced callose deposition caused *Pst* Δ CEL infection was not suppressed in Mh270 transgenic bacteria..... 64

Figure 3.17 : Western blot analysis indicates that Mh270-GFP and not YFP-Mh270 produces a stable, tagged protein in transgenic Arabidopsis..... 65

Figure 3.18: C-terminally tagged Mh270 is localised in the cytoplasm of Arabidopsis roots. 66

Figure 3.19: Localization of Mh270-GFP in Arabidopsis leaves. 67

Figure 3.20 : The interaction between full-length Mh270 and AtVDAC3 was confirmed in double-transformed yeast..... 69

IV. List of abbreviation

%	Percent
Δ	delta
μm	Micrometer
ACO1	Acotinase-1
Amp	Ampicilin
APS	Ammonium persulfate
AT	<i>Arabidopsis thaliana</i>
ATM	<i>Arabidopsis thaliana</i> medium
Avr	Avirulent
BAK1	<i>BR1</i> -associated receptor kinase
BCIP	5-bromo-4-chloro-3'-indolyphosphate p-toluidine salt
BDGR	Binding domain of glucocorticoid receptor
BLAST	Basic Local Alignment Search Tool
BR1	Brassinosteroid receptor-1
BR11	BRASSINOSTEROID-INSENSITIVE 1
BSA	Bovine serum albumin
CALB	Calcium-dependent-lipid-binding
CaMV	Cauliflower mosaic virus
CC	Coiled coil
CDS	Coding sequence
<i>C.elegans</i>	<i>Caenorhabditis elegans</i>
<i>CLE44</i>	Clavata-ESR related-44
CRT	Calreticulin
DIG	Digoxigenin
DNA	Desoxyribonucleic acid
dNTP	Nucleosidtriphosphate
dpi	Days post infection
DUF	Domain of unknown function
EDV	Effector detector vector
<i>eds1-2</i>	Enhanced disease susceptibility
EIFA 3A-1	Eukaryotic initiation factor 3A-1

elf	Elongation factor
ET	Ethylene
ETI	Effector triggered immunity
ETS	Effector triggered susceptibility
EDTA	Ethylenediaminetetraacetic acid
flg22	Flagellin 22
FLS2	Flaggelin sensitive 2
FRK1	Flaggelin induced receptor-like kinase
g	Gramm
Gent	Gentamycin
GFP	Green fluorescent protein
GST1	Glutathionine S-transferase 1
H	Histidine
H ₂ O	Water
<i>H. glycines</i>	<i>Heterodera glycines</i>
HCl	Hydrochloric acid
HDC	Histone deacetylation complex 1
HIGS	Host-induced-gene-silencing
HR	Hypersensitive response
IAA	Indole-acetic-acid
J2	Stage 2 Juvenile
JA	Jasmonic acid
Kan	Kanamycin
kDa	Kilodalton
l	Liter
L	Leucin
LRR	Leucin-rich-repeat
LB	Lysogeny broth
ml	Milliliter
mM	Milimolar
mm	Millimeter
M	Molar
<i>MAT-4</i>	Methionine adenosyltransferase
Mbp	Mega base pairs

min	Minute
<i>M. chitwoodi</i>	<i>Meloidogyne chitwoodi</i>
<i>M. incognita</i>	<i>Meloidogyne incognita</i>
<i>M. graminicola</i>	<i>Meloidogyne graminicola</i>
<i>M. hapla</i>	<i>Meloidogyne hapla</i>
<i>M. javanica</i>	<i>Meloidogyne javanica</i>
MES	2-(N-morpholino)ethanesulfonic acid
MS	Murashige and Skoog
NADPH	Nicotinamidadeninucleotidphosphate
NBT	Nitro-blue tetrazolium chloride
NCBI	National Center for Biotechnology Information
nM	Nanomolar
OMM	Outer mitochondrial membrane
OD	Optical density
PAMP	Pathogen associated molecular pattern
PEG	Polyethylene glycol
<i>PG-1</i>	Polygalacturonase
PRR	Pattern recognition receptor
<i>Pst-LUX</i>	<i>Pseudomonas syringae</i> pv <i>tomato</i> DC3000 - <i>LUX</i>
PVP	Polyvinylpyrrolidone
qRT-PCR	Quantitative real time polymerase chain reaction
R-gene	Resistance gene
<i>rboh/f/d</i>	Respirator burst oxidase homolog f/d
RKN	Root-knot nematode
RNA	Ribonucleic acid
RNAi	RNA interference
ROS	Reactive oxygen species
SA	Salicylic acid
<i>SAM-1</i>	S-adenosylmethionine synthetase-1
SC	Synthetic complete
SDS	Sodium dodecyl sulfate

SEM	Standard error of mean
Spec	Spectinomycin
t3	Transformant generation 3
tRNA	Transfer RNA
TEMED	Tetramethylethylenediamine
TRP	Transthyretin-related proteins
TTR	Transthyretin
TTL	Transthyretin-like proteins
TTSS	Type three secretion system
<i>TOM-3</i>	Tomabovirus multiplication protein 3
<i>Ubq</i>	Ubiquitin
<i>VDAC3</i>	Voltage-dependent anion channel
W	Tryptophan
YEB	Yeast extract broth
YFP	Yellow fluorescent protein
YPAD	Yeast extract peptone dextrose medium

V. Abstract

Root-knot nematodes (*Meloidogyne sp.*) present a constant threat to agriculture worldwide. When present in the field, they can infect roots and cause a distorted root structure. This strongly reduces crop production and cause crop losses worth billions of dollars annually. Due to recent banning of many front-line nematicides and the limited number of naturally of resistant plant cultivars, it is essential to understand how these pathogens are able to infect host plants and establish their feeding sites so that we can engineer novel resistance strategies. Nematodes can secrete proteins during the infection process to help them manipulate plant responses and establish feeding sites. We call these proteins “effectors.” Recent publications have shown that root-knot nematodes potentially secrete hundreds of effectors. Unfortunately, root-knot nematodes are a challenging pathogen to study, and all but a handful of root-knot nematode effectors have been characterized. To characterize novel nematode effectors, I employed a rapid screen that delivers effectors into the plant cell using the type three secretion system of *Pseudomonas syringae* pv. *tomato* DC3000. This screen was called the “effector detector vector” (EDV) screen. Seven effector candidates were identified from a bioinformatic search of the *M. hapla* proteome and were used in this EDV screen. Two candidates that could enhance bacterial growth on wild type Arabidopsis were prioritized for additional study. One candidate effector, called *Mh270*, became the focus of my thesis. *Mh270* showed an increase in gene expression in the pre- and early stages of the nematode life cycle, which hinted at a role in parasitism. *Mh270* encodes a transthyretin-like protein (TTR) whose transcript hybridized to chemosensory pores (the amphids) of the nematode. TTR proteins are often found the excretory/secretory products of parasitic nematodes, but their roles are unknown. Transgenic Arabidopsis lines ectopically expressing *Mh270* were tested for altered nematode susceptibility and PAMP-triggered immunity (PTI). Several different elicitor-induced PTI responses were studied in the *Mh270* transgenic plants (ROS burst, callose deposition, root growth inhibition, PTI-marker gene expression). The transgenic lines did not show altered susceptibility to root-knot nematode nor were they affected in any of the PTI responses that were tested. In addition, only when *Mh270* was delivered by *Pst* DC3000 and not by less virulent *Pseudomonas* strains, which lacked certain effectors, could *Mh270* enhance bacterial growth, suggesting *Mh270* may work in conjunction with other proteins in the virulent bacteria in order to help enhance virulence. To gain even more information about the function of *Mh270*, the subcellular localization of *Mh270* in plants was studied. A C-terminal GFP tagged *Mh270* showed cytoplasmic localization in the roots while in the leaves, it showed chloroplastic localization. Meanwhile, a yeast-two-hybrid screen revealed that *Mh270* can interact with a mitochondrial

membrane-localized *Arabidopsis thaliana* voltage dependent anion channel (AtVDAC3) in yeast. Possible explanations regarding Mh270's differential in localization in roots and leaves and in regards to its interaction with an AtVDAC-partner will be discussed

1. Introduction

1.1 The importance of root-knot nematodes – *Meloidogyne sp.*

Root-knot nematodes (RKN) are small round worms belonging to the phylum Nematoda, which have adapted a plant parasitic life-style. As soil borne pathogens they infect root tissue, manipulate the plant to form a feeding site, and cause root swelling. This abnormality of the root is termed a gall, and it inhibits water and nutrient transport to the shoot (Figure 1.1). In addition, fitness reduction of infected plants often leads to secondary infections by other pathogens (Barker et al., 1994). Overall, nematode infections result in a reduced productivity of infected plants and a subsequent crop losses for farmers. It is expected that RKN cause up to 5 % of all crop losses worldwide and are the most damaging group of plant parasitic nematodes (Perry et al., 2009).



Figure 1.1: Tomato roots heavily infected with *M. incognita*. Infection of the tomato roots by the southern root-knot nematode *M. incognita* causes intense swelling of the root (right) in comparison to a uninfected tomato root (left). Galling causes problems for the plant including a reduction of water uptake and nutrients (from Mitokowski, 2001).

With a demand for food is increasing, mainly due to a growing world population, food production and security is becoming ever more important. It is estimated that the world's population will reach 8 billion in 2020 and that the demand for food will rise even more (FAO, 2014). To ensure food security, efficient methods to control RKNs will become all the more important. With bans on many front-line nematicides (Gowen, 1992), a broad host range that may preclude crop rotation, and a paucity of natural resistance genes, scientists are looking for new approaches for controlling RKN.

Generally, most research has focused on RKNs which possess a broad host range. Nematodes such as *M. incognita*, *M. javanica*, and *M. hapla* have host ranges that include most vascular plants, including major food crops (Trudgill and Blok, 2001). For example, *Meloidogyne hapla*, the northern root-knot nematode, can reproduce on most dicotyledons including the model organism *Arabidopsis thaliana*, and *M. hapla* infections have been reported on all continents where agriculture is present (Figure 1.2). Some RKN species have a more limited host range. For example, the rice root knot nematode *M. graminicola* has a relatively narrow host range and is primarily a parasite of grasses. However, the fact that it can devastate rice, a major food crop, means that it receives a lot of attention (Choi-Pheng and Birchfield, 1979). While only the genomes of two root-knot nematodes (*M. incognita* (Abad et al., 2008) and *M. hapla* (Opperman et al., 2008)) have been sequenced and annotated, extensive work has been done to generate proteomic and gene expression datasets for several other species which will help contribute to broad our knowledge of these important root pathogens (Fosu-Nyarko et al., 2009; Haegeman et al., 2013; Mbeunkui et al., 2010; Roze et al., 2008).

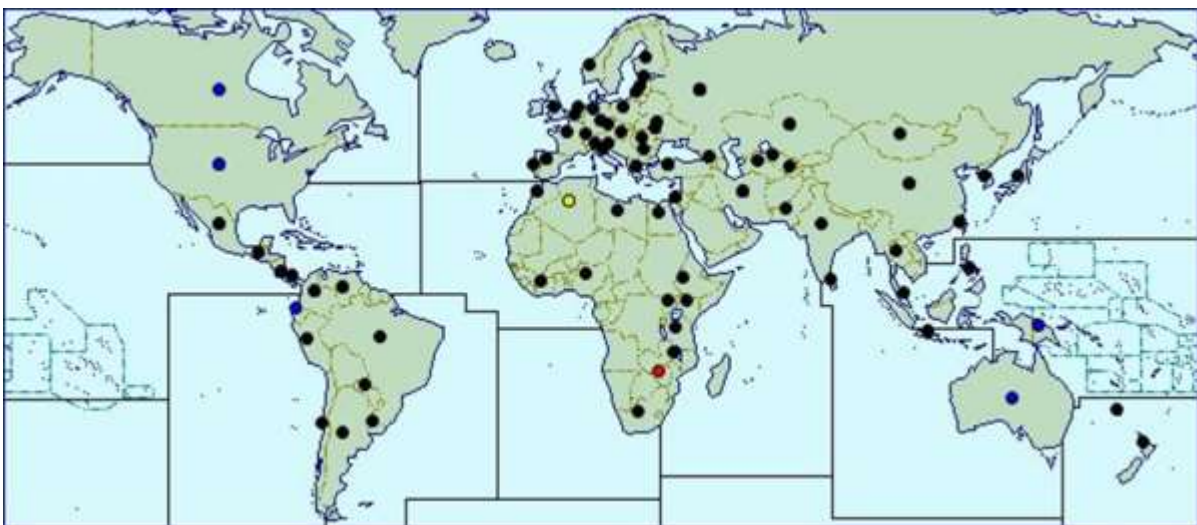


Figure 1.2 : Worldwide distribution of *M.hapla*. Black dots indicate the presence of *M.hapla*, blue dots indicate a widespread contamination and yellow dots show only an occasional contamination (from CABI.org, 2015)

1.2 *Meloidogyne sp.* biology

The life cycle of root-knot nematodes

The nematode begins life inside an egg, within which a stage 1 juvenile develops and subsequently moults to reach the infective juvenile 2 stage (J2). Hatching of J2 is mainly influenced by temperature and soil moisture content. Additionally, J2 will hatch faster if root exudates are present. These root exudates also allow the J2 to locate and move towards their host plant root system. The amphids, chemosensory organs located at the head of the nematode, are mainly thought to be involved in detection of molecules that lead the nematodes to the plant root (Chitwood and Perry, 2009). Although the identity of the nematode attractants in the root exudate are not fully known, previous studies have shown that pH gradients and indole-acetic acid (IAA) can attract J2 to the roots (Bird, 1959; Curtis, 2008). It was also shown that the most attractive part of the root for J2 is the elongation zone directly behind the root tip (Bird, 1959).

Plant parasitic nematodes secrete enzymes, such as cellulases, that soften cell walls and allow them to enter and move intercellularly through the root without causing significant root damage

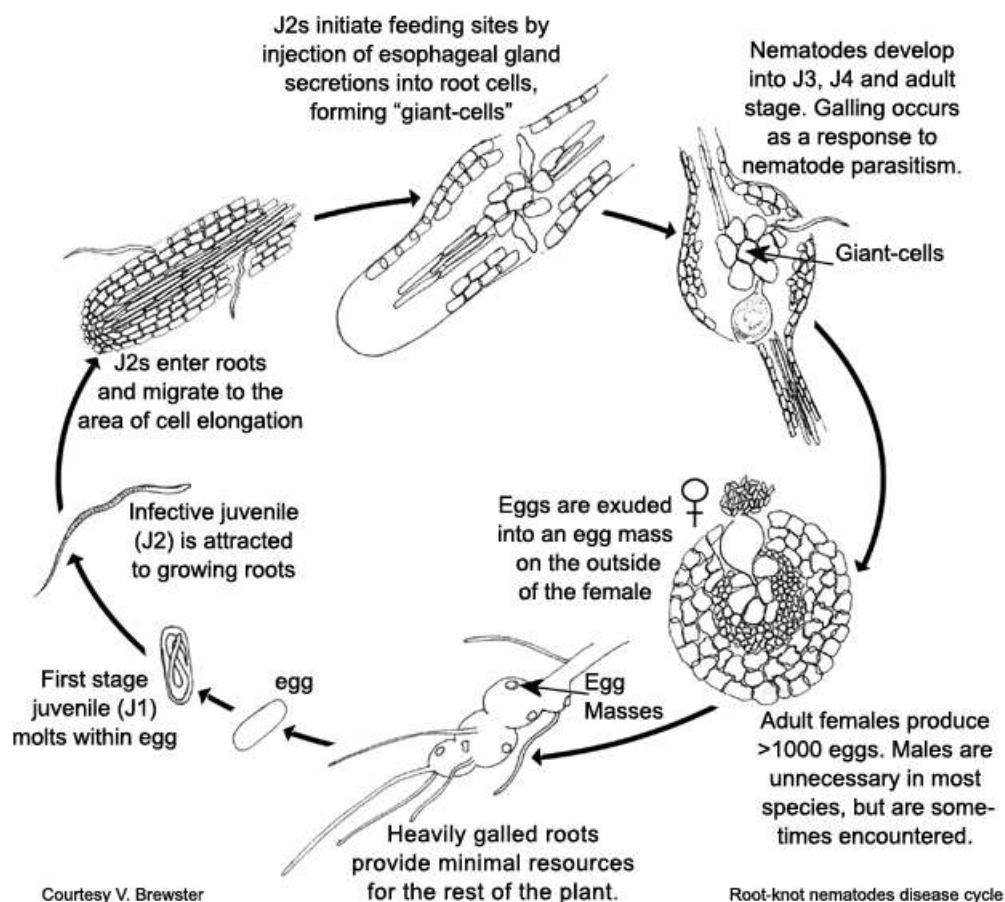


Figure 1.3 : The life cycle of *Meloidogyne sp.* Stage 1 juveniles moult within the egg. Infective J2 hatch and move towards the root, enter and migrate to the vascular cylinder to establish a feeding site. After manipulation and feeding is complete they moult twice and subsequently become adult males or females. While males leave the root, the females continue feeding and finally lay eggs in a gelatinous matrix (from Mitokowski, 2001).

(Wubben et al., 2010). The infective juveniles first migrate towards the root tip in order to bypass the Casparian strip and enter the vascular cylinder. Subsequently, they migrate up through the vascular cylinder. It is within the vascular cylinder that the nematode stops migrating and tries to establish a feeding site. These feeding sites contain of up to 12 cortical cells which undergo mitoses without cytokinesis. The resulting hypertrophied, multinucleated feeding site is called a giant cell. The giant cells act as nutrient sinks within the plant, and the nematode uses them to obtain the necessary nutrients to moult and develop. Depending on nematode and host, swelling of the plant tissue that surrounds the feeding sites and nematodes leads to the formation of the gall. The J2 feed and then moult into stage 3 and stage 4 juveniles. The J4 will eventually perform one last moult to become either adult male or female. Depending on the stress conditions and nematode species, the ratio of male to females can vary drastically. Generally, *Meloidogyne sp.* males are observed during unfavorable conditions for nematode feeding. Adult males leave the root without feeding while females start to feed again to eventually lay their eggs (Starr et al., 2009). Adult females produce eggs in a gelatinous matrix either outside or inside swollen and infected root tissue (Figure 1.3). The matrix surrounding the eggs is thought to be mainly made of glycoproteins, which keep the eggs together in an egg mass. The egg mass can protect the individual eggs against abiotic stresses and predation (Starr et al., 2009). Furthermore, it has been shown that the egg mass matrix possesses antimicrobial characteristics which protect the eggs against attacks by microorganisms (Orion et al., 2001).

For the establishment of the feeding sites, the nematode uses a straw-like, protractible stylet to pierce the plant cell wall and form a hole in the plasma membrane. It does not ingest from the cytoplasm directly, but forms a proteinaceous feeding tube in the plant cytoplasm, which is presumed to act as a sieve to filter the cytoplasm (Eves-van den Akker et al., 2014a). The nematode feeds on the amino acids and solutes in the giant cells.

As the nematode migrates and feeds esophageal secretions are released from the nematode through the stylet. There are three esophageal glands in RKNs that can produce secretions through the stylet: two subventral and one dorsal. Two subventral glands secrete proteins during root invasion and migration, whereas the dorsal gland secretes proteins during the formation of the feeding sites (Davis et al 2008). In addition to the esophageal glands, the nematode has amphids, which are chemosensory organs at the head of the nematode. The amphidal pocket is open to the outside, and secretions made in the amphid may diffuse into plant apoplast (Goverse and Smant, 2014). In addition, the nematode can secrete proteins from its surface cuticle

(Davies and Curtis 2011). Since cuticle secretions are in direct contact with the plant, they may be important for parasitism. Only a few studies have actually looked at the localization of nematode secretions *in planta*. Previous studies have shown that certain nematode proteins, when secreted *in planta* by the nematode, can accumulate in the plant's apoplast, the cell wall, and within the giant cell itself (Jaouannet et al., 2012; Rosso et al., 2011; Vieira et al., 2011). Overall, secretions from the stylet, amphids, and cuticle are thought to play key roles as effectors. Nematode effectors can alter host cell physiology, generate a feeding site, and suppress the immune response.

Manipulation of the host plant by *Meloidogyne sp.*

RKNs are entering the plant and secreting effectors that alter root cell morphology and help to form the feeding site (Figure 1.4). If the generation of giant cells fails, the nematode is not able to finish its life cycle. Interestingly, due to the wide host range of some RKN species, it is thought that RKN effectors target and manipulate conserved plant pathways involved in defense and development (Trudgill, 1997). The understanding of this manipulation of the plant may hold the key to engineer plant defenses against nematodes.

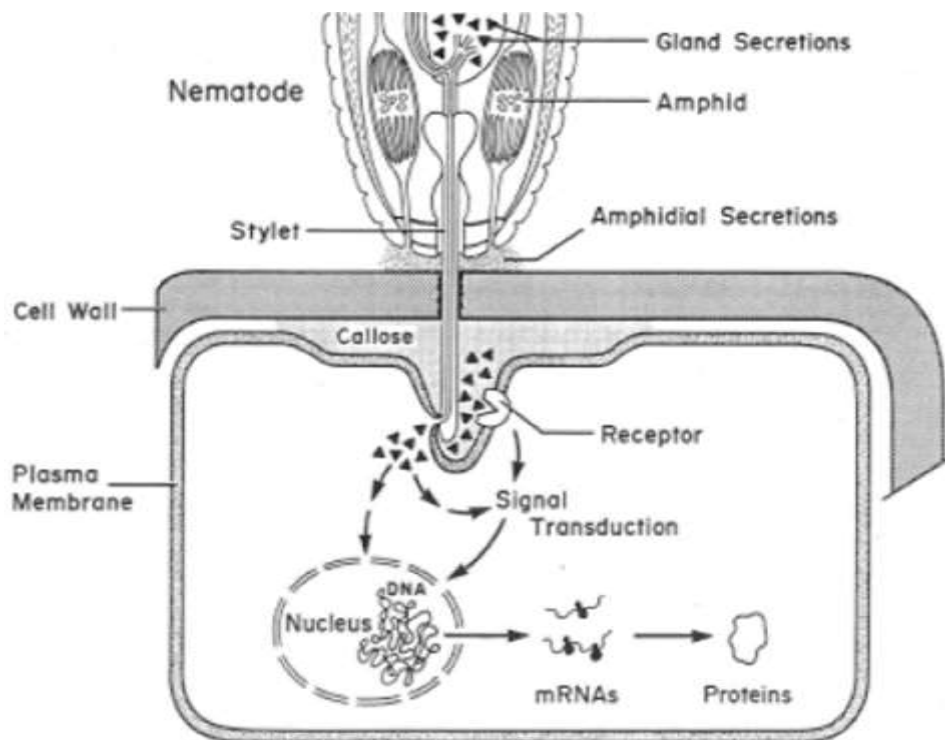


Figure 1.4: Schematic of a root-knot nematode manipulating a plant cell. The head of the nematode is directed towards the plant cell. Secretions are translocated towards the plant cell directly via the amphids or coming from the dorsal or esophageal gland through the stylet. Secreted molecules are thought to act at the in the apoplast or inside the plant cell to manipulate the plant cell towards becoming a feeding site while potentially downregulating defense mechanisms (from Williamson and Hussey, 1996).

Giant cells undergo drastic changes during their transition from standard vascular cells to mature feeding sites (Kyndt et al., 2013), and several investigations have been performed to understand the transcriptional alterations that are happening during the giant cell development. Analyses of laser dissected giant cells in rice, tomato, and Arabidopsis showed intense alterations in comparison to non-infected vascular cylinder cells. Transcriptome analysis of microdissected Arabidopsis giant cells at 3 dpi revealed that 1161 genes were differently regulated in comparison to control roots, with the majority down-regulated (Barcula et al., 2010). Interestingly, gene expression in the giant cells was shown to have significant overlap with genes regulated during infection with the root biotroph *Agrobacterium tumefaciens* (Barcala et al., 2010). Laser dissected giant cells at 4 and 7 dpi in tomato also showed that major transcriptional changes were occurring. These changes included an upregulation of genes in general metabolism and protein synthesis and turnover (Fosu-Nyarko et al., 2009). The differences in the gene expression profiles between these Arabidopsis and tomato may be a result of the different plants studied or it may be a result of the nematode influencing different plant genes at early (3 dpi) and later (4 and 7 dpi) time points of infection. In summary, it can be stated that strong transcriptional reprogramming precedes the physical development of the feeding site.

Considering that auxin is a phytohormone that is involved in turning plant tissue into tumors, it is not too surprising that enhanced auxin levels have been seen in developing gall tissue (Gheysen and Mitchum, 2011). Evidence for the important role of auxin comes from the fact that auxin signaling mutants are much less susceptible to root-knot nematodes (Goverse et al., 2000). Using the artificial DR5 promoter, which contains auxin responsive elements, scientists have seen strong *DR5::GUS* and *DR5::ER-GFP* expression in the roots infected by RKNs (Absmanner et al., 2013; Karczmarek et al., 2004). Due to the recent availability of transcriptomic datasets of giant cells, it could also be shown that auxin responsive genes are manipulated during feeding site formation. For example, two auxin responsive factor genes (*ARF*) and one auxin responsive gene (*IAA8*) are upregulated in the 3 dpi giant cell (Barcula et al. 2010). Interestingly, cyst nematodes have the ability to manipulate the polar auxin transport by manipulating the basal and temporal expression of PIN auxin transporters (Grunewald et al. 2009). Cyst nematodes generate a feeding cell that is very morphologically different to that of RKNs and the role of PIN auxin transporters in giant cells is still unknown (Grunewald et al., 2009).

Salicylic acid (SA) is a phytohormone known to be involved in stimulating plant defense responses (Nicaise et al., 2009). Although SA is classically associated with the resistance to biotrophic pathogens, no evidence has been found to directly connect SA-induced responses with an effect on the RKN-plant compatible interaction. In contrast, the antagonistically acting hormone jasmonic acid (JA) has been found to negatively influence RKN infection of susceptible plants. Exogenous jasmonic acid application (Nahar et al., 2011) or JA-induced by wounding (Snyder et al., 2006) induces nematode resistance. The nature of this resistance is not known, but it may be linked to JA causing a decrease in the attractiveness of the roots. It has also been shown that the hormone ethylene (ET), that often has a close association with JA signaling, is involved in RKN infection, and it also affects root attractiveness to nematodes. The testing of ethylene biosynthesis and signaling mutants in *Arabidopsis* showed that to ET overproducing mutants presented a nematode repellent phenotype (Fudali et al., 2012). Ethylene-dependent lignification of the roots may also limit nematode penetration (Fujimoto et al., 2015).

1.3 The plant defense system and pathogen effectors

Root-knot nematodes can enter a prolonged, intimate interaction with host plants and yet, they do not seem to activate host immune responses in a compatible interaction. Since plants are generally resistant to most pathogens (Staskawicz et al., 2001) it is important to understand the layers of plant defense and how the nematode may be manipulating these responses.

During evolution plants have develop different mechanism and layers of defense to fight off pathogens. Constitutive defenses are physical barriers that are able to block most potential threats which include cell walls and waxy epidermal cuticles. If physical barriers fail, plants also have inducible defense responses which can lead to production of toxic compounds, specific cell wall strengthening or cell death to prevent further development of the pathogen. These responses are tightly regulated to not interfere with normal plant growth and development (Freeman and Beattie, 2008).

The first inducible layer of plant defense

The most conserved and first layer of inducible defense is based on the recognition of pathogen derived molecules that are essential for their life style as flagellin from bacteria or chitin from fungi (Postel and Kemmerling, 2009). These molecules are termed pathogen associated molecular patterns (PAMP). The recognition of these molecules is performed by plasma membrane bound pattern recognition receptors (PRRs). This recognition leads to several

downstream events that, if successful, lead to PAMP triggered immunity (PTI) (Zipfel, 2008). PRRs in plants are either receptor kinases or receptor-like proteins with different ligand ectodomains that have the ability to bind to pathogen derived molecules. As soon as these receptors bind to their respective target, the cytosolic domain activates a signaling cascade. One of the most researched receptor complexes is the PRR flagellin sensing 2 (FLS2) which recognizes the bacterium derived flagellin proteins and the peptide flagellin22 (flg22). FLS2 possesses an external leucine-rich-repeat (LRR) domain and a cytosolic kinase domain. After recognition of flg22 FLS2 associates with the co-receptor BR1- associated receptor kinase (BAK1) which in turn leads to downstream signaling of the internal kinase domains (Zipfel, 2014). Subsequent responses of the plant cell include calcium flux into the cell (Tuteja and Mahajan, 2007) and an apoplastic burst of reactive oxygen species (ROS) (Wojtaszek, 1997). Additionally, transcriptional changes can be observed that lead to the production of antimicrobial compounds and to the deposition of callose that the plant uses to stop pathogens from entering the cell (Clay et al., 2009; Vidhyasekaran, 2013).

Effector triggered susceptibility and plant derived R-genes

Because pathogens need to overcome the induced plant defenses to successfully colonize the host, they acquired a diverse range of proteins that try to control plant defenses. These proteins are called effectors and support the pathogen in the compatible interaction in what is termed effector triggered susceptibility (ETS). To counteract these effectors plants acquired resistance (R) proteins that enable them to detect effectors and react to pathogen infections, leading to effector triggered immunity (ETI). Resistance genes (R-genes) that confer resistance on a gene for gene basis are often nucleotide-binding leucine rich repeat (NB-LRR) proteins and classified into two groups, depending on their N-terminal domain. One group contains a toll-interleukin-1 receptor (TIR) while the other a coiled-coil (CC) domain (Elmore et al., 2011). Activation of either R-gene variant causes a strong defense response including the generation of ROS with

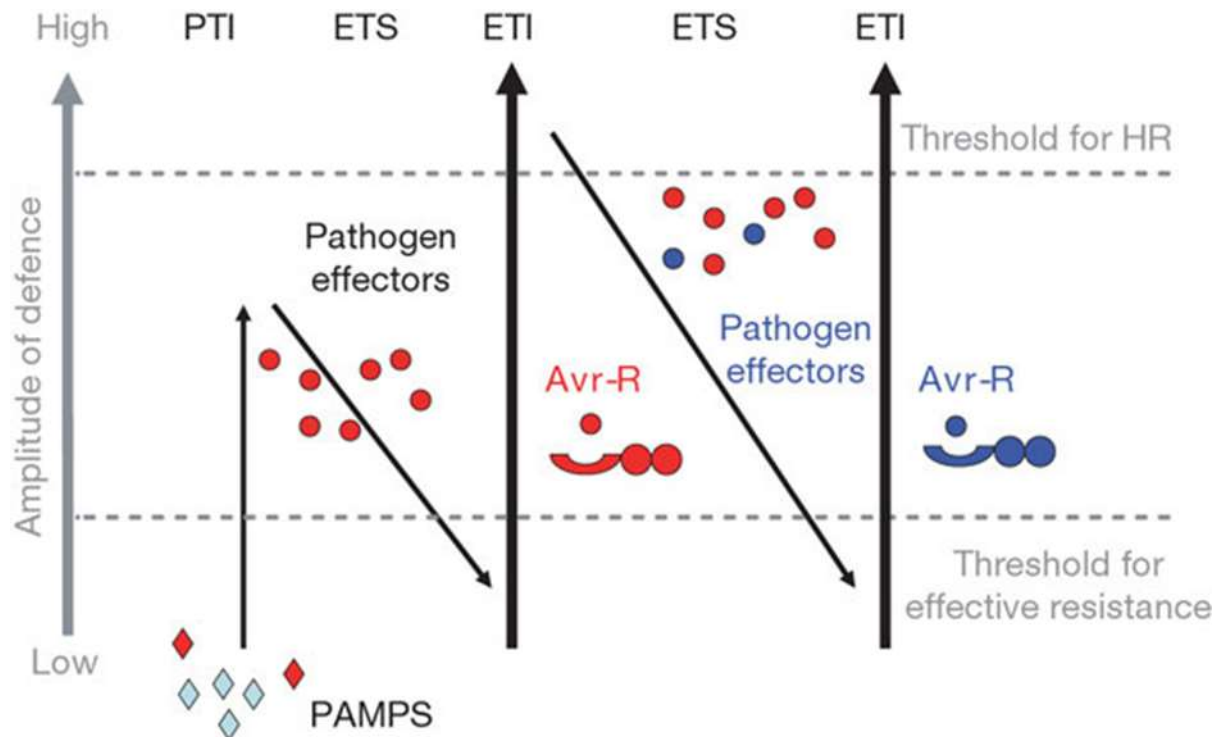


Figure 1.5 : Zig-Zag model – coevolution of defense mechanism with pathogen derived effectors. Plants use PRRs to recognize conserved molecules derived from pathogens causing PAMP triggered immunity. Effectors secreted by pathogens allow them to overcome plant defenses and establish a compatible interaction leading to effector triggered susceptibility. If an R-gene is present to detect the secreted effector, defense responses are triggered leading again to resistance due to effector triggered immunity and hypersensitive response. Pathogens effector efficiently targeting R-gene mediated resistance can subsequently establish a compatible interaction once more (Jones and Dangl, 2006)

subsequent cell death (Jones and Dangl, 2006). Thus, ETI is generally known to cause a much stronger defense response than PTI and often results in a hypersensitive responsive (HR) (Cui et al., 2015). Depending on how a pathogen is suited to infect a certain host plant, the presence of pathogen effectors and their respective plant resistance gene will determine the success of the infection (Figure 1.5).

RKNs and their impact on PTI

While PAMPs of bacterial or fungal pathogens were identified relatively early, PAMPs of plant parasitic nematodes have remained elusive. Just recently, a newly identified PAMP of nematodes, a pheromone called ascaroside, was shown to trigger defense reactions in plants (Manosalva et al., 2015). Plants treated with a plant-parasitic nematode specific ascaroside were less susceptible to diverse pathogens, including *Pseudomonas syringae* pv. *tomato*, *Phytophthora infestans* and the sedentary cyst nematode *Heterodera schachtii* as well as the root-knot nematode *M. incognita*. In line with the reduced susceptibility against various pathogens, ascaroside treatment caused MAP kinase activation and induced PTI marker gene expression (Manosalva et al., 2015). Ascarocides were identified to be conserved among nematodes influencing behavior as attraction and avoidance, and plants may have evolved to recognize this conserved nematode signature (Choe et al., 2012).

Although a nematode PAMP has been recently identified, in the compatible plant-nematode interaction, there is no evidence, yet, for basal defenses triggered by nematode infection. This suggests that the nematode may be actively suppressing PTI by secreting effectors. The RKN may also have to suppress basic plant defenses to efficiently establish their feeding sites.

Because nematode effectors are a key element of to the plant-nematode interaction, many approaches have been taken to identify nematode effectors. For example transcriptomic analysis on gland tissue cytoplasm has been performed (Wang et al., 2001). More recently, a proteomic analysis of *M. incognita* gland secretions has provided useful peptide information about possible effectors secreted through the nematode stylet (Bellafiore et al., 2008). The completion of the genomic sequence of two root-knot nematodes (*M. incognita* and *M. hapla*) and a cyst nematode species, has also aided the identification of nematode effectors (Abad et al., 2008; Cotton et al., 2014; Opperman et al., 2008)). T

Most current effector research has been performed in the cyst nematode-plant pathosystem because it is an easy nematode in which to work. In cyst nematodes several effectors and their respective targets were identified. Effects like the modification of cell walls a by cellulose binding protein (Hewezi et al., 2008), suppression defense responses by annexin-like 4F01 (Patel et al., 2010), or the alteration of cell fate by a CLAVATA3-like (CLE) proteins (Replogle et al., 2011) are examples on how cyst nematode effectors can manipulate the plant host. In fact, cyst nematode CLE peptides are particularly interesting since it was shown that they are secreted directly into the plant cell where they are recognized by plant machinery and undergo

plant-mediated protein modifications. The processed peptides are then delivered to the apoplast where they act as mimics of plant CLE peptides, triggering signaling pathways that somehow promote parasitism (Chen et al., 2014; Mitchum et al., 2012). Another example of an effector from cyst nematode is the venom allergen-like protein (VAP). Expression of the cyst nematode *Gr-VAPI* in *Arabidopsis* resulted in a suppression of basal immune responses and enhanced susceptibility to several, unrelated pathogens (Lozano-Torres et al., 2014).

So far, only 6 root-knot nematode effectors have been identified and characterized. For example, a protein secreted by RKN called *Mj-FAR-1* identified to influence defense signaling cascades by manipulating lipid based signaling. *Mj-FAR* secreted from the cuticle of the nematode influenced JA responses by potentially binding lipid precursors. Although, *FAR* could not increase infection rate of RKN, gall development was enhanced and more J2 became adult females (Iberkleid et al., 2013).

The root-knot feeding cells are highly metabolically active. Therefore, it was not surprising that an effector was discovered that may affect metabolic status of host cells. RKN secrete chorismate mutases into the plant cell (Doyle and Lambert, 2003). Chorismate mutase catalyzes the conversion of chorismate to prephenate. Chorismate is the precursor for salicylic acid and auxin. Soybean hairy roots expressing the nematode derived chorismate mutase exhibited a phenotype with less lateral roots and distorted vascular tissue. This lead to the conclusion that RKN might secrete these proteins to alter plant cell fate and establish their feeding site (Doyle and Lambert, 2003). Interestingly, smut fungi also secrete chorismate mutase into the plant cell, which leads to a reduction of available chorismate for salicylic acid biosynthesis (Djamei et al., 2011).

In RKNs, a *M. incognita* effector – calreticulin (*CRT*) – was identified to suppress PAMP triggered responses. PAMP induced gene expression was nearly completely abolished in plants expressing *Mi-CRT*. Furthermore, when the *Mi-CRT* transgenic *Arabidopsis* plants were treated with an elicitor, elf18, there was reduced callose deposition compared to the controls. Correspondingly, pathogen infection assays with *M. incognita* and *Phytophthora arabidopsidis* revealed an increased susceptibility of *Mi-CRT* expressing plants in comparison to the wild type control (Jaouannet et al., 2013).

So far, the only RKN effector with an effect on basal plant immunity identified thus far is *Mi-CRT*. Other effectors have been identified, but their mode of action is still unknown. For example, *M. javanica* derived *NULG* was able to positively influence the success of RKN

parasitism when expressed *in planta*. When the *M. incognita* effector 7E12 was expressed in tobacco plants, the plants were also more susceptible to nematodes (Souza et al 2011).

Nematode effectors and ETI

There are a handful of natural resistance genes against plant parasitic nematodes. For example, *Gpa2* confers resistance in potato to the potato cyst nematode. In tomato, the gene *Mi-1* confers resistance to the tropical and apomictic species *M. incognita*, *M. arenaria* and *M. javanica* but fails to protect the plant against other RKN species including *M. hapla* (Liu and Williamson, 2006; Vos et al., 1998). Another nematode R gene, *Ma* makes *Prunus cerasifera* highly resistant to all RKN (Lecoq et al., 1999) and *Me* confers resistance to *M. incognita*, *M. arenaria* and *M. javanica* in pepper (Djian-Caporalino et al., 2007). Researchers are interested in the cognate avirulence proteins in the pathogen that is recognized by these R genes particularly because resistance breaking nematode strains have already been observed for *Mi-1* (Ornat et al., 2001) in tomato and *R MCI* in potato (Janssen et al., 1998). So far, only two root-knot nematode effectors have been identified that are associated with nematode resistance responses, and in particular, the resistance mediated by *Mi-1*. *CGI* was shown to be involved in the recognition by *Mi-1* since silencing the gene resulted in resistance-breaking nematodes; *MAP1* was only found in avirulent *M. incognita* strains, suggesting that it may be recognized by *Mi-1* (Gleason et al., 2008; Semblat et al., 2001).

In cyst nematodes an effector called SPRYSEC-19 was shown to inhibit cell death mediated by CC-NB-LRR proteins and therefore preventing ETI (Postma et al., 2012). Although no effector has been identified in RKN to suppress ETI this finding shows that sedentary plant parasitic nematodes do possess the ability to act against this layer of defense and that further research will potentially reveal similar effectors in RKN.

1.4 Goal of this thesis

RKN are an important plant pathogen. To engineer novel resistance strategies to these pests, we must first understand the compatible plant-nematode interaction. I focused on the species *M. hapla*, which is suited for temperate climates and found in organic farms in Germany (J. Hallmann et al., 2007). This thesis focused on the potential effectors involved in the early stages of *M. hapla* infection with the special interest on effectors potentially downregulating plant defenses, in particular PTI. The first aim of my thesis was to identify several novel effector candidates from the *M. hapla* proteome which had no previously known function. Unfortunately, RKN are challenging pathogens on which to work. Because they cannot be transformed, there are limited options for the functional analysis of their genes, such as generating stable transgenic lines. To speed up effector discovery, the second goal of my thesis was to develop a novel screen to quickly and easily determine if those candidates, when expressed in bacteria, could increase bacterial virulence in plants.

In this screen, candidate genes introduced into this vector are directed towards the type three secretion system (TTSS) by the N-terminal attachment of a signal peptide deriving from *avrRPS4*. The TTSS gives *Pseudomonas syringae* the ability to directly translocate effectors into the plant cell, and effects on bacterial virulence can be quantified. After an initial screen of several *M. hapla* effector candidates in a bacterial system, I focused on one candidate in particular called *Mh270*. *Mh270* encodes a transthyretin-like protein, which has been found in the secretions of other parasitic nematodes. The transcript was localized to the head of the nematode and possibly secreted during parasitism. Because *Mh270* affected bacterial growth in planta, I hypothesized it may be affecting basal plant defenses. Thus, the third goal of this thesis was to determine, what, if any, effects *Mh270* expression in the plant might have on plant basal immune responses. Ectopic expression in *Arabidopsis* followed by a series of PTI-assays, including callose deposition, ROS burst, and PTI- marker gene expression assays, were performed. However, no effects of *Mh270* on these PTI-readouts were detected. A yeast-two-hybrid was then performed to identify the plant target. This assay gave tantalizing possibility that mitochondrial-based cell death pathways may be a target of *Mh270*, although additional experiments are needed. Based on these assays, I have gained a better understanding *Mh270* and have ruled out many possibilities for its role in the plant-nematode interaction.

2. Materials and Methods

2.1 Materials

2.1.1 Devices

Listed below are the all the used devices that were used during the different experiments of this thesis (table 2.1).

Table 2.1 : Equipment used during the experiments of this thesis. Device type, model and producer are listed.

Device	Model	Source
Autoclave	3870 ELV	Tuttnauer
Autoclave	VX95	Systec
Balance	Extend	Sartorius
Balance	SPO51	Scaltec
Blotting Device (semi-dry)		University Göttingen
Blotting Device (wet)	Criterion Blotter	BioRad
Chambers for PAGE		University Göttingen
Chambers for PAGE	Mini-PROTEAN® tetra cell	BioRad
Chambers for DNA-gel		University Göttingen
Chemocam		Intas
Confocal microscope	SP5 DM6000	Leica
Cooling centrifuge	Sorvall RC6+	DuPont
Cooling centrifuge	Rotina 38R	Hettich
Cooling micro centrifuge	Fresco17	Thermo Scientific
Counting chamber	Thoma	
Electroporator	Gene Pulser® II	BioRad
Fluorescence microscope	DM5000 B	Leica
Gel documentation device		MWG Biotech
Heating block	TH26	HLC
Heated shaker	MHR11	HLC
Heated stirrer	IKA® RH basic 2	IKA
Ice machine		Ziegra

Incubator	Certomat BS-1	Sartorius stedim biotech
Microcentrifuge	Pico17	Thermo Scientific
Microscope	DM5000B	Leica
Luciferase Camera	ImageEM	Hamamatsu
Luminometer 96 well reader	Centro XS ³ LB960	Berthold Technologies
PCR Cycler	MyCycler	BioRad
pH -Meter	pH211	Hanna Instruments
Photometer	Libra S11	Biochrom
Photometer for microtiter plates	Synergy HT	BioTek
qRT-PCR cycler	iCycler	BioRad
RNA-/DNA-Calculator	NanoDrop 2000	Thermo Scientific
Sonication device	Soniprep 150	MSE
Clean bench	Heraguard	Thermo Scientific
Clean bench	SAFE 2020	Thermo Scientific
Water deionization device	arium® pro DI	Sartorius
Vacuum pump	Cyclo 1	Roth
Vortex	Vortex Genie 2	Scientific Industries

2.1.2 Consumables

Products that are used generally only once are listed in the table below. The product specification and the producer are indicated (table 2.2).

Table 2.2 : Disposable materials used. Product type and producer are presented.

Product	Producer
Blotting paper 3MM	Whatman
Cover slips	Roth
Filter paper Miracloth	Calbiochem
Kim-Tech-Science (KimWipes)	Kimberly-Clark
Leukopor®	BSNmedical
Micotiter plates 96-wells	Greiner bio-one
Object plates	Roth
Parafilm M	Pechiney Plastic Packaging
Plastic one-way material	Biozym, Eppendorf, Greiner, Roth, Sarstedt
PVDF membrane Immobilon-P	Milipore
Tissue Culture Plate Square	Sarstedt
Tissue Culture Plate 6 well	Sarstedt

2.1.3 Chemicals

The chemicals used in buffers and media are listed in the table below. The name of the chemical compound and the corresponding manufacturer are indicated. In the material and method parts of this thesis only the chemical name is stated (table 2.3).

Table 2.3 : Chemical compounds that were used in the different experiments. Chemical description and producer are presented.

Chemical	Source
30 % (w/v) Acrylamide: N,N'-methylenebisacrylamide (37.5:1)	Roth
Agarose	Biozym
Ampicillin (Amp)	AGS
Anti-GFP antibody	Roche

Anti-rabbit antibody	Amersham Pharmacia Biotech
APS (Ammonium persulfate)	Biometra
BCIP	AppliChem
Beef extract	BD Biosciences
Bromophenol blue	Roth
Blocking reagent	Boehringer
BSA	Serva
Commercial bleach	Dan Klorix
Daishin Agar	Duchefa Direct
dNTPs	MBI
DIG PCR labeling mix	Roche
Deionised foramid	Roth
EDTA	Applichem
Ethidiumbromide	Roth
Fat-free milk powder	
Ficoll Type 400	Sigma Aldrich
Fish sperm DNA	Roche Diagnostics
Fluoresceine	BioRad
GELRITE	Duchefa
Gentamycine (Gent)	Duchefa
Hypochloric solution	Sigma Aldrich
Kanamycine (Kan)	Sigma
Luminol	Sigma Aldrich
Maleic acid	Roth
beta-Mercaptoethanol	Roth
MES	Roth
Murashige and Skoog medium (MS medium)	Duchefa
NBT	AppliChem

Orange G	Sigma
Peptone	BD Biosciences
Phenol	Sigma
Ribunucleic acid from Yeast	AppliChem
Rifampicine (Rif)	Duchefa
PVP	Sigma
Select Agar	Life Technologies
Select yeast extract	Gibco BRL
SDS	Roth
Sucrose	Roth
SYBR Green I	Cambrex
TEMED	Roth
Tryptone	Oxoid
Tween20	Roth

2.1.4 Media

In the tables below all the media and their compositions used in this thesis are listed. All media were autoclaved to ensure sterility (table 2.4-2.16).

MS plant media

Table 2.4 : Composition Murashige and Skoog plant media. Ingredients and corresponding quantities are presented.

Ingredient	Amount
MS basalt salt mixture incl. Vitamins	2.2 g
Sucrose	10 g
Adjust pH to 5.7	-
Fill up to 500ml with H ₂ O	
Add Gelrite	3.4 g

KNOPs media (Sijmons et al., 1991)

Table 2.5 : Composition KNOPs media. Ingredients and corresponding quantities are presented.

Ingredient	Amount
10x KNOPs stock	50 ml
Sucrose	5 g
Adjust pH to 6.4	-
Fill up to 500ml with H ₂ O	
Add Daishin agar	3.4g

KNOPs 10x salt stock

Table 2.6 : Composition of the 10x salt stock for KNOPs. Ingredients and corresponding quantities are presented.

Ingredient	Amount
MgSO ₄	0.488 g
Ca(NO ₃) ₂ 4H ₂ O	2.999 g
KH ₂ PO ₄	2.041 g
KNO ₃	1.28 g
72mM FeEDTA	2.77 ml
2000x micronutrient stock	5 ml
Fill up to 1l with H ₂ O	-

2000x micronutrient stock (KNOPs)

Table 2.7 : Composition of the 2000x micronutrient stock for KNOPs. Ingredients and corresponding quantities are presented.

Ingredient	Amount
MnSO ₄	0.55 g
ZnSO ₄	0.080973 g
CuSO ₄	0.029962 g
CoCl ₂ 6H ₂ O	0.011422 g
H ₃ BO ₃	1.11294 g
Na ₂ MoO ₄ H ₂ O	0.0510 g

MgCl ₂ 6H ₂ O	0.69122 g
NaCl	0.226747 g
KCl	0.33 g
Fill up to 1l	-

***Arabidopsis thaliana* culture medium (ATM) (Estelle and Somerville, 1987)**

Table 2.8 : Composition of the *Arabidopsis thaliana* culture medium. Ingredients and corresponding quantities are presented.

Ingredient	Volume (end concentration)
1 M KNO ₃	5 ml (5 mM)
1M MgSO ₄	2 ml (2 mM)
1M Ca(NO ₃) ₂	2 ml (2 mM)
20 mM Fe-Na-EDTA	2.5 ml (50 µM)
Micronutrient stock	1 ml
Adjust ph to 5.5	
Fill up to 1l with H ₂ O	

Micronutrient stock (ATM)

Table 2.9 : Composition of ATM micronutrient stock. Ingredients and corresponding quantities are presented.

Ingredient	Amount (end concentration)
H ₃ BO ₃	4.32 g (70 mM)
MnCl ₂ -4H ₂ O	2.77 g (14 mM)
CuSO ₄	80 mg (0.5 mM)
ZnSO ₄ -7H ₂ O	288 mg (1 mM)
NaMoO ₄ -2H ₂ O	48 mg (0.2 mM)
NaCl	0.58 mg (10 mM)
CoCl ₂ -6H ₂ O	2.38 mg (0.01 mM)
Fill up to 1l with H ₂ O	

Kings B medium

Table 2.10 : Composition of Kings B medium. Ingredients and corresponding quantities are presented.

Ingredient	Content (end concentration)
Proteose-Pepton No 3	10 g
K ₂ HPO ₄	1.5 g
Glycerol (86%),	15 g
Adjust pH to7.0	
Fill up to 1l with H ₂ O to 1l and autoclave	
MgSO ₄ – liquid and sterile (1M)	2 ml (2 mM)

LB medium

Table 2.11 : Composition of LB medium. Ingredients and corresponding quantities are presented.

Ingredient	Content (end concentration)
Tryptone	10 g
Yeast extract	5 g
NaCl	10 g
Adjust pH to 7	
Fill up to 1l with H ₂ O to 1l and autoclave	

YEB medium

Table 2.12 : Composition of YEB medium. Ingredients and corresponding quantities are presented.

Ingredient	Content (end concentration)
Beef extract	10 g
Yeast extract	2 g
Peptone	5 g
Sucrose	5 g/L sucrose
Adjust pH to 7.0	
Fill up to 1l with H ₂ O to 1l and autoclave	
MgSO ₄ – liquid and sterile (1M)	2 ml (2 mM)

YPAD (500 ml)

Table 2.13 : Composition of YPAD medium. Ingredients and corresponding quantities are presented.

Ingredient	Amount
Difco peptone	10 g
Yeast extract	5 g
adenine	50 mg
Adjusted pH to 5.8 with KOH	
Added H ₂ O to 450 ml	
Select agar (for solid media)	9 g
Autoclave at 121°C for 15 minutes	
40% sucrose(added when the media temperature is around 55°C)	50 ml

Yeast transformation medium

Table 2.14 : Composition of the yeast transformation medium. Ingredients and corresponding quantities are presented.

Ingredient	Amount
50 % PEG4000 (filter sterilized)	240 µl
1M LiAC pH 7.5 (filter sterilized)	36 µl
Single-stranded DNA(denatured by boiling at 100 °C for 10 minutes) from fish sperm (2mg/ml)	25 µl
Plasmid	250-500 ng

Semi-solid SC (synthetic complete) drop out medium for Y2H screen (SC –LWH)

Table 2.15 : Semi-solid SC media composition. Ingredients and corresponding quantities are presented.

Ingredient	Amount	Final concentration
Difco yeast nitrogen base	3.35 g	
CSM -Ade - His -Trp -Leu	0.305 g	
Adenine	60 mg	
Added H ₂ O to 450 ml		
Autoclave at 121°C for 15 minutes		
1% gelrite (autoclaved and immediately added to SC drop out media)	25 ml	0.05 %
40% sucrose(added when the media temperature is around 55°C)	50 ml	2 %
1 M 3-amino-1,2,4-triazole solution (if required)	2.5 ml	5 mM
Ampicilin stock conc. 100mg/ml (if required)	500 µl	100 µg/µl

Synthetic Complete dropout (SC dropout) medium (500 ml)

Table 2.16 : Composition SC dropout media for yeast. Ingredients and corresponding quantities are presented.

Ingredient	Amount	Final concentration
Difco yeast nitrogen base (W/O amino acid)	3.35 g	
*General list of amino acid, specific drop out medium can be made by leaving out the amino acid of choice		
Arginine	25 mg	
Aspartic acid	40 mg	
Histidine	10 mg	
Isoleucine	25 mg	
Leucine	50 mg	
Lysine	25 mg	
Methionine	10 mg	
Phenylalanine	25 mg	
Threonine	50 mg	
Tryptophan	25 mg	
Tyrosine	25 mg	
Uracil	10 mg	
Valine	70 mg	
Serine	10 mg	
Adenine	60 mg	
**Alternatively use commercially available amino acid dropout mixtures		
Adjust pH to 5.6 with KOH		
Added H ₂ O to 450 ml		
Selected agar (for solid media)	9 g	
Autoclave at 121°C for 15 minutes		
40% sucrose (added when the media temperature is around 55°C)	50 ml	2%
1 M 3-amino-1,2,4-triazole solution (if required)	2.5 ml	5mM

2.1.5 Buffers

Below listed in tables are all buffers used for the experiment of this thesis (table 2.17-2.29).

Alkaline Phosphatase Buffer – staining buffer

Table 2.17 : Composition of alkaline phosphatase buffer used for *in situ* hybridization. Ingredients and corresponding quantities are presented.

Ingredient/concentration of stock	Amount (end concentration)
1M Tris-HCL pH9.5	100 ml (100 mM)
NaCl	5.85 g (100 mM)
MgCl ₂	10.17 g (50 mM)
Fill up to 1l with H ₂ O	-

Böhringer blocking reagent 10%

Table 2.18 : Composition of Böhringer blocking reagent mix used for *in situ* hybridization. Ingredients and corresponding quantities are presented.

Ingredient/concentration of stock	Amount (end concentration)
Blocking reagent	10 g (10%)
Fill up and dissolve in 100ml maleic acid buffer	-

Denhardts 50x (100ml)

Table 2.19 : Composition of Denhardts (50x) buffer mix used for *in situ* hybridization. Ingredients and corresponding quantities are presented.

Ingredient	Amount
Ficoll (400kDa)	1.25 g
PVP	1.25 g
BSA	1.25 g
Fill up to 100ml with H ₂ O	-

Hybridization buffer (200ml)

Table 2.20 : Composition of hybridization buffer used for *in situ* hybridization. Ingredients and corresponding quantities are presented.

Ingredient	Amount (end concentration)
Deionised formamid	100 ml (50%)
SSC 20x	40 ml (4x)
Böhringer blocking reagent 10%	20 ml (1%)
SDS 20%	20 ml (2%)
Denhardts 50x	4 ml (1x)
EDTA pH8 0.5M	0.4 ml
Fish sperm DNA 10mg/ml	4 ml (200 µg/ml)
tRNA Yeast (28mg/ml – 500 units)	1.25 ml (3.125 U/ml)
Fill up to 200ml with H ₂ O	-

Maleic acid buffer (100ml)

Table 2.21 : Composition of the maleic acid buffer used for *in situ* hybridization. Ingredients and corresponding quantities are presented.

Ingredient	Amount (end concentration)
Maleic acid	11.61 g (100 mM)
NaCl	8.76 g (150 mM)
Adjust pH to 7.5 with NaOH	-
Fill up to 100ml with H ₂ O	

Callose staining buffer

Table 2.22 : Composition of the callose staining buffer. Ingredients and corresponding quantities are presented.

Ingredient	Content (end concentration)
K ₂ HPO ₄	26.127g (150mM)
Adjust pH to 9.5	
Adjust to 1l with H ₂ O and autoclave	
Add 0.01% (w/v) aniline blue to stain mixture	

Immunoprecipitation extraction buffer (50 ml)

Table 2.23 : Composition of the immunoprecipitation extraction buffer. Ingredients, amounts and the final concentration of the corresponding ingredient are presented.

Ingredient	Amount	Final concentration
1 M Tris-HCl	2.5 ml	50 mM
5 M NaCl	1.5 ml	150 mM
0.5 M EDTA	100 µl	1 mM
1 M Dithiotheritol (DTT) stock	250 µl	5 mM
NP40	100 µl	0.2 %
100x Protease inhibitor (excluded Protease inhibitor for wash buffer)	100 µl	1x
Added H ₂ O to 50 ml		

Acrylamide gel for Western blot

Table 2.24 : Acrylamide gel composition used to run SDS-PAGE. Ingredients, amounts and the final concentration of the corresponding ingredient are presented.

Ingredient	Amount	Final concentration
Acrylamide	2.68-13.3 ml	4-20%
1.5 M Tris-HCl pH 8.8	5 ml	375 mM
H ₂ O	11.9 – 1-28 ml	
10% APS	200 µl	1 %
10% SDS	200 µl	1 %
TEMED	20 µl	

Ingredient	Amount	Final concentration
Acrylamide	670 μ l	4%
1 M Tris-HCl pH 6.8	625 μ l	0.125 mM
H ₂ O	3.6 ml	
10% APS	50 μ l	1 %
10% SDS	50 μ l	1 %
TEMED	5 μ l	

Blocking buffer

Table 2.25 : Composition of the blocking buffer for Western blot. Ingredients, amounts and the final concentration of the corresponding ingredient are presented.

Ingredient	Amount	Final concentration
Skimmed milk powder (Sucofin ®)	0.4 g	2 %
Added TBST to 20 ml		
First or secondary antibody (if needed)	4 μ l	1:5000

Transfer buffer (1L)

Table 2.26 : Composition of the transfer buffer used for Western blot. Ingredients, amounts and the final concentration of the corresponding ingredient are presented.

Ingredient	Amount	Final concentration
Tris	5.82 g	48 mM
Glycin	2.93 g	39 mM
20% SDS	2 ml	0.04%
MeOH	200 ml	20%
Added H ₂ O to 1 liter		

10X running buffer (1L)

Table 2.27 : Composition of concentrated running buffer for SDS-PAGE. Ingredients, amounts and the final concentration of the corresponding ingredient are presented.

Ingredient	Amount	Final concentration
Tris	30.24 g	250 mM
Glycin	142.75 g	1.9 M
20% SDS	50 ml	1 %
Added H ₂ O to 1 liter		

10xTBS (1L)

Table 2.28 : Composition of concentrated 10xTBS buffer. Ingredients, amounts and the final concentration of the corresponding ingredient are presented.

Ingredient	Amount	Final concentration
Tris	24.2 g	200 mM
NaCl	80 g	1.37 M
Adjust pH to 7.6 with HCl		
Added H ₂ O to 1 liter		

1x TBST

Table 2.29 : Composition of TBS working solution. Ingredients, amounts and the final concentration of the corresponding ingredient are presented.

Ingredient	Amount	Final concentration
10X TBS	100 ml	1x
Tween 20	1 ml	0.1%
Added H ₂ O to 1 liter		

2.1.6 Primers

This section presents the primers used for qRT-PCR (table 2.30) and cloning (table 2.31). Primers for qRT-PCR were designed using Primer3 (Rozen and Skaletsky, 1998).

Oligonucleotides qRT-PCR

Table 2.30 : Sequence list of used qRT-PCR primers in the direction 5'-3'. Name of the primer and the corresponding sequence are presented.

Name of nucleotide	Sequence 5' - 3'
Mh265 Forward Primer	ATTGGACAAACTAGCTGCTG
Mh265 Reverse Primer	CAAGCATCCTCCAAAATAGA
Mh270 Forward Primer	GCAATTTGCCGACGTCGTAGT
Mh270 Reverse Primer	AACCTCATTCTCCCCACCCCT
AtWRKY22 Forward Primer	ATCTCCGACGACCACTATTG
AtWRKY22 Reverse Primer	TCATCGCTAACCACCGTATC
AtWRKY33 Forward Primer	CAAAGGAAAGGAGAGGATGG
AtWRKY33 Reverse Primer	GTAGACTGAGGTTTAGGATGG
AtWRKY53 Forward Primer	GCAACGAAACAAGTCCAGAG
AtWRKY53 Reverse Primer	GTCTTTACCATCATCAAGCCC

AtUbq5 Forward Primer	GACGCTTCATCTCGTCC
AtUbq5 Reverse Primer	GTAAACGTAGGTGAGTCCA
AtGST1	Quantitec
AtFRK1	Quantitec
AtCYP81F2	Quantitec
Mi18S Forward Primer	ACCGTGGCCAGACAAACTAC
Mi18S Reverse Primer	GATCGCTAGTTGGCATCGTT
MhActin Forward Primer	ACACGCCAGCCATGTATGTTGCT
MhActin Reverse Forward	AAATCACGTCCAGCCAAGTC

Oligonucleotides for cloning and control amplifications (excluding Att sites)

Table 2.31 : List of primers used for cloning. Name of the primer and the corresponding sequence are presented.

Name of nucleotide	Sequence 5' - 3'
Mi – PG1 Forward Primer	AAGGCTGAAGTTGAGGAAGA
Mi- PG1 Reverse Primer	ATTATGTGTTCCCTCCGTTAG
Mh270 – SP Forward Primer	ATGGAGCAACAAATATAACAGTTCGAG
Mh270 – SP Reverse Primer	TTAATCATCACACGTTTCTTTGTCTC
Mh270 for hairpin construct Forward Primer	CGACGTCGTAGTGTTAAAGGA
Mh270 for hairpin construct Reverse Primer	CGTTTCTTTGTCTCTATGTCCAG
Mh270 no stop Reverse Primer	ATCATCACACGTTTCTTTGTCTCTA
AT3G17390 Methionine adenosyltransferase, <i>MAT4</i> Forward Primer	ATGGAATCTTTTTTGTTCACATCTG
Reverse Primer	TCAAGCTTGGACCTTGTTAGACTTG
AT4G36980 Unknown protein Forward Primer	ATGTGGCACGAAGCGAGAAGATCGG
Reverse Primer	TCAGTGCCTTGACCTGCTGCTTCTT

AT5G28150 Plant protein of unknown function (DUF868) Forward Primer	ATGAAGGATTTTCCTTCTTGCTTTG
Reverse Primer	CTACTCGCTCTTCCAAGCGTACAGA
AT5G08450 Histone deacetylation complex 1, RXT3-LIKE, <i>HDC1</i> Forward Primer	ATGAGTGGTGTTCCAAAGAGATCTC
Reverse Primer	TTAGTTGGGGGAGAGAAAATGAACA
AT2G21850 Cysteine/Histidine-rich C1 domain family protein Forward Primer	ATGGCAGAGCTCAAGCATTCTCCC
Reverse Primer	TTATAACACCTCCAAGAGATGACGC
AT5G37740 Calcium-dependent lipid-binding (CaLB domain) family protein Forward Primer	ATGGAGAATCTTGTAGGTCTTCTTC
Reverse Primer	CTAAATACCCCTTGAACCCGGGACA
AT4G13195 CLAVATA3/ESR-related 44, <i>CLE44</i> Forward Primer	ATGGCAACTACAATTGATCAAACCA
Reverse Primer	CTAGTTGGAGATAGGGTTTGGACCA
AT4G35830 Acotinase 1, <i>ACO1</i> Forward Primer	ATGGCTTCCGAGAATCCTTTCCGAA
Reverse Primer	TTATTGTTTGATCAAGTTCCTGATA
AT5G47690 Unknown protein Forward Primer	ATGGCTCAGAAGCCGGAGGAACAGT
Reverse Primer	CTATATTGCTGTCCTCGAGATTGAC
AT4G11420 Eukaryotic translation initiation factor 3A, <i>ATEIF3A-1</i> Forward Primer	ATGGCGAATTTTGCCAAACCAGAGA
Reverse Primer	TCAACGCTGTGTTGGCCTGGGCCTG
AT5G15090 Arabidopsis thaliana voltage dependent anion channel 3, <i>ATVDAC3</i> - Forward Primer	ATGGTTAAAGGTCCAGGACTCTACA

Reverse Primer	TCAGGGCTTGAGAGCGAGAGCAATC
AT4G31800 Arabidopsis thaliana WRKY DNA-binding 18, <i>ATWRKY18</i> Forward Primer	ATGGACGGTTCTTCGTTTCTCGACA
Reverse Primer	TCATGTTCTAGATTGCTCCATTAAC
AT2G02180 Tobamovirus multiplication protein 3, <i>TOM3</i> Forward Primer	ATGAGAATCGGCGGGCGTCGAGGTTA
Reverse Primer	TCAGCGAATCTGATGGTATTGTGTA
AT1G02500 S-adenosylmethionine synthetase 1, <i>ATSAM1</i> Forward Primer	ATGGAGACTTTTCTATTCACATCTG
Reverse Primer	TTAAGCTTGAGGTTTGTCCCACTTG

2.1.7 Organisms

This section lists the organisms used during this thesis. If applicable selection resistance is also mentioned (table 2.32).

Table 2.32 : Organisms used during the experiments of this thesis. Name of organism, resistance conditions, and the use of the specific organism are presented.

Organism	Selection resistance (µg/ml)	Use
<i>Agrobacterium tumefaciens</i> – GV3101	Rif (25), Gent (25)	Stable transformation of Arabidopsis
<i>Meloidogyne hapla</i> – VW9	-	Infection, RNA extraction, <i>in situ</i> hybridization
<i>Meloidogyne incognita</i> – “Morelos”	-	<i>In situ</i> hybridization
<i>Arabidopsis thaliana</i> -Col-0		
<i>Solanum lycopersicum</i> – “Green Zebra”		Nematode rearing
Yeast “AH109”	-	Library screen
Yeast “PJ69-4a”	-	Double transformations
Yeast “Y178” (provided by Joachim Uhrig)		Yeast-two-library screen
<i>Pseudomonas syringae</i> pv. tomato DC3000 – <i>LUX</i> (provided by Jonathan Jones – Sainsbury Laboratory Norwich) -	Rif (25), Kan (25)	EDV screen, infection assays
<i>Pseudomonas syringae</i> pv. tomato DC3000 ΔCEL	Rif (25), Kan (25)	Infection assays
<i>Pseudomonas syringae</i> pv. tomato DC3000 Δ <i>AvrPto</i> /Δ <i>AvrPtoB</i>	Rif (25), Spec (50)	Infection assays

2.1.8 Plasmids

Below all plasmids are listed that were used either for cloning or directly for experiments.

Plasmid name, use, and selection resistance are shown.

Table 2.33 : Plasmids that were used for cloning or experimental procedures. Plasmid name, its use, and the resistance for selection in bacteria and plant are presented.

Plasmid	Use	Resistance
pDonr201	Entry vector	Kan
pB2GW7	Expression vector for Arabidopsis transformation	Spec/Basta
pUBN-YFP	Expression vector fusing YFP to the N-terminal	Spec/Basta
pUBC-GFP	Expression vector fusing GFP to the C-terminal	Spec/Basta
pEDV6 – (provided by Jane Parker – MPI Cologne)	Expression of candidates in <i>Pst</i> DC3000 - EDV	Gent
pEDV containing ATR13 ^{Emco5} (provided by Jane Parker – MPI Cologne)	Reference for <i>Pst</i> DC3000 – EDV screen	Gent
pB7GWIWG2(II)	RNAi – hairpin vector for Arabidopsis transformation	Spec
pASII	Bait vector for yeast-two-hybrid	Amp
pGAD	Fish vector for yeast-two-hybrid	Amp

2.1.9 Kits

The table below presents the kits used during the creation of this thesis.

Table 2.34 : List of kits used during this thesis. Kit name and producer are presented.

Kit name	Producer
NucleoSpin Gel and PCR Clean Up	Macherey & Nagel
NucleoSpin Plasmid	Macherey & Nagel

2.2 Methods

2.2.1 General molecular methods

Phusion DNA polymerase reaction – High fidelity amplifications

Amplification was performed according to the manufacturer's protocol. An example reaction is presented in the table below. An example cycler protocol to amplify a fragment of less than 500bp is presented.

Table 2.35 : Contents of a standard phusion taq amplification mix. Components and corresponding quantities are presented.

Stock component	Volume in 40 μ l reaction
Buffer (HF/GC) 5x	8 μ l
dNTPs 40mM (10 mM each)	0.8 μ l
Forward primer (10 μ M)	2 μ l
Reverse primer (10 μ M)	2 μ l
Template	1 μ l (~50ng)
Polymerase	0.2
H ₂ O	24.6

Table 2.36 : Standard PCR cycler program to amplify a fragment of 500b. Cycle step, temperature and cycle numbers are presented.

Cycle step	Temperature and duration	Cycles
Initial denaturation	98°C ,30 sec	1
Denaturation	98°C, 30 sec	40
Annealing (adjust to primer)	55°C, 30 sec	
Extension	72°C, 30 sec	
Final extension	72°C, 5 min	1

Measurement of DNA and RNA concentrations

The concentration of nucleic acids was determined by measuring their absorption in a NanoDrop 2000 at a wave length of 260 nm (maximum nucleic acid absorption value, due to the π -electron systems of the heterocycles of the nucleotides). Absorption at 280 nm (due to the presence of aromatic rings from amino acids and phenol compounds) was used for references of the purity of the DNA or RNA samples. The optimal ratio of OD₂₆₀/OD₂₈₀ for RNA is from 1.9-2.0 and for DNA 1.8.

Separation of DNA on agarose gels

The DNA was separated by electrophoresis in horizontal 1 % agarose gels with 1x TAE buffer. The agarose gel concentration was either 2 % agarose (< 500 kb) or 1.0 % agarose (< 4000 bp),

depending on the size of the DNA fragments to be separated. DNA samples were mixed with 1/10 volume of 10x DNA loading buffer, loaded in separate lanes and run at 120 V for 45 min. The gels were stained in ethidium bromide solution (0.1 % w/v) for 15 min, and the detection of the DNA was performed on an UV-transilluminator (260 nm). The signals were documented with a gel-documentation station. For elution of DNA fragments from the gel the visualization was done with larger wavelength UV-light (320 nm) and the DNA fragments in the gel slices were eluted with the NucleoSpin® Gel and PCR Clean-up Kit (Macherey-Nagel).

Gateway cloning

The Gateway® technology is based on the site specific recombination of bacteriophage lambda and thereby provides a fast method to exchange DNA fragments between multiple vectors without the use of conventional cloning strategies (Hartley et al., 2000; Landy, 1989). All cloning steps done with the Gateway® system were performed as described in the Invitrogen manual, Version E, September 22, 2003. Briefly, the Gateway BP II Clonase enzyme kit was used according to the manufacturer's instructions to transfer PCR fragments into the entry vector pDONR207. For introduction into the destination vectors, LR reactions were composed of the entry clone, the destination vector (150 ng/ µl) and 2 µl LR Clonase II. After a 1 hour incubation at room temperature, the reaction was used to transform *E. coli* DH5α.

Isolation of high-quality plasmid DNA

High-purity plasmid DNA was isolated for sequencing, cloning and transformation according to the manufacturer instructions of the Macherey-Nagel Mini, Midi and Maxi KitNucleoSpin Kits.

Sequencing of DNA

Sequencing of plasmid DNA was performed with SeqLab. Minimum 600 ng plasmid DNA was mixed with 20 pmol required primer and water was added to a final volume of 7 µL.

Transformation of *E. coli*

The transformation of chemical competent *E. coli* DH5α cells was done with the heat shock method according to (Hanahan, 1983). An aliquot of competent cells (200 µL) was thawed for 10 min on ice, 50 ng of plasmid DNA were added and the mixture was incubated for 30 min on ice. The cells were shocked at 42°C for 90 sec. The cells were then placed on ice for 2 min before 800 µl dYT medium were added. The transformed cells were incubated for 1h at 37°C with shaking. The cells were streaked on plates containing LB medium and the required antibiotics. Incubation took place overnight at 37°C.

Transformation of *A. tumefaciens*

Electrocompetent *A. tumefaciens* GV3101 cells were transformed by electroporation method. Thawed cells were mixed with high-quality plasmid DNA, an electric pulse (2.5 kV, 25 μ F, 400 Ω) was applied for 5 s and the cells were immediately incubated with 1 mL YEB medium for 2 h at 30°C. The transformed cells were spread on selective YEB plates and incubated for 2-3 days at 30°C. For plasmid extraction, clones were individually picked and placed in 25 mL YEB liquid medium with the appropriate antibiotics at 30°C with shaking, overnight. 5 mL aliquots of the overnight cultures were used for plasmid extraction (3.2.1.1.1.2) to check for positive clones by PCR. 1 ml of overnight culture was mixed with 1 ml 87% glycerol and stored at -80°C for storage.

Transformation of *Pseudomonas syringae* strains

Electrocompetent *Pseudomonas syringae* cells were transformed by electroporation method. Thawed cells were mixed with high-quality plasmid DNA, an electric pulse (2.5 kV, 25 μ F, 400 Ω) was applied for 5 s and the cells were immediately incubated with 1 mL Kings B medium for 2 h at 30°C. The cells were spread on Kings B media containing the appropriate antibiotics and incubated for 2-3 days at 30°C.

Agrobacteria-mediated Arabidopsis transformation

The transformation of Arabidopsis is based on the floral dip method (Clough and Bent, 1998). Briefly, six weeks old *Arabidopsis thaliana* Col-0 (or otherwise stated) were grown under long day conditions (22°C/ 18°C, 80-100 μ mol photons/m²/s, 16h light/8h dark, 60 % humidity). An overnight Agrobacteria culture was grown in 500 mL YEB media with appropriate antibiotics. After centrifugation (4000 rpm in swing bucket centrifuge, 20 min), the pellet was resuspended in 5% sucrose solution + 0.01% Sylvet77 to OD₆₀₀ = 0.8. The inflorescence were dipped in *Agrobacterium tumefaciens* GV3101 cultures, and covered with a plastic lid overnight. Plants were allowed to set seed in the long day chamber.

2.2.2 Plant growth conditions

***Arabidopsis thaliana* seed sterilization**

Seeds were surface sterilized by vortexing in 1ml 70% ethanol for 10 min in a 1.5ml Eppendorf tube. The seeds were then washed with 100% ethanol and allowed to dry under the laminar airflow.

Growth of plants on substrate

Surface sterilized seeds were sown on steamed soil (Archut, Fruhstorfer Erde, T25, Str1 fein) supplemented with Confidor (50 mg/L) and fertilizer (0,5 ml/L Wuxal) and stratificated at 4°C for two days. The plants were grown under short day conditions (22°C/ 18°C, 80-100 $\mu\text{mol Photones/m}^2/\text{s}$, 8h light/16h dark, 60 % humidity), long day conditions (22°C/ 18°C, 80-100 $\mu\text{mol photones/m}^2/\text{s}$, 16h light/8h dark, 60 % humidity) or 12h/12h-light cycle conditions (22°C/ 18°C, 80-100 $\mu\text{mol photones/m}^2/\text{s}$, 12h light/12h dark, 60 % humidity).

Plant growth on axenic plates

Surface sterilized seeds were sown on MS-MES plates under the clean bench and sealed with Leukopor®. After stratification of 2 days at 4°C the plants grown under 14h/10h-light cycle conditions (22°C/ 18°C, 80-100 $\mu\text{mol Photones/m}^2/\text{s}$, 14h light/10h dark, 60 % humidity) for 12 to 14 days.

Selection of transgenic plants on axenic plates using BASTA

Seeds were surface sterilized by vortexing in 1ml 70% ethanol for 10 min in a 1.5ml Eppendorf tube. The seeds were then washed with 100% ethanol and allowed to dry under the laminar airflow. Seed were put on MS plates containing BASTA-PPT (Phosphinothricin/Glufosinate Ammonium – 250 $\mu\text{l}/500 \text{ ml MS}$) and grown until plant responded to selection via whitening of cotyledons and growth reduction.

2.2.3 Pathogen assays

Cultivation of *Pseudomonas syringae*

Glycerol stocks frozen at -80°C were used for preparing freshly grown colonies on King's B agar plates with appropriate antibiotics. The streaked bacteria were incubated overnight at 30°C. For infection of *A. thaliana* plants, 20 mL King's B with 100 μL 1 M MgSO_4 and the required antibiotics were inoculated with a single colony of bacteria. The bacteria were incubated overnight at 30°C and 220 rpm. The overnight cultures were centrifuged for 10 min

at 4000 rpm and the pellet was washed 2 times with 20 mL 10 mM MgCl₂. The OD₆₀₀ of the washed cells were measured and the required OD₆₀₀ was prepared by dilution with 10 mM MgCl₂.

***Pst*-lux infection assay measuring bioluminescence**

Four week old Col-0 wild type plants were grown under short day conditions (8 h day/14 h night) on peat substrate were put under high humidity conditions for at least 1 h. Next plants were sprayed with a bacterial suspension of OD₆₀₀=0.2 supplemented with 10 mM MgSO₄ and 0.05% Silwet L-77. 10 mL of bacterial suspension were sprayed on 5 individual plants. Plants were kept for 1h under high humidity conditions. Subsequently, plant leaves were allowed to dry and put back into a short day growth chamber for 3 additional days. On day 3 luciferase activity was measured. Plants were put into the CCD digital camera (Hamamatsu) chamber and kept in the dark for 5 minutes. Photos were taken with the following settings: EM gain: 1200, Exposure time: 300 sec, Image acquisition: slow. Signal intensity was analyzed using HOKAWO software. After pictures were taken plant leaves were cut and above ground fresh weight was measured.

***Pst* infection assay measuring colony forming units**

Four week old Col-0 wild type plants grown under short day conditions (8 h day/14 h night) on peat substrate were leaf infiltrated with bacteria OD = 0.0001 (*Pst-LUX*) or OD₆₀₀ = 0.001 (*Pst* Δ*Cel* and *Pst* Δ*AvrPto/ΔPtoB*) in 10 mM MgSO₄. Leaves were punched out after 1 h and 3 days. Leaf discs were vortexed for 10 min in 10 mM MgSO₄ containing 0.05% Silwet L-77. Dilution series were performed using 10 mM MgSO₄ buffer and 10 μl of the dilutions were aliquoted onto Kings B media containing the appropriate antibiotics. Plates were incubated for two days at 28°C and colonies were counted at each dilution. Next, colony forming units (CFU) was calculated relative to dilution and leaf disc surface.

Nematode egg sterilization

Infected tomato (*Solanum lycopersicum* cultivar green zebra) roots were mixed vigorously for 4 min in a 10% sodium hypochlorite solution and then poured through two sieves (250 and 25 μm sequentially). The eggs were then collected and centrifuged at 4000 rpm for 5 min in a swing bucket centrifuge. The eggs were then surface sterilized by applying 10% sodium hypochlorite for 5 min with continuous shaking. at the eggs were pelleted by centrifugation at 4000 rpm for 5 min (repeated twice). The eggs were then washed with sterile H₂O 3 times, centrifuged and then re-suspended in CT solution (water with 1% SDS and 2% Plant Protection

solution). The egg containing CT solution was then transferred to a small beaker containing 4 layers of Kimwipes sitting over 50 mL CT solution. The eggs were placed on the Kimwipes and allowed to hatch for 3 days. Hatched juveniles migrate through the Kimwipes and settle in the solution at the bottom of the beaker.

Nematode infection and penetration assay

Plants grown for seven days on axenic MS plates were transferred onto six well plates containing 3ml MS media. After one week plants were infected with 200 sterile root-knot juveniles and incubated in the dark for 4 weeks at room temperature. Galls were visually counted under the stereomicroscope. To estimate penetration of nematodes, infected roots were stained with acid fuchsin 5-7 days after inoculation.

Acid Fuchsin staining (Byrd et al., 1983)

Plants to be stained were placed into sodium hypochlorite solution for 2 min. the plants were rinsed with H₂O and then placed into a boiling, 1/30 diluted, acid fuchsin staining solution (35 mg / 100 mL). The plants were incubated in the boiling solution for at least 1 min. The stained plants were shortly rinsed in H₂O and observed under a microscope.

2.2.4 RNA extraction and gene expression analysis

RNA extraction

TRIZOL method (Chomczynski 1993) was used to extract RNA from plant tissue. Phenol/chloroform (dichloromethane) extraction dissolves RNA in the aqueous phase while other compounds like chlorophyll or proteins are solved in the hydrophobic chloroform phase. RNase activity is inhibited by two thiocyanate compounds in the extraction buffer. Deep frozen fine powder (~200 mg) of ground plant tissue (2 mL reaction tube) was dissolved in 1.3 mL extraction buffer (380 mL/L phenol saturated with 0.1 M citrate buffer pH 4.3, 0.8 M guanidinthiocyanate, 0.4 M ammoniumthiocyanate, 33.4 mL 3 M Na-acetate pH 5.2, 5 % glycerol) and shaken for 15 min at RT. Chloroform (260 µL) was added to each sample and after an additional shaking step of 15 min at RT the samples were centrifuged for 30 – 40 min at 12.000 rpm and 4°C. The clear supernatant (~ 900 µL) was transferred into a new 1.5 mL reaction tube and 325 µL of precipitation buffer (HSB, 1.2 M NaCl, 0.8 M Na-citrate) and 325 µL of 2-propanol were added, the samples inverted and incubated for 10 min at RT. After centrifugation for 20 min at 12.000 rpm and 4°C the supernatant was discarded, the pellets were

washed two times with 70 % ethanol and afterwards dried at RT. The pellets were dissolved in 20-60 μ L water (ultra-pure).

cDNA synthesis

RNA samples were treated with DNase (DNase I, RNase free; 1U/ μ l, 1000U). The 10 μ l solution contained 0.5-1 μ g total RNA, 1 μ l of DNase buffer (Buffer DNase I + MgCl₂; 10X reaction buffer) and 1 μ l of DNase containing solution. The reaction mixture was then incubated at 37°C for 30 min followed by adding 1 μ l of 25mM EDTA. The mixture was then incubated at 65°C for 10 min.

cDNA synthesis was performed by adding 0.2 μ l of 100 μ M oligo dT primers and 1 μ l of 200 μ M random monomer to the reaction solution. The mixture was then incubated at 70°C for 10 min. 4 μ l RT buffer (5X reaction buffer for reverse transcriptase), 2 μ l of 10 mM dNTPs, 0.3 μ l Reverse Transcriptase (RevertAid H Minus Reverse Transcriptase; 200 U/ μ l, 10000 U) and 1.5 μ l H₂O were added and the solution was incubated at 42°C for 70 min and finally at 70°C for 10 min.

Quantitative Realtime -PCR (qRT-PCR)

For quantification of cDNA qRT-PCR was performed and fluorescence intensity was measured with the iCycler from BioRad. Reaction mix and cycler protocol are presented in table 2.37 and table 2.38. Calculations were performed using the $\Delta\Delta$ Ct method (Livak and Schmittgen, 2001).

Table 2.37 : Standard reaction mix for qRT-PCR using biolione taq polymerase. Stock component as well as the volume for a 25 μ l reaction are presented.

Stock component	Volume in a 25 μ l reaction
10X NH ₄ reaction buffer	2.5 μ l
MgCl ₂ 50 mM	1 μ l
dNTPs 40 mM (10 mM each)	0.25 μ l
F and R primers (each 4 mM)	2.5 μ l
Sybr Green (1/1000)	0.25 μ l
Flourescein (1 mM)	0.25 μ l
Biotaq DNA polymerase (2500 U)	0.05 μ l
cDNA template (~0.05 μ g)	1 μ l

Table 2.38 : Program of qRT-PCR cycler using bioline taq polymerase. Cycle step, temperature and cycle numbers are presented.

Cycle step and repeats	Temperature and duration	Cycles
Initial denaturation	95°C, 90 sec	1
Denaturation	95°C, 20 sec	39
Annealing	55°C, 20 sec	

Extension	72°C, 40 sec	
Final extension	72°C, 4 min	1
Generation of melt curve	95°C, 1 min	1
	55°C, 1min	1
	55°C, 10 sec (+0.5°C/cycle)	81

2.2.5 PAMP associated assays

Root growth inhibition assay

Sterilized seeds were put on square ATM plates and grown vertically under long day conditions. On day seven plants were transferred on ATM plates either lacking or containing 100nM flg22. Location of main root was marked and plants were grown upright in the long day chamber for an additional five days. Subsequently, pictures were taken and root length was measured using the length measurement tool in Image J.

PAMP induction assay for gene expression

Roughly 20 sterile seeds were grown fully immersed (4 ml / well) in 24 well plates in liquid AT media containing 0.5% sucrose. After 9 days of growth under short day conditions (8 h day/14 h night) media was replaced. On day 10 half of the media was removed and fresh media added containing or lacking 150 nM flg22. After 1.5h plants were harvested and quick frozen for subsequent RNA extraction.

ROS-burst assay

Plants were grown under short day conditions (8 h day/14 h night) for four weeks on peat substrate. Leaf discs were punched out and transferred into a 96 well plate containing 100 µl sterile water. The plate was sealed and put in the dark overnight. Next, water was replaced with 50 µl of a HRP (horse radish peroxidase) and luminol containing mixture (table 2.39). Shortly before the plate was placed into the reader, 100 nM flg22 or buffer only was added to each well. Measurements of relative light units were taken each minute for 1 h using a luminometer (Centro X³ LB920, Berthold Technologies).

Table 2.39 : Reactive oxygen species detection mix. Ingredients and amounts including end concentration are presented for a master mix of 6ml.

Content	Amount (end concentration)
Horse radish peroxidase (1 mg/ml)	6µl (10 µg/ml)
Luminol (17 mg/ml)	6µl (17 µg/ml)

Fill up to 6ml using H ₂ O	-
---------------------------------------	---

Callose deposition

Four week old Col-0 wild type plants grown under short day conditions (8h days/ 16h night) were infiltrated with bacterial suspensions of an OD₆₀₀=0.2. Twenty four hours after infiltration, the leaves were de-stained using 100% ethanol for 4-6h under constant agitation. Next, the solution was replaced with 70% ethanol and left overnight again with agitation. The ethanol was replaced with callose staining buffer containing 0.01 % (w/v) aniline blue, and incubated overnight at room temperature, in the dark. Leaves were placed on glass slides and callose deposition was analyzed by using an ultraviolet epifluorescence microscope. Microscopic images were saved in JPEG format. The numbers of bright spots (corresponding to callose deposits) per microscopic field in the photograph were counted using Image J software.

2.2.6 *In situ* hybridization on *Meloidogyne sp.*

DIG labeled probe generation for *In situ* hybridization

Probes were generated using the standard PCR amplification protocol of Phusion polymerase (New England Biolabs). Firstly, PCR using non-tagged dNTPs was performed using plasmid DNA as a template. Primer dimers were removed from the PCR product using the NucleoSpin Gel and PCR Clean-up Kit, following the manufacturer's instructions (Macherey-Nagel). The PCR product was then used as a template for Asymmetric PCR (one-primer PCR) that incorporated digoxigenin (dig)-labeled dUTP into the product. An example reaction is presented in table 2.40.

Table 2.40 : Phusion polymerase mix to amplify DIG-labeled DNA probes. Content and volume in a 40µl reaction are shown.

Content	Volume in µl
Buffer	8
DIG-dNTPs	4
Primer	10
Template (minimum 50ng)	2
Phusion polymerase	0.2

Water	15.8
Total	40

Probes were precipitated adding 1/10 of 3M sodium acetate and 3x the volume of 100% ethanol. Subsequently, mixture was kept at -80°C for at least 1h. Probes were pelleted and re-suspended in 200 µl hybridization buffer for 10 min at 37°C. Probes were subsequently kept at -20°C for storage.

In situ* hybridization on *Meloidogyne sp. (de Boer et al., 1998)

On day 1 hatched nematodes (3 days old) were pelleted. This and all subsequent pellet steps were performed using the microcentrifuge at 13,300 rpm. The juveniles were fixed in 1ml of 3.7 % formaldehyde in 1x PBS solution and kept at 4°C over night. The next day nematodes were pelleted and all but 50-100 µl of the liquid was removed. The pellet was resuspended in 1x PBS and the nematodes were transferred onto a glass slide. Nematodes were then cut with a vibrating razor blade for 30 seconds until most of the juveniles were seen to be cut in half. Nematodes halves were collected in 1x PBS and washed twice more with 1ml PBS: Subsequently, pelleted nematodes were incubated in 1x PBS containing 1mg/ml proteinase K at 37°C for 1h under constant agitation. Next, nematodes were washed three times with 1ml of 1x PBS and then pelleted nematodes were stored at -80°C for 15 minutes. After storage at -80°C the pellet was re-suspended in cold methanol (-80°C) via vortexing and kept at room temperature for 2 minutes. Methanol was removed and nematodes re-suspended in cold acetone (-80°C) and stored at -80°C for 15 minutes. The acetone was removed and the pellet washed with preheated 500 µl hybridization buffer (50°C). Next, nematodes were pre-hybridized in 500 µl hybridization buffer (50°C) for 30 min at 50°C under constant agitation. Subsequently, hybridization buffer was removed and 100 µl hybridization buffer containing denatured probes was added to nematodes. Probes are denatured by keeping them at 100°C for 5 minutes and 3 min on ice. Hybridization was performed over night at 40°C under agitation. The next day nematodes were washed with 1 ml 4x SSC and 0.1% SDS at room temperature under agitation for 10 minutes. Next, a washing step with 1ml 0.1 SSC with 0.1 % SDS at 50°C with shaking was performed. Then, nematodes were washed with 1ml 1x maleic acid buffer for 30 seconds. After that, nematodes were incubated at 37°C for 30 minutes in 1x Boeringer blocking reagent in 1x maleic acid buffer. After removing the blocking solution, nematodes were incubated for 3h in 1ml of anti-body solution which contained 1x Boeringer blocking reagent in 1x maleic acid buffer with the addition of 1:500 anti-DIG antibody at 37°C. After the antibody solution

was removed, nematodes were washed three times for 15 minutes in 1ml of 1x maleic acid buffer at 37°C. Nematodes were washed once in 1 ml alkaline phosphatase buffer. Signal was revealed in 1ml of alkaline phosphatase buffer over night at 4°C by adding 50 mg /ml BCIP and 77mg /ml NBT. Staining was observed using a light microscope.

2.2.7 Subcellular localization of fluorescence tagged proteins

Fluorescence tagged proteins expressed in Arabidopsis were analyzed using confocal microscope Leica SP5-DM6000 (Leica GmbH). Leaf discs from fully expanded leaves of four week old plants were used for analysis. Appropriate filter set was used to distinguish between the different fluorophores and auto-fluorescence. Z-stack pictures were taken to obtain a better view on subcellular localization. Pictures were acquired and analyzed using Leica's LAS - AF and LASAF lite.

Table 2.41 : Excitation and detection values in nm for YFP, GFP and autofluorescence for fluorescence microscopy. The excitation and detection wavelengths of YFP, GFP, and the autofluorescence of chloroplast are presented.

Fluorophore/signal	Excitation in nm	Detection in nm
YFP	514	525-600
GFP	488	500-540
Autofluorescence of chloroplasts	561	680-700

2.2.8 Protein analysis using Western blot

Co-immunoprecipitation

Frozen leaf tissue from Arabidopsis was ground to powder. The leaf powder was extracted by adding Co-IP extraction buffer in ratio 2:1 (buffer: powder). Samples were centrifuged using FiberLite® F13-14x50cy fixed angle rotor at 10,000 rpm at for 15 minutes and clear supernatants were transferred into 2ml Eppendorf tubes. Immunoprecipitation was performed by adding 10 ml of GFP-trap M beads (Chromotec) to 2ml of supernatant and incubating the samples for 2 hours at 4 °C on a rotation wheel. The magnetic beads were separated from the solution by using magnetic rack. The purified beads were washed 3 more times with co immunoprecipitation washing buffer before adding 45ml of 1x Laemmli buffer containing 5% β-mercaptoethanol. Beads were boiled at 95 °C for 8 minutes. The samples were loaded directly onto SDS-PAGE gels or stored at -20 C.

SDS-polyacrylamide gel electrophoresis (SDS-PAGE)

In this study, separating gels used ranging from 4 to 20 % and were overlaid with 4% stacking gels. In short, the preferred separating gels were poured between 1.5mm glass slide and then overlaid with Isopropanol. When the separating gels were completely solidified, isopropanol was removed and a 4% stacking gel was poured on top. Combs suitable for 1.5mm spaced glass was inserted and the gel was left at room temperature until completely polymerize. Polymerized SDS-PAGE gels can be either used directly or wrapped with wet towel papers in a box and stored at 4 degree. SDS-PAGE-gels were placed in Mini Protean tetra cell (BioRad) chambers and loaded with 1xSDS-running buffer according to the manufacturer protocol. The combs were removed and samples were loaded. Gels were run at 100 to 160 Volts for approximately 1-2 hours or until the Page ladder reach the bottom of the gel.

Western blot analysis

The samples from finished SDS-PAGE gel were blotted onto activated polyvinylidene fluoride membrane covered by 3 layers of Whatmann paper wetted with 1x transfer buffer in semi blot chamber (homemade, University of Göttingen). The transfers of the protein were carried out for 90 minutes at 1mA/cm². After proteins were successfully transferred, the membranes were washed briefly in 1x transfer buffer and blocked in 2% nonfat milk powder in TBS-T for at least 30 minutes. After blocking, the first primary antibody (αGFP) was applied and incubated at room temperature for 120 minutes or 4 °C overnight. After the first antibody incubation, the membranes were washed to remove unattached antibody with 1xTBS-T for 10 minutes at room temperature 3 times. The secondary antibodies were added and incubated for 120 minutes at room temperature. After the incubation, the secondary antibodies were removed by washing with 1xTBST for 5 minutes for 5 times. The membranes were developed by using Super Signal™ West Femto Maximum Sensitivity Substrate and chemiluminescence was visualized using the Intrac ChemoCam camera.

2.2.9 Protein interaction assays using yeast

Yeast transformation

Overnight culture of yeast strain AH109 in YPAD was sub-cultured into new YPAD media and incubated at 28 °C until the OD₆₀₀ was between 0.6 - 1.2. Yeast cells were collected and wash with sterile H₂O by centrifugation at 4000 rpm for 5 minutes at room temperature in 50 ml falcon tube. The cells were resuspended in 1 ml of water and transferred into a sterile Eppendorf

tube before briefly centrifuging at 13,000 rpm to pellet the cells. Cells were resuspended in 550 μ l of 100 mM LiAc pH 7.5 and were distributed into 11 x 50 μ l sterile tubes. Supernatant was removed by brief centrifugation followed by adding a transformation mix containing 240 μ l of 50% PEG 4000, 36 μ l of 1M LiAc pH 7,5, 25 μ l single stranded DNA and 250-500 ng of plasmid. The mixture was vortexed vigorously to resuspend the cells. Next, the mixture was incubated at 30 °C for 25 minutes with occasional shaking. Transformation was performed by heat shock. The yeast was incubated at 42 °C for 25 minutes. Subsequently, cells were centrifuged at 4000 rpm for 10 seconds and supernatant was removed. Yeast cells were resuspended in 200 μ l of sterile water. Aliquots were spread onto suitable selective drop out media. Plates were allowed to air dry and incubated at 30 °C for 3 days or until the colonies developed.

For double transformation to confirm interactions, the full length coding sequence of potential interaction candidates were amplified from either Arabidopsis root/leaf/flower cDNA and cloned into the plasmid (pGAD1) vector system using Gateway technology. Mh270 was cloned into pASII. The fish and Mh270 (bait) plasmids were co-transformed into yeast

Yeast library screening

To screen for potential interaction partners, yeast libraries containing cDNA fragments from *Arabidopsis thaliana* root and cell line were provided by Joachim Uhrig.

cDNA libraries containing fish plasmids (pGADI), were quickly thawed in a water bath at 42 °C and resuspended in YPAD for 1 hour at 30 °C 200 rpm or until the OD₆₀₀ = 1.2. The AH109 containing bait plasmid (pASII-effector candidate) was cultured overnight at 30 °C at 200 rpm in SC-W. 1.85*10⁸ yeast cells (Y187) of each library were 1.85*10⁸ yeast cells (AH109) containing the bait construct. Cell were pelleted by centrifugation and resuspended in 10 ml of YPAD containing 20% PEG6000 and transferred into a 100 ml Erlenmeyer flask. The mixture was incubated over night with 80rpm at 30°C. The next day, mixture was pelleted by centrifugation at 4000rpm for 4 minutes in 50 ml tubes and resuspended in 500ml SC –LWH containing 0.05% gelrite, 5mM 3`-AT and ampicillin. Mating efficiency was determined by spreading 10 μ l of the mixture onto SC –LW plates. Colonies for mating efficiency were observed after 2 days of incubation and after 10-14 days of incubation for interaction. Colonies developing in the interaction media were transferred on new selection plates and inserts were amplified using PCR.

3. Results

3.1 Bioinformatic screen reveals seven potential effector proteins in *M. hapla*

To discover new effector candidates a pipeline was created to identify candidates from *Meloidogyne hapla* using publically available resources (Figure 3.1). The first step was to look at the published *M. hapla* proteome (Mbeunkui et al., 2010). This publication lists 516 non redundant proteins that were identified via a bioinformatic analysis of the *M. hapla* genome and then confirmed through LC/MS analysis of *M. hapla* J2 proteins. The 516 proteins had been annotated by a BLASTp search of the Uniprot database and protein domains via a search of the Pfam22 database, which provided initial annotations that could be visually screened for potential proteins of interest. Since I was interested in novel *M. hapla* proteins, the list was first screened for proteins that were described as a “protein with unknown function”. Effectors with no conserved domain or no significant homology to anything in the database would be quite interesting pioneer effectors to study. This search provided a list of 57 candidates.

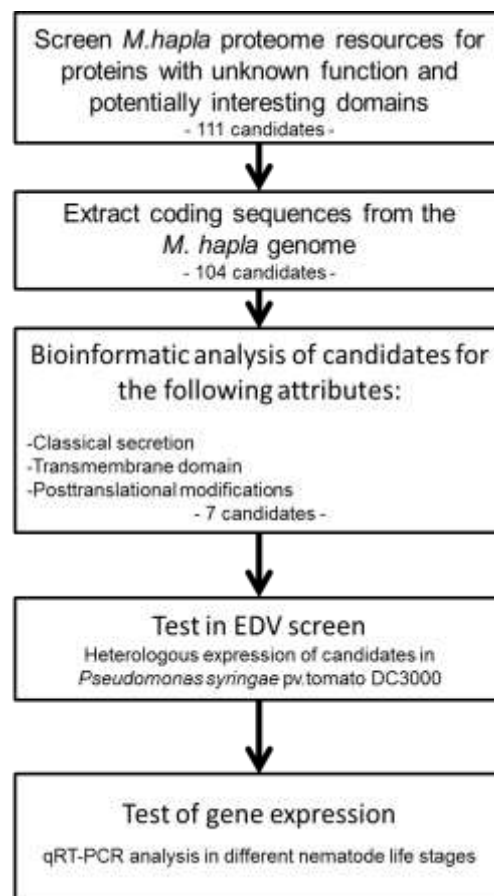


Figure 3.1 : Pipeline for the identification of potential *M.hapla* candidates for subsequent testing. Initial candidate list was taken from the *M.hapla* proteome. Subsequent extraction of full length CDS from the *M. hapla* genome followed and bioinformatics analyses revealed 7 candidates to be tested in the lab.

In order to identify new nematode effectors that affect plant immunity, the published list of proteins was also screened for candidates that contain conserved domains potentially involved in plant defense responses. This included proteins with predicted functions in the regulation of gene expression, detoxification or in binding of signaling molecules as lipids or calcium. With these criteria, I picked an additional 54 candidates, leading to 111 protein candidates in total (Supplemental table 1).

Each peptide listed in the Mbeunkui et al. (2010) paper contained the corresponding gene's contig location in the *M. hapla* genome database. Using the *M. hapla* GBrowse interface, sequence information for each protein of interest, including predicted introns and exons, could be found but for all but seven candidates. For these 7 candidates, no complete open reading frame could be found and they were excluded from further analyses.

Because nematode effectors are predicted to be secreted from the nematode, I hypothesized that nematode effectors should contain a secretory signal and no transmembrane domain. The nematode gland secretions are proteins and peptides that are released in small vesicles from the nematode stylet. SignalP, (Petersen et al., 2011) which predicts both the probability of a classical secretion signal and the chance of a signal anchor, was used to predict the presence of a secretion peptide in the candidates. Only candidates that presented both a classical secretion signal with D-cutoff value higher than 0.450 and which had no predicted signal anchor were kept for further analyses. Additionally, a TMHMM algorithm (Krogh et al., 2001) which predicts potential transmembrane domains, was also used to remove candidates with a predicted transmembrane domain in the mature protein. Twenty eight protein sequences with predicted secretion signals and no transmembrane domains remained for further analysis.

Candidates were going to be expressed in a bacterial system, and production of eukaryotic proteins can be hindered by the lack of correct post-translational modifications in bacteria (Tokmakov et al., 2012). Proteins can undergo multiple post-translational modifications, and after phosphorylation, glycosylation and acetylation are the two most common post-translational modifications (Khoury et al., 2011). In fact, some effectors need appropriate glycosylation to be functional (Chen et al., 2014). First, GlycoEP (Chauhan et al., 2013) was used to check for potential eukaryotic glycosylation sites with a standard SVM threshold of 0.0. Seven candidates did not have predicted glycosylated sites, and they were kept for further analysis. Using the publically available tool from the ExPASy Bioinformatics Research Portal, an additional search was performed on the seven remaining candidates to exclude proteins with predicted acetylated sites. NetAcet was used with default setting for prediction of prediction of

N-terminal acetylation sites (Kierner et al., 2005), and none of the seven proteins were predicted to be acetylated.

From the remaining seven candidates three were originated from the list of “unknown proteins” while four came from the list of potentially interesting candidates with homology to known proteins. To retrieve more specific and potentially newly published information about the candidates, a new BLASTp search of the non-redundant protein database in NCBI was performed. The BLASTp analysis of the protein sequences of the remaining candidates showed that six out of the seven candidates had similarity to proteins in other nematodes. Interestingly, five of the candidates had similarity to proteins in animal parasitic nematodes (Table 3.1). Two of the candidates had low amino acid identity (31 and 32% respectively) to *Pristionchus pacificus*, which is a free living nematode, and the plant burrowing nematode *Radopholous similis*.

Table 3.1 : List of remaining candidates after all bioinformatic analyses were performed. Final list of candidates that were chosen for subsequent testing. Designation as well as highest hit with pairwise identity found in an NCBI protein BLAST using standard settings including E-Values are presented. Detectable conserved domains are also shown.

Designation	Length in bp	Highest similarity NCBI Protein Blast	Identity	E-Value	Domain
Mh7	381	Transthyretin-like family protein [<i>Ancylostoma duodenale</i>]	61%	1,00E-51	DUF290
Mh222	519	Chondroitin proteoglycan 3 [<i>Ascaris suum</i>]	41%	3,00E-21	-
Mh247	1050	No significant similarity found	-	-	-
Mh257	801	Hypothetical protein PRIPAC_3335 [<i>Pristionchus pacificus</i>]	31%	9,00E-06	-
Mh265	645	Fatty acid retinoid binding protein [<i>Ancylostoma duodenale</i>]	32%	0.10	-
Mh270	465	Transthyretin-like protein 2 precursor [<i>Radopholus similis</i>]	70%	8,00E-60	DUF290
Mh309	954	Reticulocalbin-2 [<i>Toxocara canis</i>]	50%	9,00E-101	Ef-Hand 7

Mh7 and Mh270 show a similarity to transthyretin-like proteins in other nematodes and contain a conserved DUF-290 (domain of unknown function 290). These proteins are nematode specific and show a higher presence in parasitic nematodes with a focus on the parasitic life stages (Jacob et al., 2007). So far, the potential involvement of these proteins in nematode-host interaction remains unknown.

Mh222 displays a 41% similarity to a chondroitin proteoglycan in the animal parasitic nematode *Ascaris suum*. In general, chondroitin proteoglycans have a core protein with one or more covalently attached chondroitin chains. They are found in many organisms, including *C. elegans*, where they play a role in embryonic development and vulval morphogenesis (Olson et al., 2006).

Candidate Mh247 revealed no significant similarity to other proteins in the NCBI database.

A hypothetical protein from the free-living nematodes *Pristionchus pacificus* was found to be the most similar protein to Mh257. The protein with the second highest homology was found in the free living nematode *Caenorhabditis remanei*.

Mh265 did not show significant similarity to other known protein. However, it is noted that the top hit showed low homology (32% identity of 88 aa, E=0.1) to a fatty-acid retinoid (FAR) binding protein of *Ancylostomona duodenale*. This is interesting because FAR proteins have been shown to be involved in both the infection of cyst (Prior et al., 2001) and root-knot nematodes (Iberkleid et al., 2015).

The last candidate, Mh309, contains an Ef-hand domain and presents significant identity with reticulocabin-2 from the dog roundworm *Toxocara canis*. These proteins are known to bind calcium ions which could suggest a role in affecting calcium dependent signaling pathways. In *C.elegans* reticulocalbin was shown to be associated with neuronal activity (Hobert, 2013).

3.2 Two effector candidates are able to increase virulence of *Pst* DC3000 on *Arabidopsis thaliana*

In order to functionally characterize the effector candidates, an “Effector Detector Vector” (EDV) system was employed in which effectors are delivered into plants cells via the type three secretion system of *Pseudomonas syringae*. pv *tomato* DC3000 (*Pst* DC3000). This screen was adapted for nematode effectors as method to quickly screen the large list of nematode effectors from section 3.1 for possible effects on plant immunity. Effectors which help significantly enhance bacterial growth compared to the control, were kept for further studies.

The full length coding sequences of effector candidates, minus their signal peptides, were amplified from *M. hapla* cDNA and cloned into the pEDV6 vector, which contains a signal to direct bacterial secretion of the candidate via the type three secretion system. The constructs were introduced into *Pst* DC3000 harboring a luciferase operon - luxCDABE (*Pst-LUX*) which allows the estimation of bacterial abundance by measuring the bacterial bioluminescence (light units/fresh weight). Successful bacteria transformation was confirmed by colony PCR, and no influence on bacterial growth on rich growth media could be observed due to the presence of the transgene (data not shown).

The effector *ATR13^{Emco5}* from *Hyaloperonospora arabidopsidis* has been shown to increase the virulence of *Pst-LUX* in the EDV system (Fabro et al 2011). *Pst-LUX* expressing either pEDV6-*ATR13^{Emco5}* or pEDV6-*YFP* (control) were spray inoculated onto Col-0 plants and the bioluminescence (light units/fresh weight) was measured at 3 dpi. *ATR13^{Emco5}* significantly

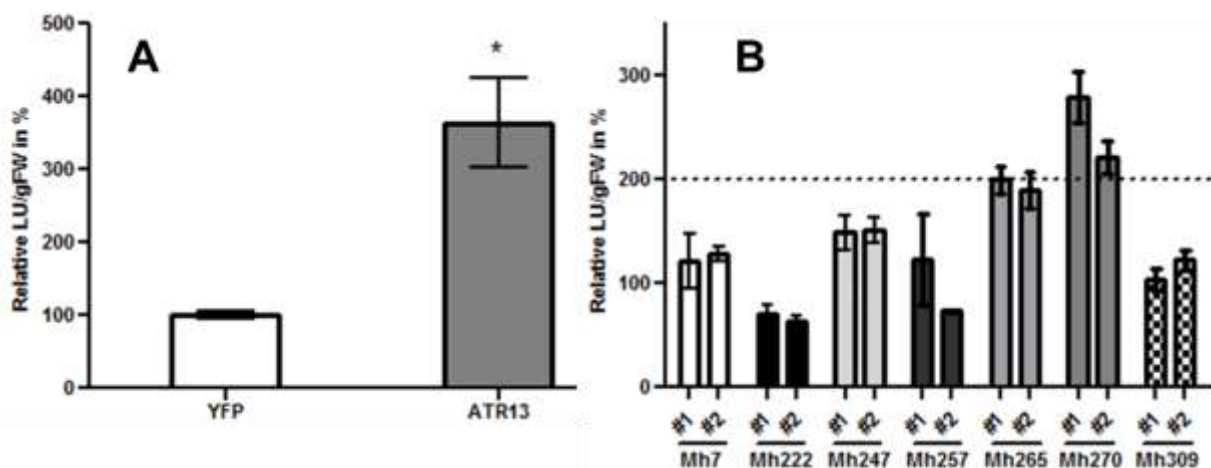


Figure 3.2 : ATR13 and some nematode effector candidates can promote *Pst-LUX* growth in planta. **A:** *Pst-LUX* delivering YFP or ATR13 were spray inoculated onto 4 week old Col-0 plants. *Pst-LUX* growth was measured at 3dpi as bioluminescence (light units / g fresh weight), and converted to a percentage relative to the LU / g fresh weight of *Pst-LUX* YFP at 3 dpi. Bars present the mean +/- SEM of two independent experiments (n=16). Asterisk indicate a significant difference using student t-test (p<0.05). **B:** Summary of *Pst-LUX* growth upon delivery of effector candidates into Col-0. Bioluminescence (LU/ g fresh weight) was measured and then converted to a percentage relative to the bioluminescence of the YFP control at 3 dpi. The experiment was performed twice, as shown. The dotted line shows the set threshold for candidates significantly enhancing bacterial growth in the plants. Error bars represent the SEM (n=6-12).

increased bacterial growth *in planta* compared to *YFP* in two independent experiments (Figure 3.2 A). Due to variability in the amount of bioluminescence that is produced by the bacteria at 3 dpi between experiments, we defined positive EDV effector candidates as those which could enhance bacterial growth over 200% in comparison to *YFP* control in each experiment.

Two independent clones of *Pst-LUX* expressing candidate constructs [pEDV6-*Mh7*, pEDV6-*Mh222*, pEDV6-*Mh247*, pEDV6-*Mh257*, pEDV6-*Mh265*, pEDV6-*Mh270*, and pEDV6-*Mh309*] were spray inoculated on Col-0 plants and bioluminescence (light units/fresh weight) was measured at three days post inoculation. Only *Mh265* and *Mh270* could increase bacterial growth *in planta* over the set threshold of 200% increase in bioluminescence at 3 dpi (Figure 3.2.B).

For *Pst-LUX* expressing pEDV6-*Mh265* and pEDV6-*Mh270*, the level of bacterial bioluminescence was compared to the bacterial numbers (colony forming units (cfu)/cm²) *in planta* at 3 dpi. *Pst-LUX* expressing pEDV6-*Mh265* and pEDV6-*Mh270* exhibited higher numbers of bacteria at 3dpi (Figure 3.3 A and B). This confirmed that the increase in bacterial luminescence correlated to an increase in the bacterial population.

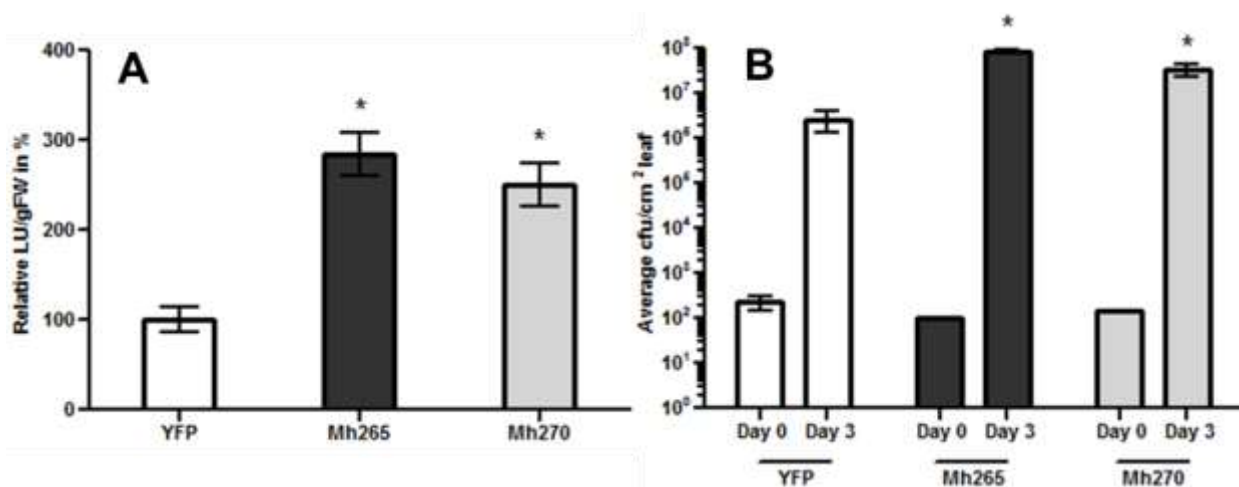


Figure 3.3 : Mh265 and Mh270 can increase *Pst-LUX* bioluminescence and this correlates with enhanced bacterial populations *in planta*. **A:** Col-0 plants were spray inoculated with a bacterial suspension of *Pst-LUX* (OD₆₀₀=0.2) expressing YFP, Mh265, or Mh270. Bioluminescence (LU / g fresh weight) was measured at 3dpi. The bioluminescence of the YFP control at 3 dpi is set to 100%. Bars present the mean +/- SEM (n=15). Asterisk indicate a significant difference to YFP control using student t-test (p<0.05). **B:** Transgenic *Pst-LUX* expressing YFP, Mh265, or Mh270 were infiltrated (OD₆₀₀=0.0001) into fully expanded leaves of 4 week old Col-0 plants. Bacteria were extracted from leaf disks at 1h and 3 days after infiltration to determine the number of bacteria in the plant. Bars present the mean CFU / cm² of three biological replicates at 0 and 3 dpi. Error bars present SEM. Asterisks indicate a significant difference at 3 dpi as calculated by student t-test (p<0.05).

3.3 Mh265 and Mh270 exhibit enhanced gene expression in the pre- and early infection stages of *Meloidogyne hapla*

Because genes involved in pathogenicity may be upregulated during the parasitic life stages of the nematode, qRT-PCR was performed to measure gene expression of *Mh265* and *Mh270* in egg, J2 and parasitic nematodes (i.e. gall tissue from infected Col-0 wild type plants at 6, 10, and 14dpi) (Figure 3.4). Acid fuchsin staining of roots revealed that at 6 dpi J2 were still migrating or establishing a feeding site while at 14 dpi most nematodes were sedentary and had started to moult (Supplemental figure 1). For the qRT-PCR analysis, the transcript levels were normalized to the geometric mean of the expression of the reference genes *Mh18S* and *MhActin*. Expression analysis showed that compared to the egg stage, there is enhanced gene expression in the J2 and in nematodes at 6 dpi for both *Mh265* and *Mh270*. At later stages of infection (10 and 14 dpi), the gene expression was similar to that of the egg stage. These results show that relative expression of the candidate genes is higher during the pre-infective (J2) and early infection stages.

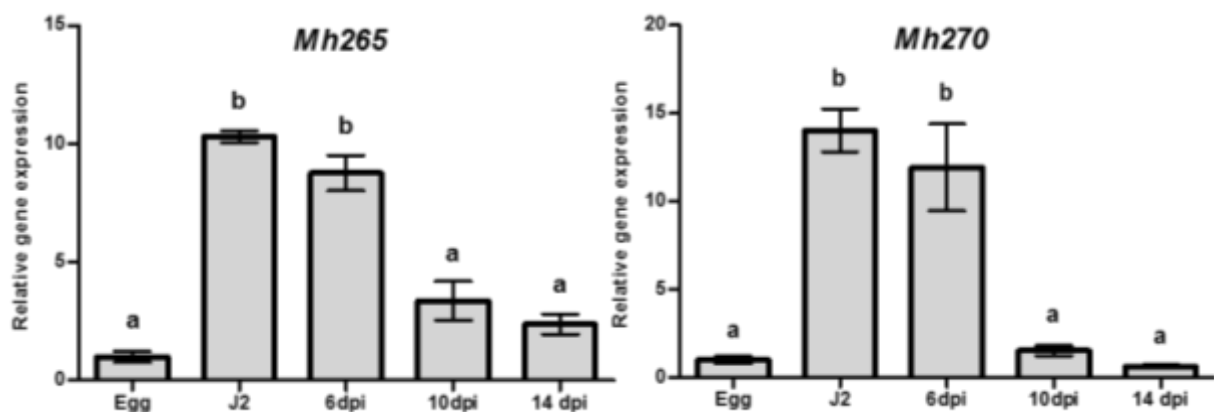


Figure 3.4 : qRT-PCR expression analysis of Mh265 and Mh270 over different life stages of *M. hapla*. The relative transcript abundance for Mh265 and Mh270 was determined for *M. hapla* eggs and pre-parasitic J2, and for parasitic *M. hapla* in *Arabidopsis* roots. For the parasitic nematodes, Col-0 was infected with J2 and gall tissue was collected at 6, 10, and 14 dpi. The transcripts were normalized using the geometric mean of the expression levels of two endogenous reference genes, *Mh18S* and *MhActin*. Each reaction was done in triplicate on two independent biological replicates. The bars represent the arithmetic mean of two independent samples \pm SEM (n=2). Expression in egg stage was set to 1. Letters indicate a significant difference in between groups using one-way ANOVA analysis ($p < 0.05$). J2= preparasitic Stage 2 juvenile, dpi = days post infection.

Both Mh265 and Mh270 have successfully passed through the initial stages of the effector candidate identification pipeline (EDV screen and qRT-PCR in nematode life-stages). Due to limitations in time, I decided to focus solely on characterizing Mh270, while Mh265 was further characterized by another member of the lab.

3.4 *In situ* localization of candidate effector *Mh270* shows labelling of the amphid region of the nematode

A potential effector is likely secreted from the nematode into the plant. Because the stylet is connected to the esophageal glands, transcripts that localize to glands are thought to encode proteins that are secreted via the stylet. However, the nematode contains many secretory organs such as the cuticle, amphids, or anus of the nematode, and secreted proteins may also be produced in these organs. To test where *Mh270* transcript hybridizes in the nematode juveniles, digoxigenin (DIG) labeled DNA probes were generated via one primer PCR spanning the full coding sequence of *Mh270*. Additionally, DNA probes for *Mi-PG-1*, a polygalacturonase, which had been previously shown to show localize to the subventral gland of *M. incognita*, was also made (Danchin et al., 2013). Hybridization of the probes on J2 nematodes was visualized by using an anti-DIG antibody coupled to alkaline phosphatase which generates a blue precipitate when NBT (nitro-blue tetrazolium chloride) and BCIP (5-bromo-4-chloro-3'-indolyphosphate p-toluidine salt) are present.

The anti-sense probe for *Mi-PG1* intensely labeled the subventral gland of *M. incognita* juvenile, confirming the previously published report (Danchin et al., 2013). The anti-sense

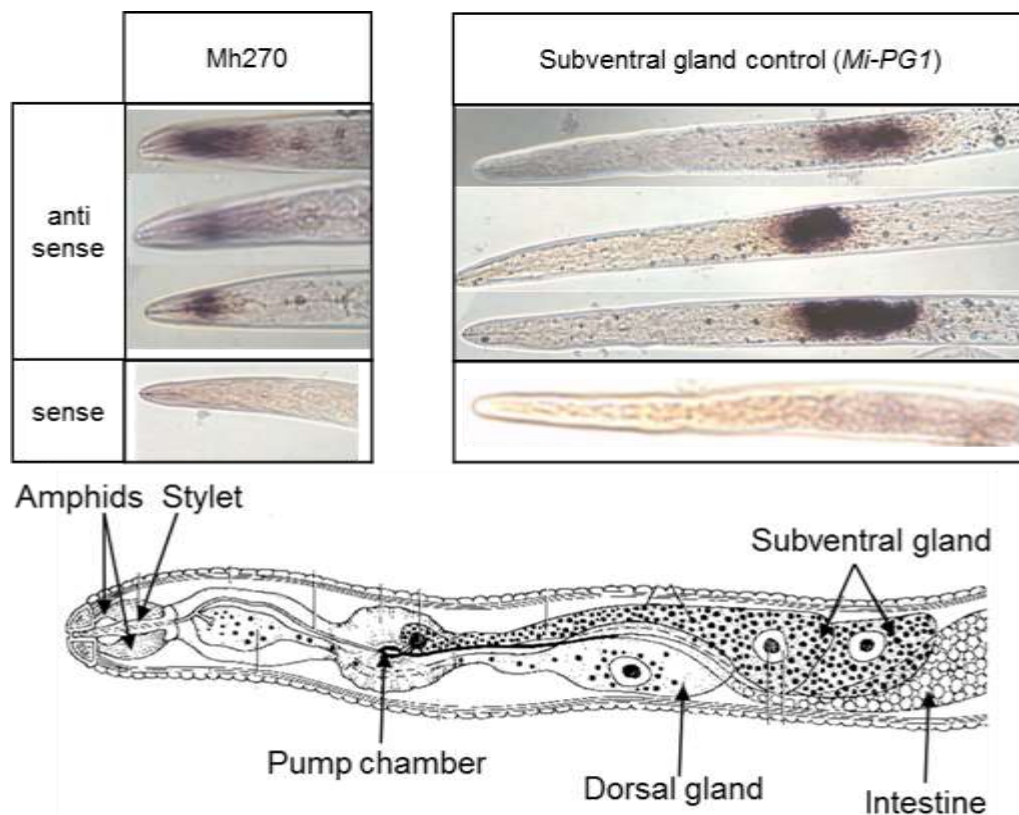


Figure 3.5: *In situ* hybridization shows localization of *Mh270* and *Mi-PG1* in pre- parasitic juveniles. Digoxigenin labelled DNA probes for *Mh270* and *Mi-PG1* were hybridized to fixed juveniles of *M. hapla* and *M. incognita* for *Mh270* and *Mi-PG1*, respectively. Antisense probe staining shows target transcript presence. Sense probe presents potential background stain. Cartoon presents the RKN anatomy with arrows indicating organs associated with ingestion and secretion (modified from Hussey, 1989).

probe of candidate *Mh270* hybridized to a head region of the nematode where the chemosensory organs called amphids are located (Figure 3.5). The sense probes for *Mi-PG1* and *Mh270* sense probe did not show any non-specific hybridization to the whole mount J2.

3.5 *Mh270* expression in plants does not affect flg22-induced PTI responses

Upon recognition of conserved PAMPs, PTI is elicited in plants. Although our knowledge of the molecular mechanisms of PTI is relatively limited, we have several signaling outputs that can be measured after PAMP perception. Typical readouts of PTI in leaves include measuring elicitor induced oxidative burst, the accumulation of callose deposits, and defense marker gene expression. This chapter will focus on the potential effect of *Mh270* expression *in planta* on these PTI outputs after induction by the elicitor flg22.

Mh270 (coding sequence minus the signal peptide) under the control of the CaMV-35S promoter was introduced to Col-0 plants. Four homozygous T3 lines were tested for their expression of *Mh270* by qRT-PCR. The lines *Mh270* 13-2 and *Mh270* 16-3 were chosen for further experiments due to their relatively high expression of *Mh270* (Figure 3.6). None of the homozygous lines showed an obvious altered growth phenotype in comparison to Col-0 (data not shown).

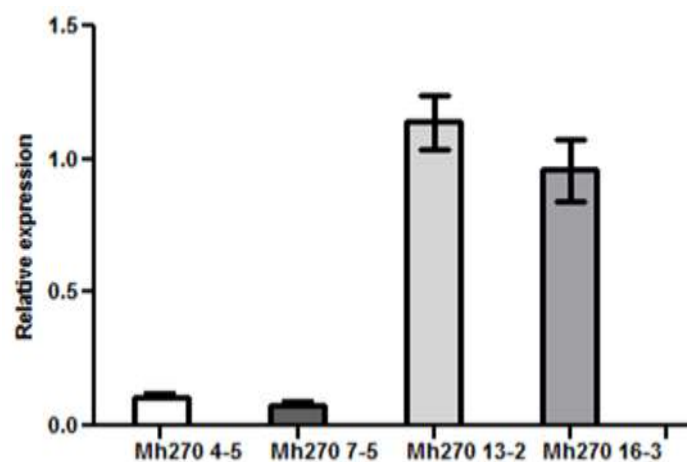


Figure 3.6 : Homozygous, stable transgenic Arabidopsis lines express Mh270. qRT-PCR was performed on four T3, homozygous Arabidopsis lines, each with single *Mh270* insertion. The expression of *Mh270* transgene was determined in relation to the Arabidopsis housekeeping gene *AtUbg5*. Bars represent the mean of two independent biological replicates \pm SEM (n=2).

3.5.1 The early PAMP response ROS-burst is not altered in *Mh270* transgenic plants

Shortly after the recognition of PAMPS such as flg22, an oxidative-burst is triggered in the apoplastic space of plants, largely due to the activity of the NADPH oxidases (Torres et al., 2006). To test whether *Mh270* expression affects elicitor-induced production of reactive oxygen species (ROS), leaf discs of Col-0 and transgenic plants were challenged with or without 100nM flg22 and the subsequent ROS-bursts were measured via a luminol based assay. The buffer-only treatments did not induce ROS production in either Col-0 or *Mh270* transgenic lines at any time point. ROS production in the flg22-treated Col-0 leaf disks peaked at 15 min after elicitor treatment and then dropped to basal levels within 25 minutes. Leaf disks from transgenic plants expressing *Mh270* exhibited no differences in the amplitude and duration of the flg22-induced ROS burst compared to Col-0 (Figure 3.7).

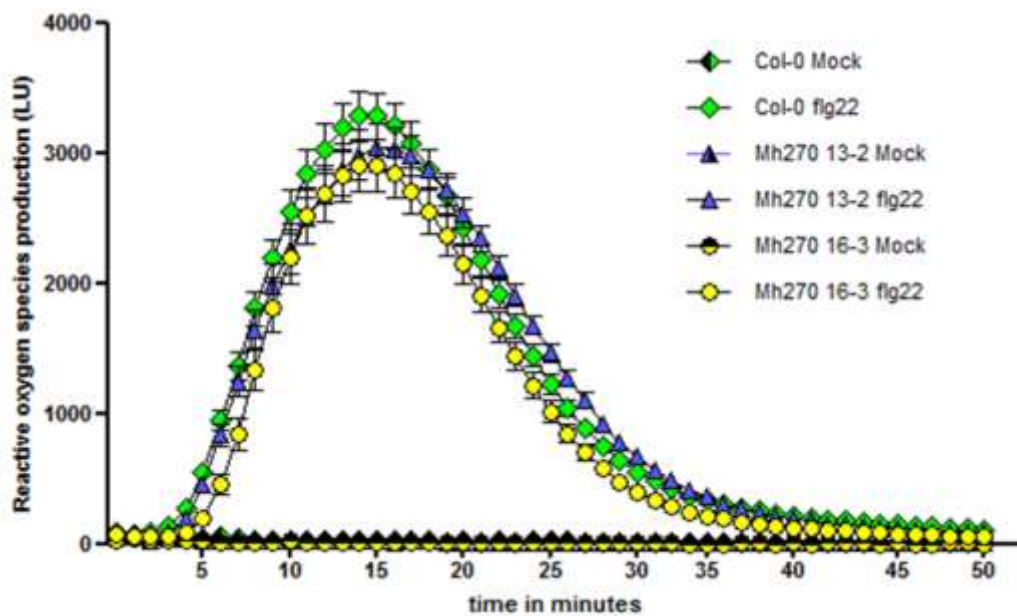


Figure 3.7 Flg22-induced ROS production is not affected in *Mh270* transgenic lines. Leaf discs from Col-0 and *Mh270* transgenic lines were incubated in buffer with and without 100nM flg22. ROS production was measured as relative light units in a time course, with measurements taken every minute for 50 minutes. n=24 for flg22 treated samples, n = 3 for buffer only samples. Values are mean +/- SEM. Experiment was repeated four times with similar results.

3.5.2 Mh270 transgenic lines do not show altered flg22-induced gene expression

Next, *Mh270* transgenic plants were examined for altered PTI-marker gene expression after flg22 treatment. *WRKY22*, *WRKY33*, *WRKY53*, *GST1*, *FRK1*, and *CYP81F2* have been well-studied and their expression can be induced in Col-0 leaves usually within 1-2 hours after flg22 treatment (Asai et al., 2002; Clay et al., 2009; Jacobs et al., 2011). Using qRT-PCR gene expression analysis, it was observed that the basal expression of these marker genes was not affected in the *Mh270* transgenic plants (Figure 3.8). After 1.5 h treatment of flg22, gene expression analysis showed no significant differences between Col-0 and the two *Mh270* transgenic lines for 6 of the PTI-marker genes (*WRKY22*, *WRKY53*, *GST1*, *FRK1*, and *CYP81F2*). Although *Mh270* 16-3 exhibited slighter lower flg22-induced expression of *WRKY33*, this reduced expression was only seen in this one transgenic lines and, thus, not

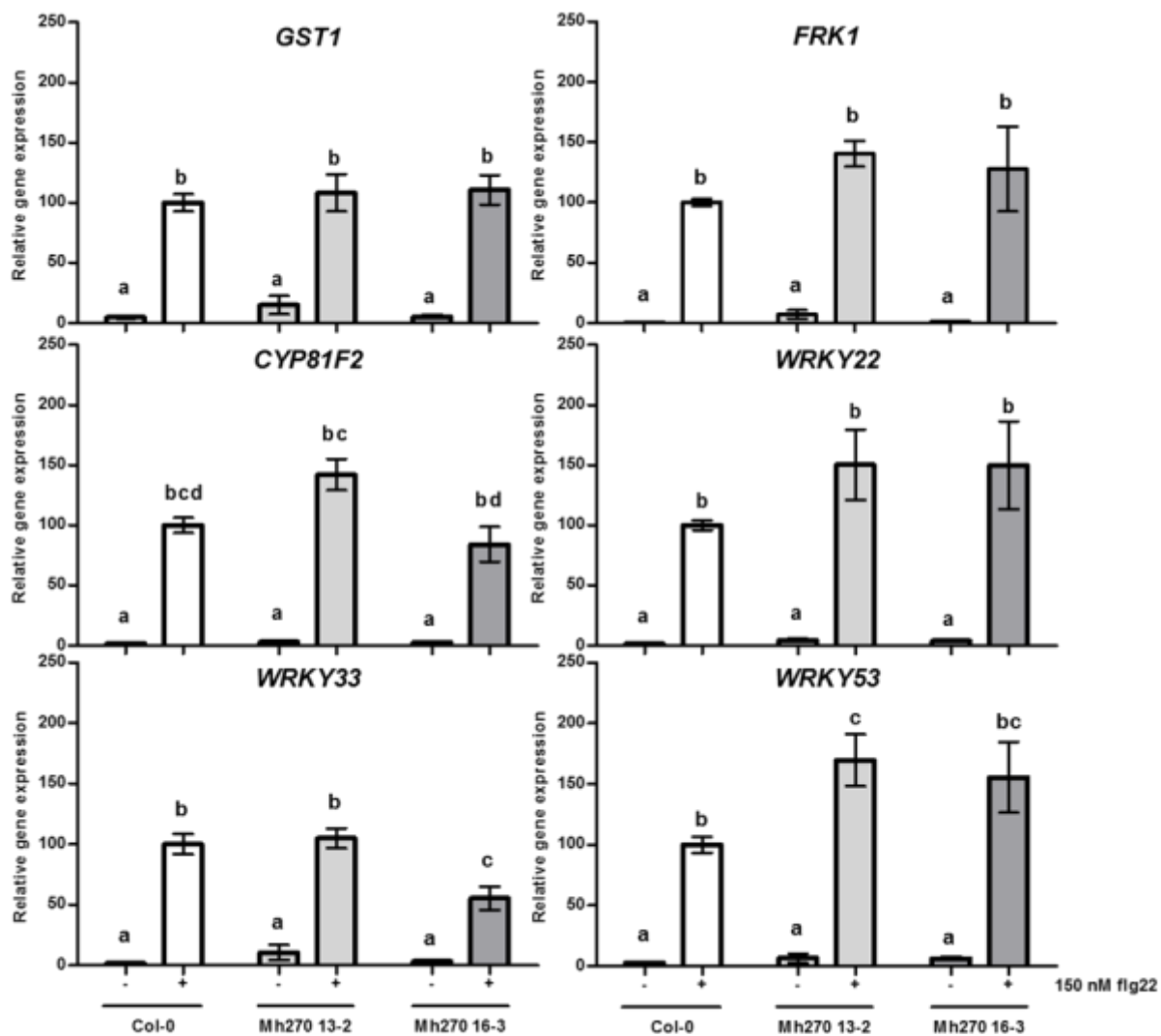


Figure 3.8 : Flg22 responsive genes were expressed at similar levels in Col-0 and transgenic M270 lines. Transcript abundance for the PTI marker genes was determined via qRT-PCR in 10 day old seedlings flooded in buffer with or without 150 nM flg2 for 1.5 hr. *AtUbg5* was used as the reference gene. Expression was set relative to flg22-treated Col-0. Bars represent the arithmetic mean of 6 biological replicates +/-SEM (n=6). Letters indicate a significant difference between groups calculated using two-way ANOVA ($p < 0.05$)

reproducible between independent transgenic lines

3.5.3 Flg22-induced root growth inhibition is not affected in *Mh270* transgenic plants

Root growth inhibition is another flg22-induced response (Ranf et al., 2011). If *Mh270* can suppress PTI, it may also suppress elicitor-induced root growth inhibition. To test if *Mh270* expression in plants could alter this response, seven day old *Arabidopsis* seedlings were placed on media with and without 100 nM flg22. After five days of growth on the new media, the length of the primary roots was measured. On media without flg22, root lengths between Col-0 and the *Mh270* lines were not significantly different, confirming that *Mh270* expression in plants does not alter root growth. When Col-0 and transgenic *Mh270* (13-2 and 16-3) seedlings were grown on flg22, both showed similar levels of pronounced growth retardation (Figure 3.9).

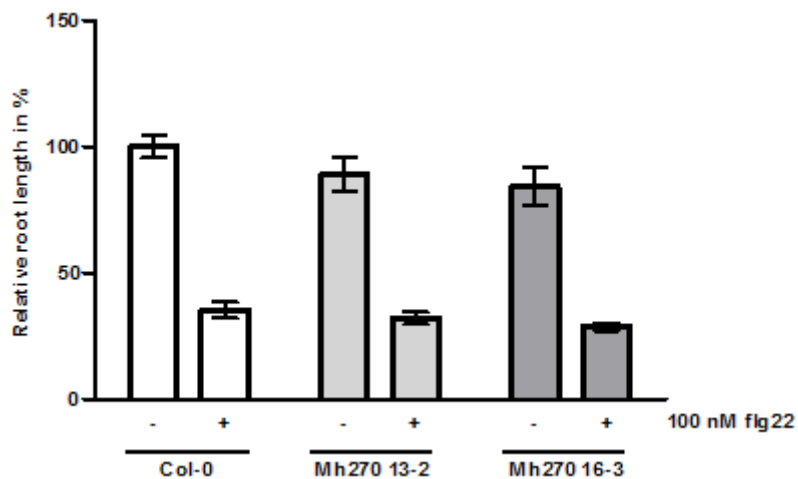


Figure 3.9: Flg22-induced root growth inhibition is the same in Col-0 and *Mh270* transgenic lines. Seven day old plants were transferred to AT media with and without 100nM flg22. Five days later, the length of the primary root was measured. Bars show the arithmetic mean of three independent experiments +/- SEM. The control condition (Col-0 root length on media without flg22) was set to 100. (n=27-34). No significant difference could be seen between treatment conditions using student t-test ($p < 0.05$).

3.6 The susceptibility of *Mh270* transgenic lines to diverse pathogens is similar to that of wildtype plants

3.6.1 Penetration assays reveal no difference in number of nematodes entering the root between transgenic and Col-0 plants

To address a potential influence of *Mh270 in planta* expression on plant susceptibility to nematodes, I performed pathogen assays with *M. hapla*. Plants with enhanced nematode susceptibility may exhibit one or more of the following three scenarios: 1) enhanced nematode penetration (more nematodes successful in finding/penetrating the root), 2) enhanced galling (more nematode able to initiate the feeding site and subsequent division of surrounding cells) and 3) enhanced egg production (conditions in which the female has greater reproductive capacity). Because we found that root-knot nematodes do not often complete their lifecycles and produce eggs in our axenic cultures, we focused on measuring nematode penetration and galling.

To address whether the initial number of nematodes penetrating the root is affected by *Mh270* expression, the number of nematodes inside the root at 4 dpi was counted. Acid fuchsin staining of the roots revealed that at 7 dpi, the nematodes were all still in the migratory J2 stage, indicating that at 7 dpi, feeding site formation had not yet begun. The transgenic lines contained the same number of juveniles (J2) per root as Col-0 (Figure 3.10). Based on this data, the *in planta* expression of *Mh270* has no effect on the attraction or penetration ability of the nematodes.

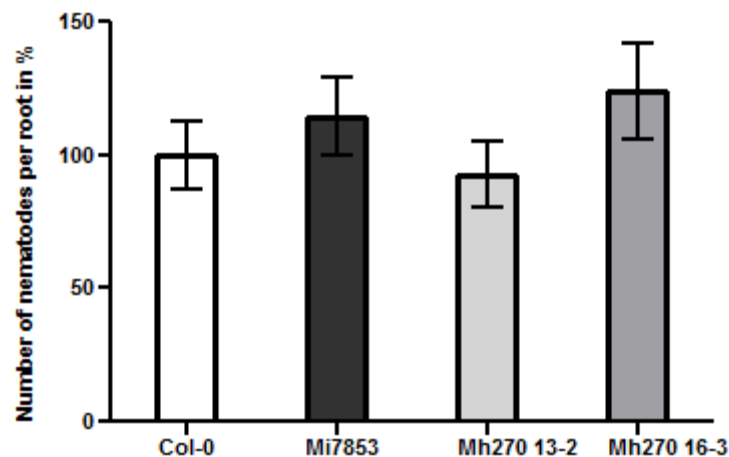


Figure 3.10: Nematode attraction and penetration were not affected in the *Mh270* lines. Penetration was measured by counting the number of juveniles at one week post-infection inside the plant root. The number of nematodes inside of the root in two transgenic *Arabidopsis* lines expressing *Mh270* was compared to the number inside Col-0 and the stable transgenic *Arabidopsis* line expressing the *M. incognita* effector candidate *Mi7853*. To visualize the nematodes, the roots were stained with acid fuchsin. The number of J2 inside Col-0 was set to 100. Bars present the arithmetic mean of three independent replicates +/- SEM (n=24).

In addition to the *Mh270* transgenic lines, a homozygous transgenic line for a putative *M. incognita* effector candidate *Mi7853* was generated in the Gleason lab. Presence of the *Mi7853* transgene had been confirmed by PCR and sequencing, and no developmental defects were observed in seedlings of this transgenic line (data not shown). Previous work in the lab had shown that *Mi7853* transgenic lines were not affected in nematode susceptibility (C, Gleason personal communication), but they had not been tested for nematode penetration. The transgenic line *Mi7853* also had similar number of J2 / root at the Col-0. Thus, *Mi7853*, which was later used as a control in galling assays, had no effect on nematode penetration (Figure 3.10).

3.6.2 *Mh270* transgenic lines are not altered in nematode susceptibility

Next, an infection assay tested whether the *Mh270* transgenic lines have altered nematode susceptibility, which is quantified as the number of galls per root system. Fourteen days old seedlings Col-0 and the *Mh270* transgenic lines were infected with 200 surface sterilized *M. hapla* J2. The number of galls per plant was counted at 4 weeks post-inoculation. The transgenic line *Mi7853* had been previously shown to have wild type-like susceptibility to RKN (C. Gleason, personal communication), and this line was used as an infection control. There was no significant difference in the galling between Col-0, *Mi7853* transgenic line, and the *Mh270* transgenic lines, indicating that *Mh270* has no effect on nematode susceptibility (Figure 3.11).

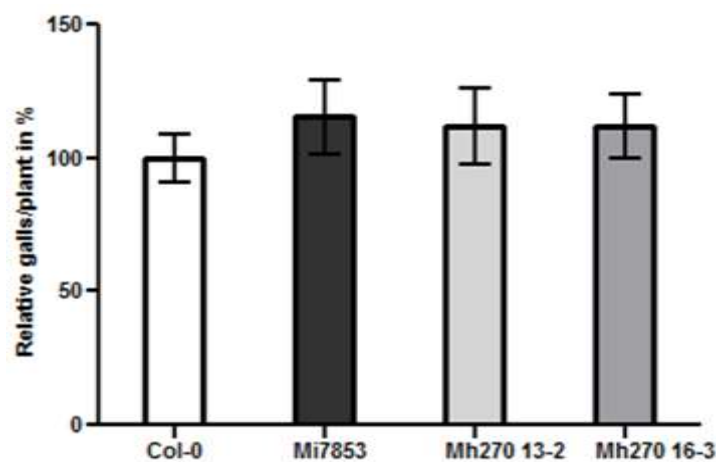


Figure 3.11: *Mh270* transgenic lines were not affected in nematode susceptibility. Susceptibility was measured by counting the number of galls per plant at 4 weeks post-infection. Galling of the root systems of two transgenic *Arabidopsis* lines expressing *Mh270* was compared to that of Col-0 and the stable transgenic *Arabidopsis* line expressing the *M. incognita* effector candidate *Mi7853*. The number of galls in Col-0 was set to 100. Bars present the arithmetic mean of three experiments combined \pm SEM (n=30).

3.6.3 Susceptibility to *M. hapla* is not altered in lines expressing a RNAi hairpin construct specifically targeting *Mh270*

Although the ectopic expression of *Mh270* in plants did not alter their susceptibility to nematodes, silencing *Mh270* in the nematode may lead to a visible phenotype in plants, such as reduced susceptibility. Thus we used host induced silencing (HIGS) in an attempt to knockdown *Mh270* and see if the knockdown has an effect on nematode infection success. For HIGS a *Mh270* RNAi construct is expressed in plants, and when the *Mh270* dsRNA is ingested by the nematodes, *Mh270* is presumably silenced via RNA interference mechanisms in the nematode.

Two homozygous lines were generated and tested for the expression of the *Mh270* RNAi hairpin construct (Figure 3.12 B). When these RNAi lines were tested in infection assays, no change in galling could be observed between Col-0, the two RNAi lines (Mh270 RNAi 9-4 and Mh270 RNAi 17-1) and the two ectopically expressing lines (Mh270 13-2 and Mh270 16-3) (Figure 3.12 A). Thus, expressing the Mh270 hairpin construct in Arabidopsis did not alter the plant's susceptibility to nematodes.

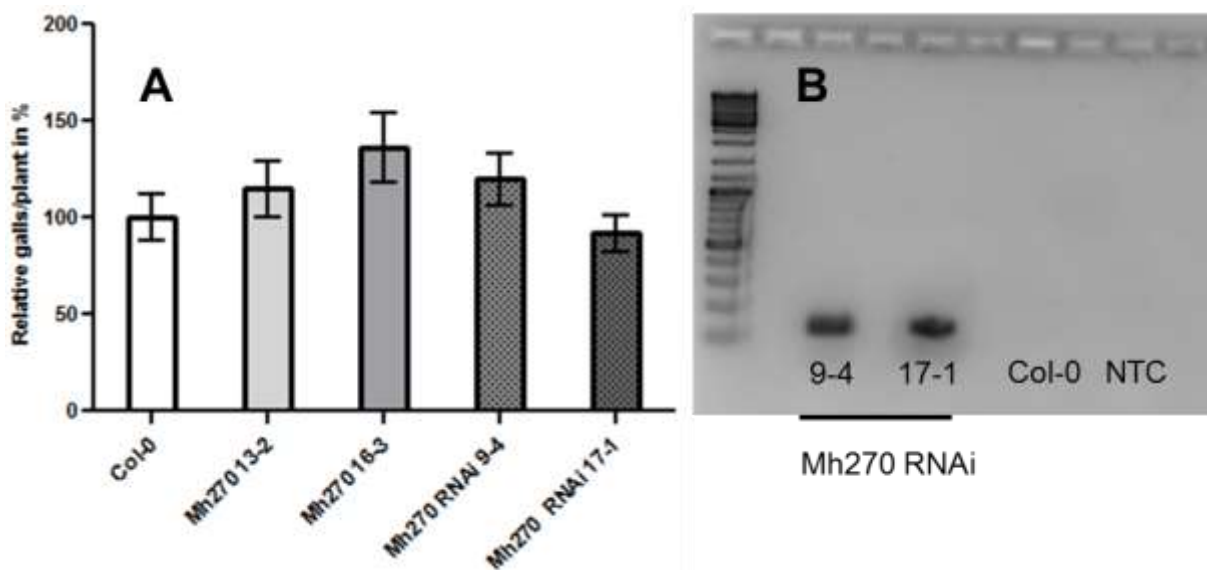


Figure 3.12 Expressing an RNAi-Mh270 construct in Arabidopsis had no effect on plant susceptibility. **A:** An RNAi construct targeting *Mh270* transcript was transformed into Arabidopsis. Col-0 and transgenic seedlings from four independent lines were infected with 200 *M. hapla* J2 per plant. The number of galls per root system was counted at 4 weeks post-inoculation. Galling in the Col-0 control was set to 100. Bars present the arithmetic mean of three independent experiments \pm SEM (n=30). **B:** PCR confirms expression of the hairpin construct in the RNAi lines. NTC = no template control.

3.6.4 *Mh270* expressing plants have no altered susceptibility to *Pst-LUX*

When *Mh270* was expressed in *Pst-LUX*, it could enhance the bacterial growth in wild-type plants. To determine if this phenotype persists when *Mh270* is stably expressed in Col-0, four week old *Mh270* transgenic plants were spray inoculated with a bacterial suspension of *Pst-LUX* and bacteria populations were measured at three days post-inoculation. No difference in bacterial growth *in planta* could be observed in between the transgenic *Mh270* lines and Col-0. The positive control *eds1-2* (enhanced disease susceptibility), which is a known hyper-susceptible mutant, showed higher bacterial growth (Figure 3.13 A). To confirm these results, *Pst-LUX* growth was also assessed by measuring bacterial numbers (colony forming units (cfu)/cm²) 0 and 3 dpi in the Col-0 and *Mh270* transgenic lines. The transgenic lines did not show any difference in bacterial growth *in planta* at 3 dpi compared to the Col-0 (Figure 3.13 B).

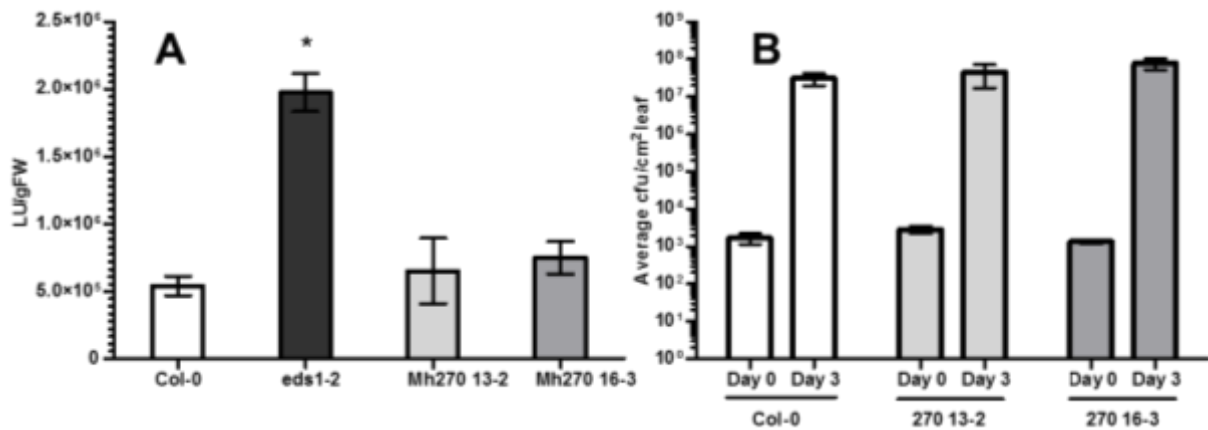


Figure 3.13: Arabidopsis plants expressing *Mh270* did not exhibit enhanced *Pst-LUX* growth. **A:** Four week old plants were spray inoculated with a bacterial suspension of *Pst-LUX*. At 3 dpi, bioluminescence (light units per gram fresh weight) was measured. Bars show the arithmetic mean of three biological replicates. Error bars represent the SEM (n=3). Asterisk indicate a significant difference in comparison to Col-0 using student t-test (p<0.05) Experiment was repeated twice with similar results. eds1-2 = hyper-susceptible mutant “enhanced disease susceptibility 1-2.” **B:** Fully expanded leaves of four week old plants were infiltrated with a *Pst-LUX* suspension (OD600=0.0001). Bacteria were extracted from leaf disks at 1h and 3 days after infiltration to determine the number of bacteria in the plant. Bars present the mean CFU / cm² of three biological replicates at 0 and 3 dpi +/- SEM.

3.6.5 Transgenic *Mh270* lines were not more susceptible to less virulent strains of *Pseudomonas syringae*

As the *Pst-LUX* strain is highly virulent, it may be difficult to assess if *Mh270* only causes a small enhancement in bacterial growth. As a result, assays with less aggressive bacterial strains may show larger differences in bacterial growth and a more robust phenotype conferred by *Mh270*. The bacterial strain *Pst* Δ CEL contains a mutation in conserved effector loci (CEL) and cannot suppress the formation of callose deposits (DebRoy et al., 2004). *Pst* Δ AvrPto/ Δ AvrPtoB can infect *Arabidopsis* but shows less virulent growth because it also lacks effectors that help it downregulate basal plant defenses. These two strains were tested on *Mh270* transgenic lines to see if *Mh270* could enhance bacterial pathogenicity.

Pst Δ CEL and *Pst* Δ AvrPto/ Δ AvrPtoB strains were leaf infiltrated into four week old wild type and transgenic plants. Bacterial abundance was measured on day 0 and three days post-infection. Plants expressing *Mh270* did not show enhanced growth *in planta* at 3 dpi for either *Pst* Δ CEL or *Pst* Δ AvrPto/ Δ AvrPtoB compared to Col-0 plants (Figure 3.14 A and B).

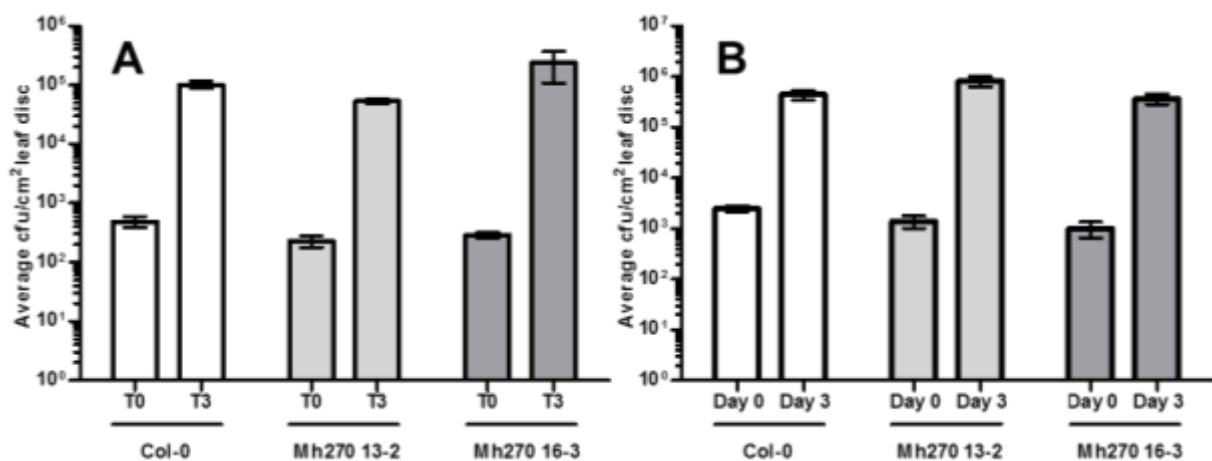


Figure 3.14 : Arabidopsis plants expressing *Mh270* did not exhibit enhanced growth of either *Pst* Δ CEL or *Pst* Δ AvrPto/ Δ AvrPtoB Four week old plants grown on substrate and under short day conditions were leaf infiltrated with a bacterial suspension (OD₆₀₀=0.01) of either *Pst* Δ CEL or *Pst* Δ AvrPto/ Δ AvrPtoB. Bacteria were extracted from leaf disks at 1h and 3 days after infiltration to determine the number of bacteria in the plant. Bars present the mean CFU / cm² of five biological replicates at 0 and 3 dpi +/- SEM (n=5). Experiments were repeated once with similar results **A**: *Pst* Δ CEL **B**: *Pst* Δ AvrPto/ Δ AvrPtoB.

3.7 Expression of *Mh270* in less virulent *Pseudomonas syringae* strains does not enhance bacterial growth

Mh270 expression *in planta* did not influence bacterial growth for either *Pst-LUX* or the less virulent mutant strains *Pst* Δ CEL and *Pst* Δ AvrPto/ Δ AvrPtoB. However, it was originally observed that pEDV6-*Mh270* expression in *Pst-LUX* resulted in enhanced bacterial growth in Col-0 plants. It is possible enhanced susceptibility may be linked to the bacterial expression of the effector. For example, the quantity of the effector secreted via the TTSS or the timing of the effector secretion during pathogenesis may be contributing to the enhanced bacterial virulence in the plant. If this hypothesis is correct, expression of *Mh270* in *Pst* Δ CEL and *Pst* Δ AvrPto/ Δ AvrPtoB may enhance bacterial growth on susceptible plants. Thus, both strains were transformed with pEDV6 containing either *YFP*, *ATR13* or *Mh270*. Positive clones were confirmed by colony PCR.

The bacterial strains carrying pEDV6-*YFP*, pEDV6-*ATR13* and pEDV6-*Mh270* were infiltrated into the leaves of Col-0, and bacterial growth was measured at 0 and 3 dpi. Neither the expression of *ATR13* nor *Mh270* could increase bacterial growth in either *Pst* Δ CEL or *Pst* Δ AvrPto/ Δ AvrPtoB (Figure 3.15 A and B). This was surprising since pEDV-*ATR13* in *Pst* Δ CEL has been previously reported to enhance bacterial growth *in planta* (Sohn et al., 2007).

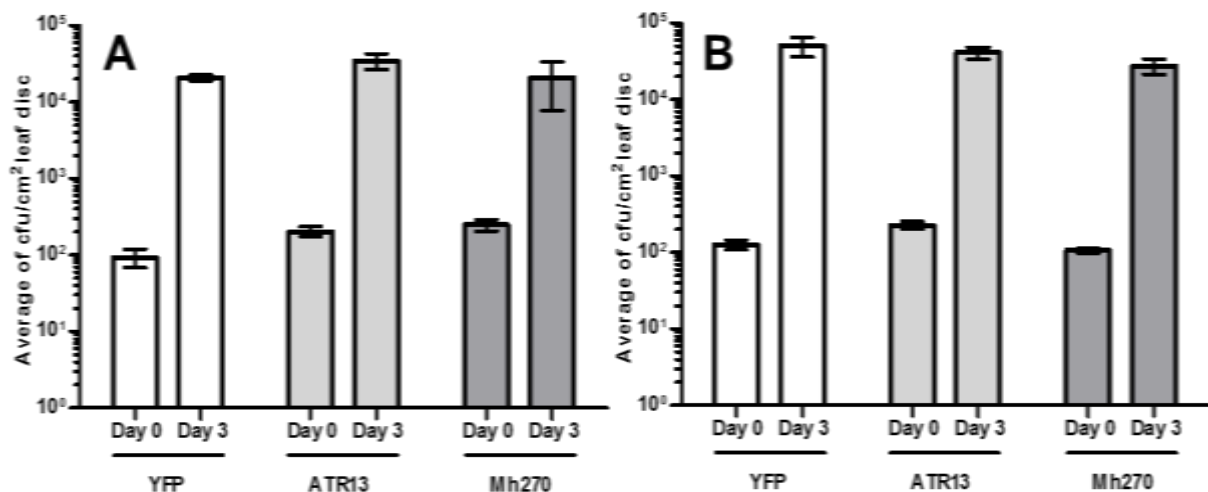


Figure 3.15 : Transgenic *Pst* Δ CEL and *Pst* Δ AvrPto/ Δ AvrPtoB expressing *Mh270* or *ATR13* did not have altered growth on Col-0 leaves. Bacterial suspensions (OD₆₀₀=0.01) of *Pst* Δ CEL or *Pst* Δ AvrPto/ Δ AvrPtoB expressing YFP, ATR13 or Mh270 were leaf infiltrated into four week old Col-0 leaves. Bacteria were extracted from leaf disks at 1h and 3 days after infiltration to determine the number of bacteria in the plant. Bars present the mean CFU / cm² of five biological replicates at 0 and 3 dpi +/- SEM (n=5). Experiment was repeated twice with similar results. **A.** *Pst* Δ CEL transformed to deliver YFP, ATR13 or Mh270 **B.:** *Pst* Δ AvrPto/ Δ AvrPtoB transformed to deliver YFP, ATR13 or Mh270.

Because *Pst* Δ CEL cannot suppress callose deposition, leaves infected with *Pst* Δ CEL show an enhanced number of callose deposits. To test if Mh270 could suppress the callose deposition induced by *Pst* Δ CEL, leaves were infiltrated with *Pst* Δ CEL carrying pEDV6-*YFP*, pEDV6-*ATR13* or pEDV6-*Mh270*. Aniline blue staining of callose deposits showed that none of the constructs could suppress callose deposition induced by *Pst* Δ CEL in Col-0 (Figure 3.16).

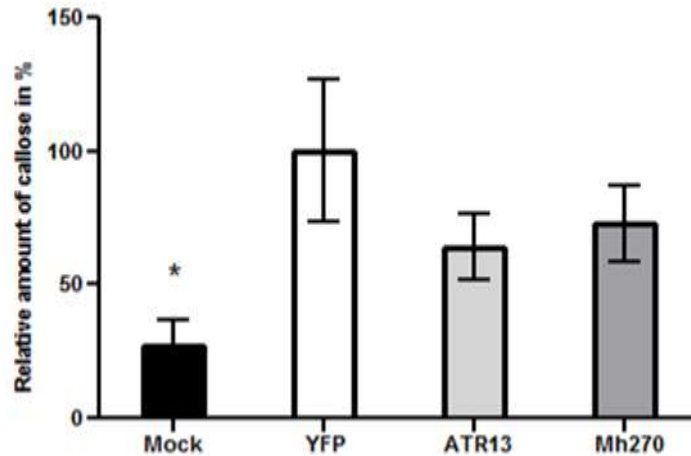


Figure 3.16 : The enhanced callose deposition caused *Pst* Δ CEL infection was not suppressed in Mh270 transgenic bacteria. Four week old Col-0 grown under short day conditions were leaf infiltrated with bacterial suspensions ($OD_{600}=0.2$) of *Pst* Δ CEL or $MgSO_4$ (Mock). One day after infiltration, the leaves were callose deposits were stain stained with aniline blue. The number of callose deposits in the field of view was determined using Image J software. Measurements were taken in triplicates. Bars present the arithmetic mean of three experiments \pm SEM (n=10). Asterisk indicate a significant difference in comparison to *Pst* Δ CEL harbouring pEDV6 – YFP ($p<0.05$).

3.8 Fluorescently-tagged Mh270 stable transgenic Arabidopsis lines were generated

Sub-cellular localization gives an insight into where a candidate protein localizes within the plant cell. The coding sequence of Mh270 (minus signal peptide) was cloned in frame to with either an N-terminal YFP or a C-terminal GFP. Both *pUbq::YFP-Mh270* and *pUbq::Mh270-GFP* were introduced into Col-0 to generate stable transformed lines with constructs driven by the plant ubiquitin promoter. Generated lines were visually screened for fluorescent signal intensity by fluorescence microscopy and the four lines with the strongest signal were chosen for further analysis.

3.8.1 Western blot analysis of fluorescently-tagged Mh270 expressed in Arabidopsis reveals instability of the N-terminal construct

To detect the Mh270 fusion proteins in the transgenic lines, Western blot analysis with GFP antibody the four transgenic Mh270 tagged lines was performed. In plants containing *pUbq::Mh270-GFP* construct, a protein of the expected size of Mh270-GFP fusion (40 kDa) was detected. However, in the plants containing the *pUbq::YFP-Mh270* construct, only a 25kD band could be detected with the anti-GFP antibody. This size is similar to that of soluble GFP, suggesting that the YFP has been cleaved from Mh270 in these lines (Figure 3.17).

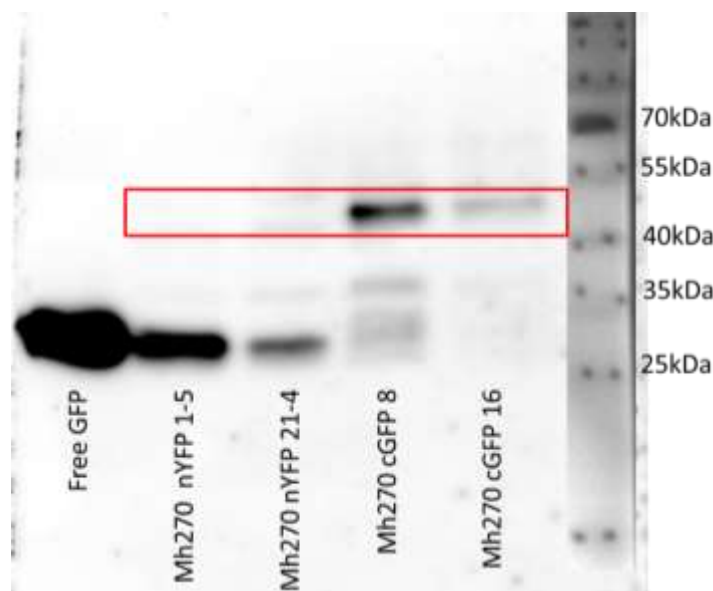


Figure 3.17 : Western blot analysis indicates that Mh270-GFP and not YFP-Mh270 produces a stable, tagged protein in transgenic Arabidopsis. Proteins from transgenic Arabidopsis lines expressing GFP, YFP-Mh270, or Mh270-GFP driven by the 35S promoter were separated on an SDS-PAGE gel and blotted onto PVF membranes. GFP and YFP were detected using the α GFP antibody. Predicted size of Mh270 fluorescently tagged proteins is 40.13kDa. Size of GFP is 27kDa. Red square indicates the size of the predicted Mh270-tagged proteins.

3.8.2 Mh270-GFP localizes to the chloroplast of Arabidopsis leaves

Roots of one week old plants expressing the pUbq::*Mh270-GFP* construct were analyzed for the subcellular localization of Mh270 using confocal microscopy. Mh270-GFP was observed in the roots of the transgenic plants (Figure 3.18). Mh270-GFP was seen in the cytoplasm of the root cells, similar to the distribution of GFP in Arabidopsis cells, when GFP is not fused to a specific plant protein (“free GFP”).

Next, leaves of plants expressing the pUbq::*Mh270-GFP* construct were analyzed by confocal microscopy. Mh270-GFP appeared to localize to the chloroplasts since the green fluorescence was co-localized with the red autofluorescence of chlorophyll in leaves (Figure 3.19). In plants expressing pUbq::*YFP-Mh270*, only a protein the size of YFP could be detected on the Western blot, and the plants had a ubiquitous fluorescent signal, similar to that of plants expressing *p35S::GFP*, in both roots and leaves (Supplemental figure 3).

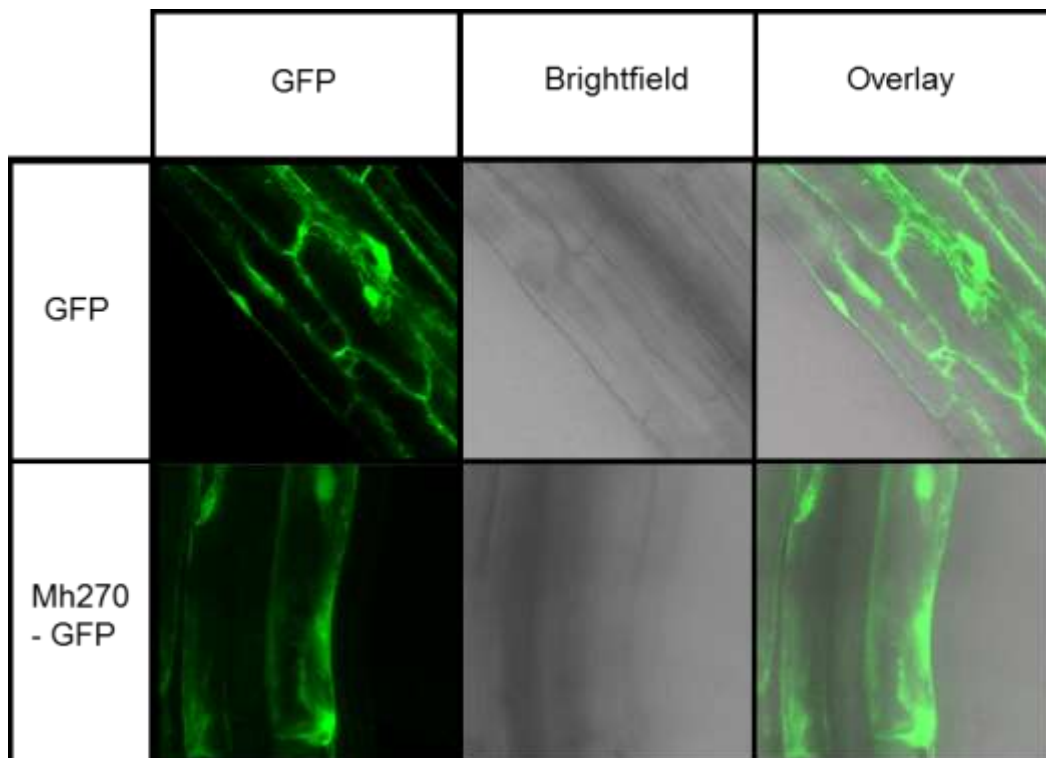


Figure 3.18: C-terminally tagged Mh270 is localised in the cytoplasm of Arabidopsis roots. One week old roots from stably transformed Arabidopsis plants with either p35S::*GFP* or pUbq10::*Mh270-GFP* were analyzed by confocal microscopy. Localization was observed in two independent lines.

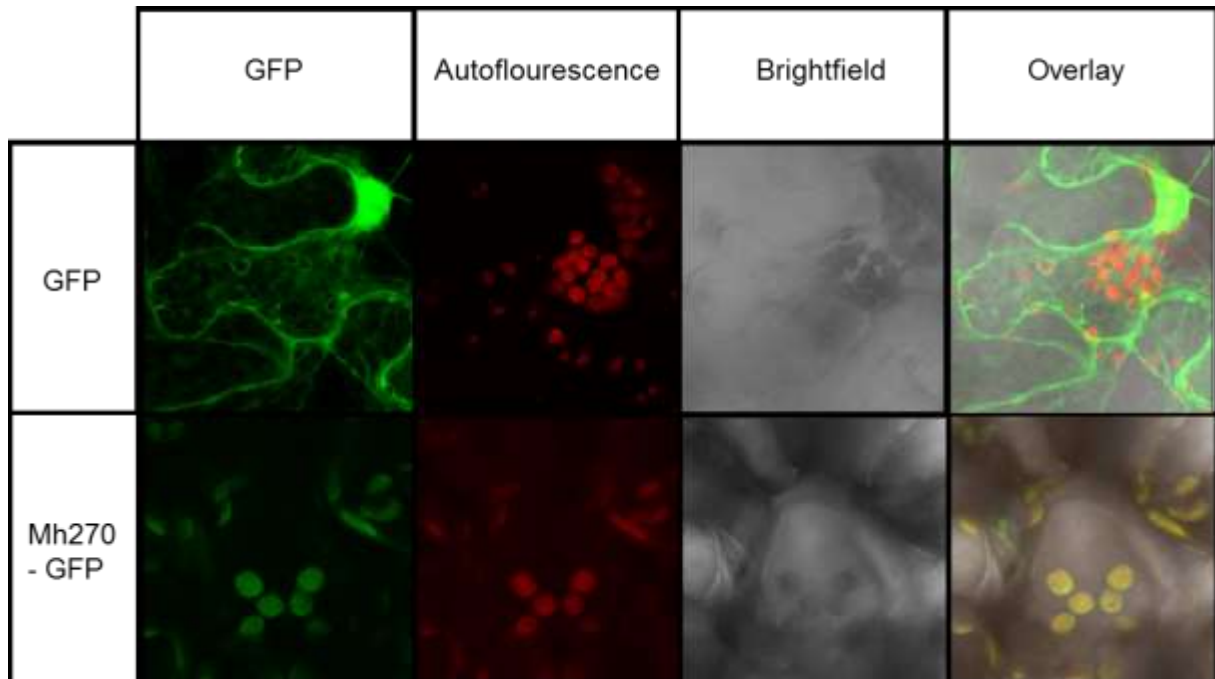


Figure 3.19: Localization of Mh270-GFP in Arabidopsis leaves. Leaves of seven day old plants were analysed for fluorescence signal using confocal microscopy under the use of the appropriate filter set. Localization was observed in two independent lines. With these optical filters, the chloroplasts exhibited autofluorescence. Brightfield and an overlay of all channels are also presented.

3.9 A yeast-two-hybrid screen reveals a potential plant interaction partner for Mh270

To find potential plant targets for Mh270, a yeast-two-hybrid screen was performed. First, *Mh270* without signal peptide was introduced into the yeast two hybrid pASII vector and transformed into the yeast strain AH109. To test for potential auto-activation, yeast harboring the *Mh270* construct were grown on synthetic complete media lacking leucine or synthetic complete media lacking the amino acids leucine and histidine with an addition of 5 mM 3-AT (3-Amino-1,2,4-triazole). While growth on control media was normal, it was completely abolished on double knock-out media, indicating that *Mh270* does not cause an auto activation of the reporter gene (Supplemental figure 2).

Two different libraries were used to screen for potential interaction partners. An Arabidopsis root library and a cell line library, both provided by Joachim Uhrig, were mated with yeast containing Mh270 in pASII. The libraries contained cDNA fragments of RNA generated from Arabidopsis roots or cells that was introduced into pGAD and transformed into yeast strain Y190. Approximately 10-14 days after mating, colonies were picked from semi liquid drop out media deficient in leucine, tryptophan, and histidine supplemented with 5 mM 3-AT. Additionally, sc plates lacking leucine and tryptophan were prepared with mated yeast to estimate mating efficiency. This resulted in 2.6 million and 7.8 million mating events for root and cell line library, respectively.

Using vector specific primers, the inserts of 65 picked colonies were amplified and sequenced (Supplemental table 2). Five ribosomal and one mRNA binding protein were removed from the list of interacting partners since they commonly occur in the libraries and are likely false-

Table 3.2 : List of positive candidates derived from both root and cell line library. Amplified sequences were analysed and candidates were compared with TAIR database available sequences. Redundant candidates and candidates presenting a frameshift were excluded from further testing. Working number, AGI code, gene name, if applicable, according to the TAIR database and the library in which the candidate was identified are presented. Occurrence indicates how often a candidate was identified in the screen.

Number	AGI-code	Gene name (TAIR)	Library	Occurrence
Y3	AT3G17390	Methionine adenosyltransferase, <i>MAT4</i>	Cell	1
Y9	AT4G36980	Unknown protein	Cell	2
Y13	AT5G28150	Plant protein of unknown function (DUF868)	Cell	2
Y14	AT5G08450	Histone deacetylation complex 1, RXT3-LIKE, <i>HDC1</i>	Cell	1
Y18	AT2G21850	Cysteine/Histidine-rich C1 domain family protein	Cell	1
Y29	AT5G37740	Calcium-dependent lipid-binding (CaLB domain) family protein	Cell	1
Y33	AT4G13195	CLAVATA3/ESR-related 44, <i>CLE44</i>	Cell	1
Y34	AT4G35830	Acotinase 1, <i>ACO1</i>	Cell	1
Y40	AT5G47690	Unknown protein	Cell	1
Y44	AT4G11420	Eukaryotic translation initiation factor 3A, <i>ATEIF3A-1</i>	Cell	1
Y49	AT5G15090	Arabidopsis thaliana voltage dependent anion channel 3, <i>ATVDAC3</i>	Root	2
Y51	AT4G31800	Arabidopsis thaliana WRKY DNA-binding 18, <i>ATWRKY18</i>	Root	1
Y53	AT2G02180	Tobamovirus multiplication protein 3, <i>TOM3</i>	Root	3
Y56	AT1G02500	S-adenosylmethionine synthetase 1, <i>ATSAM1</i>	Root	1

positives (Joachim Uhrig, personal communication, 2014). A list of 40 non-redundant candidates remained and their sequences were analyzed in more detail. Because the prey libraries were made from cDNAs that may or may not be full-length, an important criteria was that the start codon of the prey protein must be produced in frame in yeast. When the out-of-frame clones were excluded, 13 candidates remained as possible interaction partners of Mh270 (Table 3.2).

In order to confirm the interaction, a double transformation between the full-length sequence of the candidates from the original screen (13 in total) and *Mh270* were performed. An entry clone for candidate Y40 was not made because it was not possible to amplify the corresponding

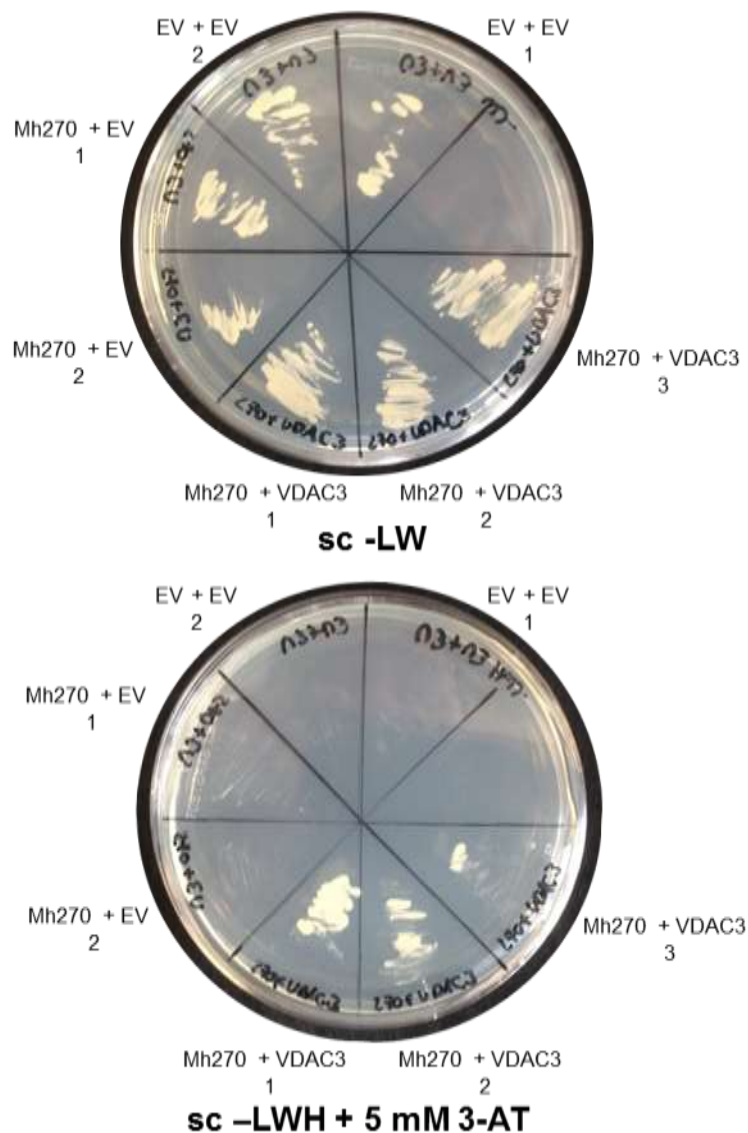


Figure 3.20 : The interaction between full-length Mh270 and AtVDAC3 was confirmed in double-transformed yeast. Yeast AH109 were transformed with the following constructs: empty vector EV + Mh270, EV + AtVDAC3, or Mh270 + AtVDAC3. They were grown three days at 28 °C on either on non-selective control plates (SC-W) or selective plates (SC-LWH +5 mM 3-AT). Two independent transformants were picked for empty vector controls and three for Mh270+AtVDAC3 double transformations.

full length cDNA. Double transformation experiments confirmed that out of the 12 full length candidates, only Y49 could interact with Mh270 in yeast. Clone Y49 contains the open reading frame for At5g15090, which encodes a voltage-dependent anion channel *AtVDAC3* (Figure 3.20).

4. Discussion

4.1 The pros and cons of the “effector detector vector” screen for identifying nematode effectors

It is widely assumed that root-knot nematodes are secreting effectors during the early stages of parasitism that help the nematode suppress plant immunity and/or help establish their feeding sites in the root. Several approaches have been undertaken to identify these secreted effectors. For example, Roze et al. (2008) studied *M. chitwoodi* effectors by generating EST (expressed sequence tags) datasets of three different nematode life stages. Subsequent bioinformatic analyses of these libraries identified proteins expressed in the parasitic stages with signal peptides, which was indicative of stylet secretion. To confirm that these proteins were indeed secreted from the nematode, the group then did *in situ* localization, and found that most of their candidates were localized to nematode organs involved in secretion (Haegeman et al., 2013). Finding that a majority of the predicted secreted proteins were localized to the glands validated their bioinformatic approach to identify nematode secreted proteins with possible roles in parasitism. Danchin et al. (2013) mined the genomes of several plant parasitic nematodes for genes with secretion signals that are present in parasitic worms but absent from non-target species (plants, chordates, annelids, insects, and mollusks). This allowed them to identify potential nematode-specific effectors that could be targets for host-induced gene silencing. Taking a more direct approach, Bellafiore et al. (2008) used mass spectrometry together with bioinformatic analyses to identify proteins from the *M. incognita* stylet secretions. Overall, they uncovered that are nearly 500 proteins secreted from *M. incognita*, which may or may not be involved in parasitism (Bellafiore et al., 2008).

Although there are hundreds of potentially secreted proteins from root-knot nematodes, only a few have been intensively studied. Unfortunately, RKN present many challenges to researchers. They are obligate pathogens, they have a complex genome organization, and they cannot be transformed. Therefore, experiments looking at effector function require quite labor intensive studies using RNA interference or making stable transgenic plants expressing the nematode gene of interest. To speed-up the effector discovery and functional analysis, I decided to adapt the “Effector-Detector Vector” (EDV) screen for nematode effectors. I could study seven putative effector candidates from *M. hapla* in an easy, bacterial assay to determine if expressing nematode effector candidates in *Pseudomonas syringae* affected bacterial growth in the plant. If the effector candidate could enhance bacterial growth, it would suggest that candidate is targeting conserved aspects of plant immunity, such as PTI. I could then prioritize the

candidates and focus on those which are likely to play key roles in the plant-nematode interaction. Despite the ease of the assay, there were drawbacks to the bioinformatic and EDV screen that should be considered.

In the bioinformatic screen that was performed on the *M. hapla* dataset, a search algorithm for predicted classical secretion signals was performed. Although the presence of signal peptide is a typical feature used to define secreted proteins, some secreted proteins lack a canonical secretion signal and are secreted via an unconventional secretion system (Nickel, 2003). In *Brugia malayi*, 4.4% of the 2572 excretory/secretory proteins identified in the secretome were classified as non-classically secreted and the *M. incognita* secretome also presented proteins that lack a secretion signal (Bellafiore et al., 2008; Garg and Ranganathan, 2012; Suh and Hutter, 2012). Recently, non-classical secretion of isochorismatases as effectors required for pathogenicity has been described for filamentous plant pathogens (Liu et al., 2014). These results reveal the potential for phytopathogens to use both classical and non-classical secretion to deliver effectors (Liu et al., 2014). The alternate secretory routes in phyto-nematodes have yet to be uncovered, but by excluding non-conventionally secreted proteins from root-knot nematodes in our initial bioinformatic analysis, we may have missed potential nematode effectors.

In addition to running candidates through search programs for signal peptides, I also used a search program for predicted glycosylation sites. Candidates with predicted glycosylation sites were removed in order to ensure that chosen candidates could be correctly produced by the plant pathogenic bacteria *Pseudomonas syringae* pv. *tomato* DC3000, which was used to deliver proteins to the plant cell in the EDV screen. However, many of the effector candidates had predicted glycosylation sites, and were excluded from the EDV-screen. In addition, glycosylation is just one of many potential post-translation modifications that could affect protein function. The fact that proteins that undergo post-translational modifications may not be suitable for the EDV screen is a major drawback of the system.

Another drawback to the EDV system is that it is necessary to consider that *Pst* DC3000 is a bacterial plant pathogen that infects leaf tissue while RKN are animals parasitizing root tissue. Additionally, *Pst* DC3000 is a hemibiotrophic pathogen which causes severe damage on the leaves. In contrast, RKN are biotrophic and establish a very intimate interaction with the respective host while causing virtually no visible phenotypes, except swelling of the root. Although it was shown that roots can respond to PAMPs in a similar manner to leaves, (Millet et al., 2010) it is still important to note the differences of these two infection systems and

possible differences in defense responses (i.e. root vs leaf). The discrepancy between life style and tissue specificity might lead to either false positive or to the exclusion of true positive candidates in the EDV screen. Nonetheless, further investigations of positive candidate effectors as gene expression analysis and *in situ* hybridization can be used as subsequent tests to confirm their potential involvement in nematode-plant interaction. In summary, the EDV system allowed a high throughput testing of selected candidate effectors for their bacterial growth enhancing capabilities in *Pst* DC3000– plant interaction, and these candidates had the potential to be involved in suppressing plant immunity.

The expression of candidates *Mh270* and *Mh265* is up-regulated in pre and early-parasitic life-stages, suggesting roles in parasitism

Gene expression analysis allows the estimation of transcript abundance of a specific target gene. In the case of nematodes it is important to note that the different life stages can have an effect on reference gene expression, which can ultimately affect relative gene expression. To account for this, I used a technique described by Iberkleid et al (2013) in which the geometric mean of two different reference genes is used to reduce the life-stage effect on the relative gene expression calculation. Although an increase in specific gene expression in the infective and motile stages of the nematode does not necessarily indicate an involvement in pathogenicity, it can be used as definite exclusion criteria to ensure that the target gene has a higher importance in a certain life stage in comparison to non-infective or sedentary stages. Generally, the analysis of gene expression is a well-established method to identify genes potentially involved in the plant-pathogen interaction (Fabro et al., 2011; Lin et al., 2013; Roze et al., 2008). Using gene expression as a second criterion for possible effectors candidates after the EDV screen, both *Mh270* and *Mh265* showed enhanced expression in the pre- and early parasitic stages of the nematode, which is enticing evidence that they may be involved in parasitism. Because *Mh270* and *Mh265* were effector candidates that 1) enhanced bacterial growth in the EDV system and 2) had enhanced gene expression in parasitic stages, they were prioritized for further studies.

***Mh270* is a transthyretin-like protein localized to the amphids**

Mh270, as the main candidate for this thesis, was identified to belong to the transthyretin-like protein group harboring a DUF290 – a transthyretin like domain. Transthyretin-like genes are part of a large gene family and are a nematode specific group of proteins.

Transthyretin-like proteins (TTLs) have similarity at the protein level to transthyretins (TTR), which have a transthyretin domain (PF00576) and are specifically found in vertebrates. The

initially identified transthyretin proteins in humans have been mostly studied for their ability to transport thyroxine and for their involvement in Vitamin A metabolism. In vitamin A metabolism, TTRs act as carrier proteins that bind to retinol-binding proteins (Yamamoto et al., 1997). Mutations in a TTR gene can cause amyloidosis which causes the aggregation of proteins. The aggregates become insoluble in intercellular space of the human body causing several different disease symptoms depending on which organ is affected (Hamilton and Benson, 2001).

In addition to the TTLs, there are transthyretin-related proteins (TRPs), which contain a transthyretin domain (PF00576) and a characteristic C terminal motif (Y-[RK]-G-[ST]) (Pessoa et al., 2010). TRPs are found in a broad range of organisms, including plants. In Arabidopsis, the TRPs are involved in brassinosteroid signaling and modulating plant growth. The Arabidopsis TRP acts as substrate of the BRASSINOSTEROID-INSENSITIVE 1 (BR1), a Leucine-rich-repeat (LRR) receptor kinase (Nam and Li, 2004). Although sequence similarities exist between TRPs from fungi, plants, and animals, they have evolved many different functions, from their role in BR-signaling in plants to acting as a 5-hydroxyisourate hydrolase in zebrafish (Pessoa et al., 2010; Zanotti et al., 2006).

Nematode specific transthyretin-like proteins are found in both non-parasitic (*C. elegans*) and parasitic nematodes. In plant parasitic worms, they have been found in *Xiphinema index*, *M. incognita*, *H. glycines* and *Radopholous similis*, but their role in plant parasitism is unknown. In animal parasitic nematodes, such as *Ostertagia ostertagi*, TTLs were identified to be expressed from the free-living stage onwards. It has also been found in the excretory-secretory (ES) products of *Ostertagia ostertagi*, *Brugia malayi*, and *Haemonchus contortus*, which suggests a role in the secretions during the parasitic stages of the worms (Saverwyns et al., 2008). Unfortunately, RNAi-mediated knockdowns of TTLs have led to little insight to their function (Wang et al 2010). In *C. elegans*, only RNAi knockdowns of 4 out of 53 TTLs tested showed any aberrant phenotype, such as hyperactivity, increased fat content, and maternal sterility (Wang et al., 2010). Knockdowns of the TTLs in the burrowing nematode *Radopholous* (*Rs-TTL-1* and *Rs-TTL-2*) also did not have any phenotype, leaving few clues as to their biological roles (Jacob, 2009). Localization studies do provide some information about the possible function of the TTLs in nematodes. For example, one of the *C. elegans* TTL was localized to the nervous system and hypodermis (Wang et al 2010). In addition, the plant parasitic *Radopholous similis* *Rs-TTL-1* and *Rs-TTL-2* were localized to the central nerve cord and the vulva, respectively (Jacob et al., 2007). Because the TTLs are a multigene family of

secreted proteins with expression in the nervous system, Jacob et al. (2007) hypothesize that *Rs-TTLs* share characteristics with neuropeptides.

Interestingly, *in situ* hybridization determined that Mh270 transcript was localized to the amphids of the J2 nematode. The amphids are two open pores on the head of the nematode that function as chemosensory sensilla (sense organs). The amphids contain a glandular sheath cell, a socket cell, and dendritic processes that are bathed in secretions (Perry, 1996). Because the amphids are open to the environment, the secretions generated by the glandular sheath cells can be released by the nematode. Recent work has identified plant-parasitic nematode effectors that localize to the amphids and are likely secreted to the plant apoplast. For example, in *Globodera pallida* a novel group of hyper-variable extracellular effectors were localized to the amphids. Silencing these effectors reduced the nematode success in infecting the plant, and these proteins were detectable during plant infection by immunochemistry in the plant apoplasm (Eves-van den Akker et al., 2014b). In RKN, the putative avirulence factor MAP-1 was also shown to be secreted from the amphids during infection, and these secretions also localized to the apoplast during infection (Vieira et al 2011).

It is interesting to speculate that Mh270 may be associated with the nerves or the amphid secretions that surround the nerves. The localization in the amphids would suggest that Mh270 is initially secreted into the apoplast during infection. However, we observed that when Mh270 was delivered by *Pst-LUX* into the plant cell via the TTSS, it enhanced bacterial virulence in the plant. This suggests that Mh270 functions in the plant cytoplasm. Therefore, we speculate that if Mh270 were secreted into the apoplast, it would have to be delivered into the plant cell by some mechanism. Unlike oomycete effectors that have a conserved RXLR-uptake motif that is required for effector translocation into the plant cell (Morgan and Kamoun, 2007), there are no known nematode translocation motifs. In the future, immunolocalization of Mh270 during infection may shed light on its destination compartment within the plant after nematode secretion.

4.2 Transgenic lines expressing *Mh270* do not show an altered infection phenotype for *M. hapla* and *Pseudomonas syringae* strains

The EDV screen identified two effector candidates which enhanced bacterial growth in plants, and I focused my research on one of these effector candidates, *Mh270*. To test the effects of *Mh270* on plant susceptibility, stable transgenic lines expressing *Mh270* were generated. These lines were tested for enhanced nematode susceptibility by studying both penetration and galling. Penetration assays test nematode abundance in infected roots, and a changed penetration phenotype could be due to many factors, including root morphology and root attractiveness. A root system that is altered in size could lead to a different number of nematodes in the root due to differences in availability of penetration sites. For example, a peptide from *M. incognita*, termed 16D10, could significantly enhance root growth when ectopically expressed in *Arabidopsis* and tomato hairy roots, and these hairy roots were more susceptible to nematodes (Huang et al., 2006). However, the *Mh270* transgenic lines did not show any obvious morphological phenotype, which precludes the possibility of increased penetration sites. Overall, there was no change in the number of nematodes at 7 dpi in the transgenic lines compared to the control, suggesting that the nematode penetration is not affected by *Mh270*.

Next, infection assays were performed to test for an effect of *Mh270* expression on nematode susceptibility. Several effectors have been identified to increase nematode susceptibility when expressed in the host plant. For example, RKN effectors. *Mi-CRT*, *Mi-NULG1a*, and *8D05* were able to increase the number of galls, indicating enhanced nematode susceptibility (Iberkleid et al., 2013; Jaouannet et al., 2013; Lin et al., 2013; Xue et al., 2013). Unfortunately, *Mh270* transgenic plants did not have altered galling, and overall, they were just as susceptible to *M. hapla* as Col-0.

The transgenic *Mh270* lines were also tested with *Pst-LUX* to see if ectopic *Mh270* expression in plants could affect bacterial susceptibility. Fabro et al. (2011) reported that when nine *Hpa* Emoy2 HaRxLs effectors were constitutively expressed in Col-0 plants, six gave results consistent with the EDV phenotype. This suggests that effectors which enhanced bacterial growth in the EDV screen should also enhance bacterial growth when the effectors constitutively expressed in plants. Unfortunately, when *Mh270* was expressed in plants, its presence did not have a positive effect on *Pst-LUX* growth. *Mh270* transgenic plants were also inoculated with less virulent strains of *Pseudomonas syringae*: *PstΔCEL* and *PstΔAvrPto/ΔAvrPtoB*. There was no enhanced bacterial growth in the transgenic plants for either *PstΔCEL* or *PstΔAvrPto/ΔAvrPtoB*. These results are surprising since only one of the

nine effectors presented in the Fabro paper that enhanced bacterial growth in the EDV screen did not have the same effect when the effector was expressed in plants. The transgenic plants expressing this effector also exhibited smaller leaves and enhanced callose deposition, and these plant phenotypes may have contributed to the bacterial phenotype (Fabro et al 2011). In contrast, the Mh270 transgenic lines did not present an altered growth phenotype nor did they have altered callose deposition, so the lack of increased *Pst-LUX* growth phenotype in the Mh270 lines cannot be linked to these responses.

Although Mh270 transgenic lines were not more susceptible to nematodes and they did not exhibit enhanced *Pst-LUX* susceptibility, it does not completely rule-out Mh270 as an effector candidate. One possibility is that the amount of Mh270 protein in the transgenic plants was too low to have an effect on nematode and *Pst-LUX* susceptibility. Since only the *Mh270* transcript level was measured in the transgenic plants, no clear statement can be given about the Mh270 protein levels in these lines. Because protein tags could potentially interfere with protein function (Terpe, 2003) we initially transformed only constructs with untagged Mh270 into Arabidopsis. Subsequent generation of homozygous, N-terminal YFP tagged constructs showed that only soluble YFP was present, suggesting that the Mh270 had been cleaved from its fluorescent tag. The C-terminal tagged Mh270 GFP lines were only recently generated, which, according to the Western blot analysis, have stable, GFP-tagged Mh270. Unfortunately, due to time limitations, these were not tested with nematodes or other pathogens as part of the thesis, but they will be tested in the future.

4.3 Expression of an RNAi construct in plants did not affect nematode susceptibility

Although the ectopic expression of *Mh270* did not increase virulence of *M. hapla* the importance of the candidate effector could still be detected via an RNAi silencing approach. If a candidate effector has a crucial importance in the infection process and it is efficiently silenced, an impact on nematode infection should be visible. In general, two methods are used to silence genes in RKNs. The first is to soak juvenile nematodes in a dsRNA solution. The silencing construct should passively enter the nematode, be processed, and target the specific gene for silencing nematodes (Lozano-Torres et al., 2014; Niu et al., 2012). Unfortunately, soaking nematodes in dsRNA often has low penetrance due to the thick nematode cuticle and results can be highly variable. Furthermore, Dalzell et al.(2009) reported aberrant phenotypes from soaking plant parasitic nematodes in non-nematode dsRNA, suggesting that soaking can lead to non-specific effects. Due to these observations, we decided to use host-induced gene

silencing (HIGS), which has been used to silence different genes in RKN and cyst nematodes (Iberkleid et al., 2013; Jaouannet et al., 2013; Lin et al., 2013). For this method we created transgenic plants producing an RNAi hairpin construct targeting *Mh270* transcripts. The RNAi construct was detected in the generated homozygous lines. However, determination of a potential reduction of *Mh270* transcript in the nematode was not performed. Unfortunately, it is technically difficult to measure RNAi-mediated knockdowns of nematode genes during parasitism. First, the initial amount of *Mh270* transcript was very low, and since the infections were not synchronized, it meant that infections contained a mixture of both feeding and non-feeding nematodes, which would have also diluted any knock-down effects on *Mh270* transcript levels. Nevertheless, I predicted that silencing of *Mh270* in nematodes could lead to reduced galling in the plants. Unfortunately, the nematode bioassays did not reveal any effect of the RNAi construct on *M. hapla* galling. Since the nematodes will potentially take up the dsRNA only when they feed on the plant cell, the knockdown of *Mh270* could have happened after *Mh270* already fulfilled its function in pathogenicity. We also cannot rule out that *Mh270* may work in coordination with other parasitism genes, and thus, targeted silencing of one gene would have limited effects. The lack of phenotype in the *Mh270* RNAi lines highlights the drawbacks of HIGS. It should be noted that while RNAi had once been touted as a technique for elucidating gene function in plant parasitic nematodes, the nematode community has begun to lose confidence RNAi due to high variability between experiments and the lack of significant, targeted effects for most genes tested (Lilley et al., 2012).

4.4 *Mh270* expression has no effect on flg22 triggered responses

PTI is the first line of active defense responses against pathogens, and host plants have to constantly cope with effectors which can affect this basal line of defense. When *Mh270* was delivered by *Pst-LUX*, the bacterial growth was enhanced in the plants, and therefore, I hypothesized that this effector candidate may be affecting very general immune responses that affects diverse pathogens, including bacteria and nematodes. In other words, it may have an effect on PTI. Several effectors from different pathogens have been identified to affect PTI. For example, in *Pseudomonas syringae*, HopAII is an effector that influences map-kinase signaling, resulting in reduced PTI defense gene expression and consequently less callose deposition (Zhang et al., 2007). Another example for an effector directly targeting plant defenses is Pep1 from *Ustilago maydis*. This effector inhibits apoplastic peroxidases to reduce the ROS burst generated during immune responses (Hemetsberger et al., 2012).

Even though the importance of basal defenses in RKN-plant interaction is not well researched, different effectors are being identified which affect PTI associated responses. Most prominently, *Mi-CRT* was shown to down-regulate the expression of the PTI marker genes *FRK1* and *CYP81F2*. Additionally, less elf18-induced callose could be detected after treatment in the Arabidopsis lines ectopically expressing *Mi-CRT* (Jaouannet et al., 2013). This indicates that RKN effectors suppress at least some PTI responses to successfully manipulate the plant host.

In the case of *Mh270*, I tested several PTI readouts. Because at the time of the experiments no nematode PAMP had been identified, flg22 was used to induce PTI in the transgenic plants. Unfortunately, the *Mh270* transgenic plants were not compromised in flg22-induced callose deposition, ROS-burst, or PTI-marker gene expression. They were also not affected in flg22-induced root growth inhibition. Altogether, any effect of *Mh270* in the plant-nematode interaction is probably not associated with PTI suppression. However, additional tests with the newly generated *Mh270*-GFP tagged lines will hopefully confirm this conclusion.

4.5 Mh270 did not enhance the virulence of *Pst*ΔCEL and *Pst*ΔAvrPto/ΔAvr PtoB

When pEDV6-*Mh270* was expressed in *Pst-LUX*, the bacteria showed more growth *in planta* compared to the controls. However, *Pst-LUX* is a virulent pathogen, and it may be easier to detect enhancement of bacterial virulence using less virulent bacteria. Thus, *Pst*ΔCEL and *Pst*ΔAvrPto/*PtoB* were transformed to express either pEDV6-*YFP*, pEDV6-*Mh270* or pEDV6-*ATR13*. Unfortunately, neither *Pst*ΔCEL nor *Pst*ΔAvrPto/ΔAvrPtoB showed an enhanced growth when expressing *Mh270* or *ATR13* in comparison to *YFP*. For *Mh270* we cannot rule out the possibility that it works in combination with other *Pst* DC3000 effectors in order to contribute to significantly enhance bacterial growth. Thus, the full complement of *Pst* DC3000 effectors is necessary to see the enhanced bacterial growth conferred by *Mh270*. In addition, neither *ATR13* nor *Mh270* were able to reduce callose deposition when delivered by *Pst*ΔCEL. The results for *ATR13* were surprising since *ATR13* had previously been shown increase bacterial growth *in planta*; it is also supposed to suppress PAMP-triggered callose deposition when delivered by *Pst*ΔCEL (Sohn et al., 2007). The reasons for the discrepancy between our data and published data may be due to differences in the experimental set-ups. For example, Sohn et al. inoculated Col-0 with 5×10^5 cfu/mL *Pst*ΔCEL carrying pEDV3 -*ATR13*^{Emoy2}, whereas I inoculated more of these bacteria into the leaves, 5×10^6 cfu/mL *Pst*ΔCEL carrying pEDV3 -*ATR13*^{Emco5} for the bacterial growth assays. The denser bacterial suspensions used in our lab may have led to stronger disease symptoms and masked any subtle differences in virulence and callose deposition due to the expression of *ATR13*.

4.6 A GFP-tagged Mh270 shows different sub-cellular location in roots versus leaves.

Based on the fact that *Pst-LUX* delivery of Mh270 into the plant enhanced bacterial growth, we presumed that nematode-secreted Mh270 is also destined for the plant cell cytoplasm. To determine where it may localize in the plant cell, stable transformed Arabidopsis lines expressing Mh270 tagged at the C-terminus with GFP (Mh270-GFP) were generated. The plants produced a GFP signal with nucleo-cytosolic localization in the roots. In contrast, in leaf tissue, Mh270-GFP showed a chloroplastic localization. Subsequent Western blot analyses of transgenic lines revealed that only Mh270-GFP is a stable protein fusion, in which full-length Mh270 was fused C-terminally to GFP. Transgenic plants expressing full-length N-terminal fusion of YFP to Mh270 were also made, but the tagged Mh270 was not detectable on the Western blot. Only a band of the size of GFP was present on the blot, suggesting that Mh270 had been degraded or cleaved from the tag.

The TargetP algorithm did not predict chloroplast transit peptide for Mh270. However, its chloroplastic localization in leaves suggests that Mh270 can be targeted to the chloroplast and that it may have a novel N-terminal transit peptide. The instability of the N-terminal fusion suggests the presence of a cleavable peptide. As chloroplast transit peptides often have cleavage sequences, the N-terminal transit peptide and the N-terminal fluorescent tag may both be cleaved from the protein (Nielsen et al., 1997; Petre et al., 2015).

In general, chloroplasts present interesting targets for pathogens as they are not only providing the plant with energy and, thus, having a strong impact on metabolism but they are also involved in the synthesis of plant hormones. The initial steps of the JA biosynthetic pathway are situated in the chloroplast (Bell et al., 1995). Additionally, the shikimic acid pathway in the chloroplast produces chorismate, which is a precursor for the defense signaling molecule salicylic acid (Mano and Nemoto, 2012; Wildermuth et al., 2001). There are examples of pathogens that contain effectors that target the chloroplast to manipulate the host to their advantage. *Pseudomonas syringae* pv. *maculicola* secretes an effector termed HopI1 that localizes to the chloroplast to suppress SA associated responses (Jelenska et al., 2007). Additionally, *Pyrenophora tritici-repentis* uses *ToxA* and *ToxB* to alter the chloroplasts of wheat to induce ROS which allows the pathogen to cause disease on infected plants (Ciuffetti et al., 2010). These examples show that pathogens may secrete effectors that are targeted to the chloroplast to efficiently manipulate the plants to their advantage.

4.6 Mh270 interacts with AtVDAC3 in a yeast-two-hybrid assay

To understand the function of a potential effector candidate it is helpful to understand if the effector targets a host protein. Thus, a yeast-two-hybrid assay was performed using two different libraries and identified AtVDAC3 as an interaction partner of Mh270 in yeast.

VDAC proteins present interesting interaction candidates for effectors. VDACs have been most prominently researched in mammalian cells, where they have been shown to control the flux of metabolites, ions, nucleotides, and calcium across the outer mitochondrial membrane to the cytosol. The structure of VDAC is typically a porin-type β -barrel diffusion pore with an estimated size of 30kDa (Benz, 1994). The VDACs normally localize to the highly permeable outer membrane of mitochondria (OMM), and in mammalian cells, the VDACs are important in apoptosis because they are involved in the release of apoptotic proteins (Brenner and Grimm, 2006) e.g. cytochrome *c*, which triggers a cascade that leads to cell death (Adrain and Martin, 2001). The importance of VDACs in cell metabolism was confirmed in silencing experiments where a *VDAC1* knockdown disrupted energy production and cell growth in human cell lines (Arif et al., 2014).

There has been less research regarding the role of VDACs in plants. In *Arabidopsis thaliana* five different VDAC isoforms are known (Lee et al., 2009), and they all localize to mitochondria (Hoogenboom et al., 2007). Expression of 4 of these *AtVDACs* can be induced by environmental stresses such as high salt (Lee et al., 2009; Zhang et al., 2015), and there is also evidence for Arabidopsis VDACs involvement in plant defense. For example, four of the *VDAC* genes were up-regulated in Arabidopsis inoculated with *Pst* DC3000 (Lee et al., 2009). Moreover, in *Nicotiana benthamiana*, *NbVDAC1* and *NbVDAC2* expression was upregulated after *Pseudomonas cichorri* infection, and silencing of these VDACs compromised plant defenses against this pathogen (Tateda et al., 2008). It has been speculated that plant VDACs are playing a role in plant defense through their involvement in mitochondria-mediated cell death. In fact, features of the hypersensitive response (HR) that occurs in plants after pathogen attack bear hallmarks of apoptosis (Gilchrist, 1998). Thus, VDACs may be a conserved mitochondrial element in both plant and animal programmed cell death. Evidence for this conservation in function lies in data showing that expression of a rice *VDAC* (*osVDAC4*) in the Jurkat T-cell line induced apoptosis (Godbole et al., 2003). In addition, four of the Arabidopsis VDACs, including the Mh270 interacting partner VDAC3, could functionally complement the yeast *VDAC* mutant, suggesting that VDAC function is conserved between plants and yeast. In yeast, VDAC has a role in mediating apoptotic changes in yeast mitochondria. Exactly how the

VDACs may be regulating plant cell death (and plant defense) is unknown, but (Tateda et al., 2008) showed that H₂O₂ production was reduced in *NbVDAC1*-silenced *N. benthamiana* plants infected with *Pseudomonas cichorii*, compared to the controls, suggesting that plant VDACs may regulate cytosolic ROS levels. In summary, plant VDACs are thought to be localized to the outer mitochondrial membrane, where, after pathogen stress, they may be involved in opening the mitochondrial permeability transition pore. This may lead to an increase in cytosolic ROS levels and cell death, which could contribute to plant defense (Kusano et al., 2009).

In the leaves containing fluorescently tagged Mh270 is localized to the chloroplasts, not to the mitochondria. Although Mh270 does not seem to localize specifically to mitochondria, an interaction between AtVDAC3 and Mh270 cannot be excluded. For example, Mh270 could be targeted to both the mitochondria and the chloroplast, as a “dually targeted protein.” This scenario is similar to the rust fungal effector CTP1, which is targeted to both the plant mitochondria and the chloroplast, although its accumulation in the mitochondria is weak (Petre et al 2015). Moreover, transit peptides of chloroplasts and mitochondria contain similar traits (Carrie and Small, 2013) which could lead to a nonspecific targeting of Mh270 to chloroplasts in leaves (Petre et al., 2015). As a result, Mh270 is possibly mis-localized to the chloroplasts, and its cytoplasmic localization, as seen in roots, represents its true sub-cellular localization. This sort of mis-localization in the aerial chloroplasts was previously documented in *Arabidopsis* expressing the binding domain of glucocorticoid receptor fused to GFP (GFP/BDGR) (Brockmann et al., 2001). These proteins were cytoplasmically localized in the roots, but were incorrectly targeted to the plastids in the leaves. Such mis-localization was explained by suggesting that the fusion proteins may be sequestered to the chloroplast through a leaf-specific chaperone (Brockmann et al., 2001). Dual localization or bifluorescence complementation studies must be performed to confirm the *in planta* interaction of Mh270 and AtVDAC3 and its subcellular localization.

Because VDAC3 is a membrane-associated protein, it was surprising to see an interaction between it and Mh270 in yeast. However, recent publications have shown that when VDAC3 is used as a bait in a traditional yeast-two-hybrid screen, it can interact with the plant-specific kinesin KP1 and with chloroplast protein thioredoxin m2 AtTRXM2 (AT4G03520) (Yang et al., 2011; Zhang et al., 2015). *Arabidopsis* VDACs can accumulate to a small degree in the cytosol, which may explain these interactions in the yeast screens (Lister et al., 2007). In addition, work in human cells suggests any modification of the N-terminus, including

placement into a yeast vector for a yeast-two-hybrid screen, may inhibit the expression of VDAC1 at the cell membranes (Schwarzer et al., 2002). This would mean that VDACS used in yeast work would likely be mis-localized to the cytoplasm. Therefore, while the interaction between Mh270 and VDAC3 may be real in our yeast-two-hybrid assay, additional experiments as a co-immunoprecipitation assay will be needed to confirm that this interaction takes place *in planta*, and is not an artifact of the yeast system used.

Assuming that the interaction between Mh270 and VDAC3 *in planta* can be confirmed, it is tempting to speculate about the protein-protein interaction and how that may affect the plant-nematode interaction. In addition from influencing cell death, the potential involvement of VDAC in ROS production and cell death presents a promising area to look at in more detail. ROS as a signal compound has received a lot of attention in the last few years. It has been shown that ROS are involved in both stress (Baxter et al., 2013) and pathogen (Torres et al., 2006) associated signaling. A direct impact of ROS altered signaling has been found for the cyst nematode *Heterodora schachtii*. NADPH (reduced form of nicotinamide adenine dinucleotide phosphate) oxidase double mutant lines *rbohD* and *rbohF* are impaired in the production of apoplastic ROS and this alters the plant responses to pathogens (Torres et al 2006). Plants with loss-of-function mutations in *rbohD* or *rbohD* and *rbohF* (*rbohD/F*), were less susceptible to cyst nematodes infection. It seems that the cyst nematode need an initial ROS burst to successfully manipulate the plant to create a feeding site. It may be using ROS to suppress the spread from the initial feeding site of SA-mediated signals that trigger plant defense responses (Siddique et al., 2014). RKN also seem to depend on the presence of functional NADPH oxidase since *M. incognita* had less success infecting *Arabidopsis robohd/F* mutant line (C. Gleason, personal communication). Thus, nematodes seem to be using ROS levels to fine-tune the plant responses during parasitism.

Overall, there are several possible ways as to how Mh270's interaction with VDAC3 might contribute to *M. hapla* infections. Interaction of Mh270 with VDAC3 could be a positive interaction, in which Mh270 influences the opening the mitochondrial permeability transition pore, resulting in increased cytosolic ROS levels. With the evidence that the nematode needs a transient elevation of ROS to prevent the spread of SA-defense signals from its feeding site (Siddique et al 2014), Mh270 could induce short-lived ROS production in the early stages of infection. However, ROS is a double-edged sword that can also induce cell death, and in the later stages of the feeding site formation, it is thought that the nematode is actively trying to suppress ROS production and cell death. With this in mind, Mh270 may block the opening of

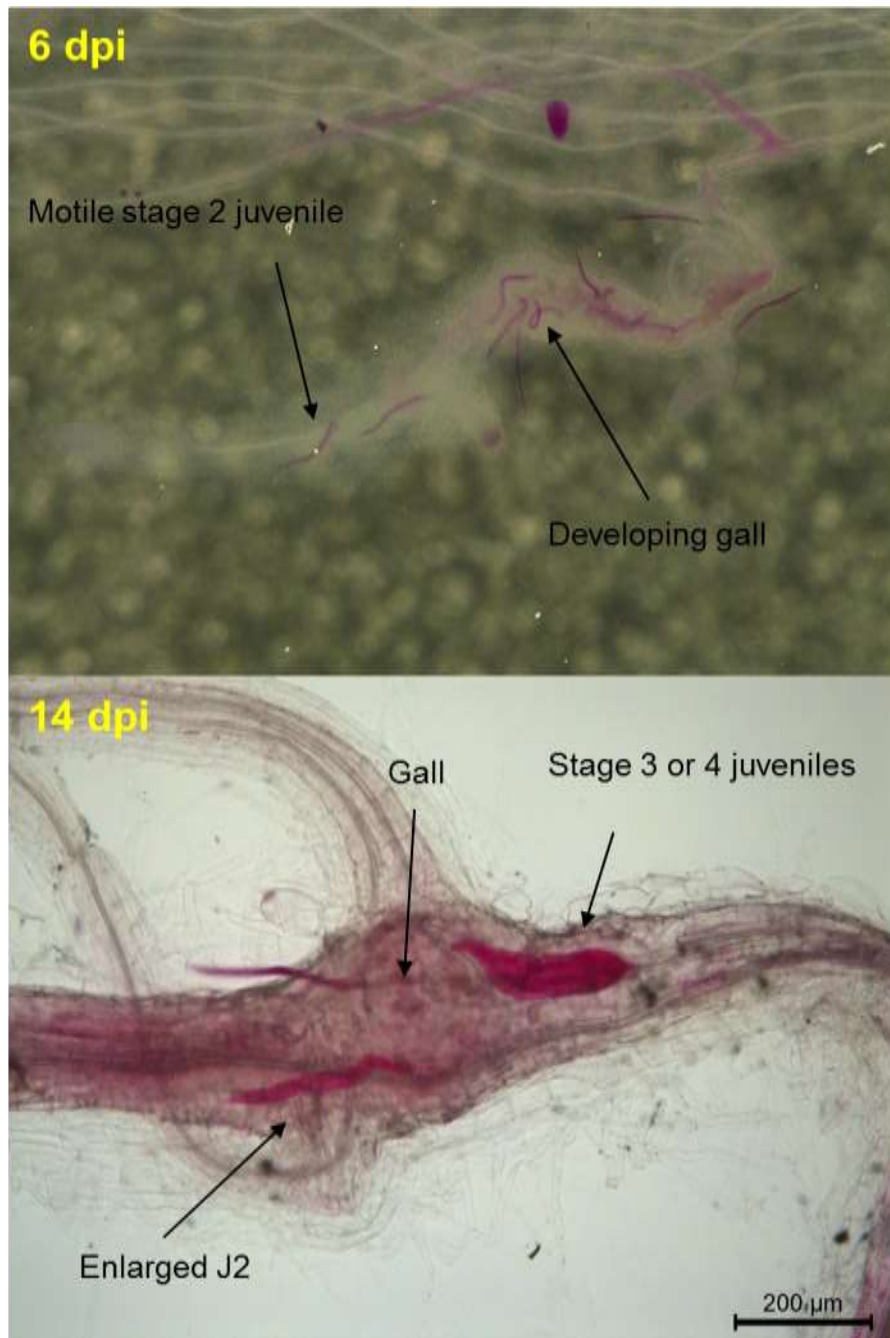
the mitochondrial permeability transition pore and prevent the leakage of compounds that can lead to cell death. In this scenario, the nematode is trying to avoid triggering a cell death response in the feeding cells. Future work on Mh270 and VDAC3 will hopefully continue to shed light on their possible roles in the plant-nematode interaction.

5. Appendix

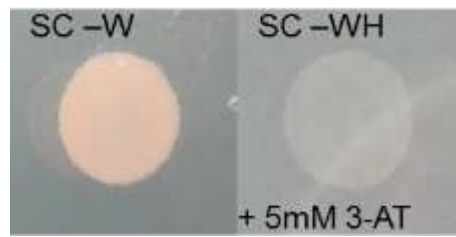
Supplemental Table 1 : Effector candidates extracted from the *M. hapla* proteome. Effector candidates that were chosen in an initial, visual screen of the proteome of Mbeunkui et al 2010 are presented. “Prot. Nr.,” indicates the number given to the peptide, as indicated in this proteome paper. Highest similarity of the proteins after a BLASTp search of the nr database is shown. SP indicates a presence or absence of classic secretion signal, FL ORF , indicates whether a complete open reading frame could be found in the *M. hapla* genome, Glycosylation, indicates whether predicted glycosylation sites are present using GlycoEP, Trans.Domain , indicates the presence or absence of predicted transmembrane domains.

Prot. Nr.	Highest similarity (NCBI blastP)	SP	FL ORF	Glycosylated	Transm. Domain
7	Transthyretin-like protein 46 [Ascaris suum]	Yes	Yes	No	No
17	No	Yes	Yes	Yes	Not tested
22	No	No	Yes	Not tested	Not tested
30	No	No	Yes	Not tested	Not tested
39	putative aminopeptidase E [Prevotella stercorea DSM 18206]	No	Yes	Not tested	Not tested
57	Protein F42A10.5 [Caenorhabditis elegans]	No	Yes	Not tested	Not tested
61	thiamin pyrophosphokinase [Loa loa]	Yes	Yes	Yes	Not tested
70	hypothetical protein A1Q1_03930 [Trichosporon asahii var. asahii CBS 2479]	No	Yes	Not tested	Not tested
78	poly(A+) RNA-binding protein, putative [Ogataea parapolyomorpha DL-1]	No	Yes	Not tested	Not tested
79	EsV-1-1 [Ectocarpus siliculosus]	No	Yes	Not tested	Not tested
86	manganese superoxide dismutase [Meloidogyne incognita] >emb CAR97796.1	No	Yes	Not tested	Not tested
88	hypothetical protein CAEBREN_07369 [Caenorhabditis brenneri]	No	Yes	Not tested	Not tested
92	CBN-CHCH-3 protein [Caenorhabditis brenneri]	No	Yes	Not tested	Not tested
93	hypothetical protein CRE_12377 [Caenorhabditis remanei]	Yes	Yes	Yes	Not tested
94	hypothetical protein WUBG_07095 [Wuchereria bancrofti]	No	Yes	Not tested	Not tested
97	GTP-binding nuclear protein RAN/TC4 [Brugia malayi]	Yes	No	Not tested	Not tested
107	phosphoribosyltransferase [Chelativorans sp. BNC1]	Yes	Yes	Yes	Not tested
123	Dystrophin-1 [Ascaris suum]	No	Yes	Not tested	Not tested
128	ATP-dependent DNA helicase [Helicobacter mustelae 12198]	No	Yes	Not tested	Not tested
135	similar to breast carcinoma amplified sequence 2 [Brugia malayi]	No	Yes	Not tested	Not tested
139	superoxide dismutase [Globodera rostochiensis]	No	Yes	Not tested	Not tested
148	SKP-1 protein [Loa loa]	No	Yes	Not tested	Not tested
149	No	No	No	Not tested	Not tested
152	hypothetical protein LOAG_01926 [Loa loa]	No	Yes	Not tested	Not tested
157	putative vitellogenin precursor-like protein [Ascaris suum]	No	Yes	Not tested	Not tested
166	hypothetical protein CRE_17428 [Caenorhabditis remanei]	Yes	Yes	Yes	Not tested
168	24 kDa protein [Anisakis simplex]	No	Yes	Not tested	Not tested
175	hypothetical protein SELMODRAFT_424859 [Selaginella moellendorffii]	No	Yes	Not tested	Not tested
178	Peptidyl-prolyl cis-trans isomerase FKBP9 [Ascaris suum]	Yes	Yes	Yes	Not tested
181	hypothetical protein CRE_19590 [Caenorhabditis remanei]	Yes	Yes	Yes	Not tested
182	C. briggsae CBR-HSP-12.2 protein [Caenorhabditis briggsae]	No	Yes	Not tested	Not tested
190	Prolyl carboxy peptidase like protein 5 [Ascaris suum]	Yes	Yes	Yes	Not tested
195	Toll-interacting protein [Ascaris suum]	No	Yes	Not tested	Not tested
197	Unknown [Ascaris suum]	No	Yes	Not tested	Not tested
209	conserved unknown protein [Ectocarpus siliculosus]	No	Yes	Not tested	Not tested
210	serine proteinase [Heterodera glycines]	Yes	Yes	Yes	No
214	Peptide transporter family 2 [Ascaris suum]	Yes	Yes	Yes	Not tested
221	No	No	Yes	Not tested	Not tested
222	Chondroitin proteoglycan 3 [Ascaris suum]	Yes	Yes	No	No
224	hypothetical protein CAEBREN_08311 [Caenorhabditis brenneri]	No	Yes	Not tested	Not tested
230	hypothetical protein PCC8801_3854 [Cyanospora sp. PCC 8801]	No	Yes	Not tested	Not tested
246	late embryogenesis abundant domain-containing protein [Toxoplasma gondii ME49]	No	Yes	Not tested	Not tested
247	No	Yes	Yes	No	No
248	Plasminogen activator inhibitor 1 RNA-binding protein [Salmo salar]	No	Yes	Not tested	Not tested
249	FI06040p [Drosophila melanogaster]	No	Yes	Not tested	Not tested
257	hypothetical protein CRE_08539 [Caenorhabditis remanei]	Yes	Yes	No	No
260	CBN-CRI-3 protein [Caenorhabditis brenneri]	No	Yes	Not tested	Not tested
263	Unknown, partial [Ascaris suum]	No	Yes	Not tested	Not tested
264	hypothetical protein LOAG_05492 [Loa loa]	No	Yes	Not tested	Not tested
265	predicted protein [Micromonas pusilla CCMP1545] >	Yes	Yes	No	No
266	hypothetical protein TcasGA2_TC010248 [Tribolium castaneum]	No	No	Not tested	Not tested
267	outer membrane lipoprotein carrier protein LoaA [Sphingopyxis alaskensi]	No	Yes	Not tested	Not tested
270	transthyretin-like protein 2 precursor [Radopholus similis]	Yes	Yes	No	No
271	hypothetical protein [Candida glabrata CBS 138]	Yes	Yes	Not tested	Not tested
275	regulatory protein [Bacteroides thetaiotaomicron VPI-5482] >ref ZP_09940686.1	No	Yes	Not tested	Not tested

Prot. Nr.	Highest similarity (NCBI blastP)	SP	FL ORF	Glycosylated	Transm. Domain
280	Phosphatidylethanolamine-binding protein [Ascaris suum]	No	Yes	Not tested	Not tested
281	FkbM family methyltransferase [Mesorhizobium alhagi CCNWXJ12-2] 2]	No	Yes	Not tested	Not tested
292	polymerase [Woodchuck hepatitis virus]	No	Yes	Not tested	Not tested
296	UDP-sugar diphosphatase [Loa loa]	No	Yes	Not tested	Not tested
298	No	No	Yes	Not tested	Not tested
299	hypothetical protein [Frankia alni ACN14a] >emb CAJ64519.1 hypotheti	Yes	Yes	Yes	Not tested
301	protein phosphatase 1, catalytic subunit, beta isoform, like [Danio rerio]	No	Yes	Not tested	Not tested
306	Deoxyribodipyrimidine photolyase [Methylophaga sp. JAM1]	No	Yes	Not tested	Not tested
308	ubiquitin conjugating enzyme protein 13 [Brugia malayi] >gb EDP3284	No	Yes	Not tested	Not tested
309	protein phosphatase 1, catalytic subunit, beta isoform, like [Danio rerio]	Yes	Yes	No	No
311	NSFL1 cofactor p47 [Ascaris suum]	Yes	Yes	Yes	Not tested
312	No	Yes	No	Yes	Not tested
313	No	Yes	Yes	Yes	Not tested
314	SPV110 hypothetical protein [Swinpox virus]	No	Yes	Not tested	Not tested
315	hypothetical protein Bm1_38120 [Brugia malayi]	Yes	Yes	Not tested	Not tested
331	hypothetical protein CAEBREN_01558 [Caenorhabditis brenneri]	No	Yes	Not tested	Not tested
333	Zinc metalloproteinase nas-30 [Ascaris suum]	No	Yes	Not tested	Not tested
337	hypothetical protein, variant [Loa loa]	No	Yes	Not tested	Not tested
341	predicted Zn-dependent peptidase [Erythrobacter sp. NAP1] >gb EAQ29	Yes	Yes	Yes	Not tested
346	Protein HMG-1.1 [Caenorhabditis elegans]	No	Yes	Not tested	Not tested
351	Pepsin inhibitor Dit33 [Ascaris suum]	Yes	Yes	Yes	Not tested
352	SR00449 [Strongyloides ratti]	Yes	Yes	Yes	Not tested
356	Protein H03E18.1 [Caenorhabditis elegans]	No	Yes	Not tested	Not tested
357	UVrD_2 Superfamily	No	No	Not tested	Not tested
360	AGAP003976-PA [Anopheles gambiae str. PEST]	No	Yes	Not tested	Not tested
363	hypothetical protein LOAG_17132 [Loa loa]	No	Yes	Not tested	Not tested
368	hypothetical protein WUBG_07172 [Wuchereria bancrofti]	No	Yes	Not tested	Not tested
380	RE40412p [Brugia malayi] >gb EDP37891.1 RE40412p, putative [Brugia malayi]	No	Yes	Not tested	Not tested
381	No	No	Yes	Not tested	Not tested
390	hypothetical protein LEMA_P076930.1 [Leptosphaeria maculans JN3]	No	Yes	Not tested	Not tested
392	hypothetical protein WUBG_04255 [Wuchereria bancrofti]	No	Yes	Not tested	Not tested
405	Nascent polypeptide-associated complex subunit alpha [Ascaris suum]	No	Yes	Not tested	Not tested
411	hypothetical protein LOAG_05514 [Loa loa]	No	Yes	Not tested	Not tested
413	hypothetical protein LOAG_05514 [Loa loa]	No	Yes	Not tested	Not tested
414	thioredoxin-disulfide reductase [Candidatus Pelagibacter ubique HTCC1002]	No	Yes	Not tested	Not tested
417	No	No	No	Not tested	Not tested
444	No	Yes	Yes	Not tested	Not tested
446	Y43F8B.1b-like protein [Bursaphelenchus xylophilus]	No	Yes	Not tested	Not tested
447	ICD-1 protein [Loa loa] >gb EFO25461.1 ICD-1 protein [Loa loa]	No	Yes	Not tested	Not tested
449	cathepsin D-like aspartic proteinase preproprotein [Meloidogyne incognita]	No	Yes	Not tested	Not tested
456	hypothetical protein CRE_18041 [Caenorhabditis remanei] >gb EFP08	No	Yes	Not tested	Not tested
457	PREDICTED: uncharacterized protein LOC100870442 [Apis florea]	No	Yes	Not tested	Not tested
459	Hypothetical protein CBG03955 [Caenorhabditis briggsae]	No	Yes	Not tested	Not tested
460	PREDICTED: uncharacterized protein LOC100870442 [Apis florea]	No	Yes	Not tested	Not tested
465	hypothetical protein LOAG_02299 [Loa loa]	Yes	Yes	Yes	Not tested
466	Protein T21G5.4 [Caenorhabditis elegans]	Yes	No	Yes	Not tested
478	glycosyl transferase family protein [Mucilaginibacter paludis DSM 186	No	Yes	Not tested	Not tested
479	AGAP012028-PA [Anopheles gambiae str. PEST] >gb EAL38787.3 AG	No	Yes	Not tested	Not tested
481	hypothetical protein DAPPUDRAFT_306287 [Daphnia pulex]	No	Yes	Not tested	Not tested
482	major facilitator transporter [Beijerinckia indica subsp. indica ATCC 9039]	No	Yes	Not tested	Not tested
484	innexin unc-9 [Trichinella spiralis] >gb EFV54609.1 innexin unc-9 [Trichinella	No	Yes	Not tested	Not tested
489	CBN-RPN-11 protein [Caenorhabditis brenneri]	No	Yes	Not tested	Not tested
487	Nucleoredoxin-like protein 2 [Ascaris suum]	No	Yes	Not tested	Not tested
491	CBN-RPN-11 protein [Caenorhabditis brenneri]	No	Yes	Not tested	Not tested
499	Glutaredoxin 3, partial [Ascaris suum]	No	Yes	Not tested	Not tested
506	No	Yes	Yes	Yes	Not tested



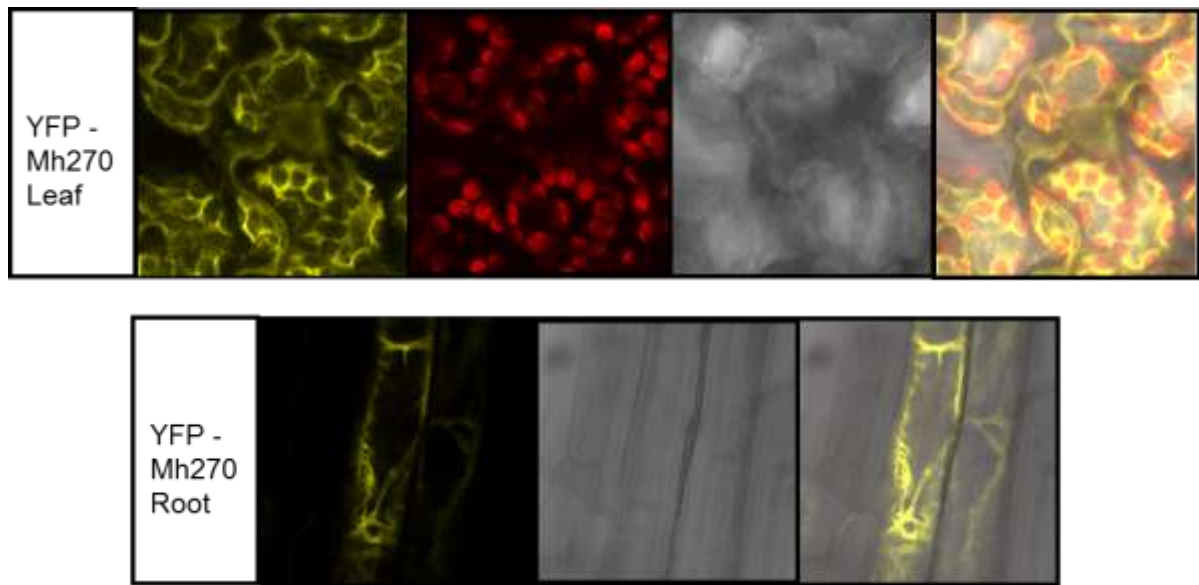
Supplemental Figure 1 : Representative photographs of *M. hapla* in Col-0 roots stained with acid fuchsin. Wild type Col-0 plants were infected with 200 surface sterilized *M. hapla* and galls were allowed to develop for 6 dpi (top) and 14 dpi (bottom). Roots were stained using acid fuchsin. Arrows indicate either nematodes, developing or mature galls dpi= days post infection.



Supplemental Figure 2: Mh270 does not cause autoactivation of the yeast reporter gene. Yeast grown on selective plates for pASII showed normal growth on control plates (SC-W). Yeast did not grow on media lacking histidine and containing additionally the enzymatic inhibitor 3-AT (SC-WH +5 mM 3-AT).

Supplemental Table 2 : Complete list of interactors found in the yeast-two-hybrid screen. Working number, the library in which the candidate was identified the AGI code, and the gene name (“Protein”) according to TAIR.

Working Nr.	Library	AGI code	Protein
Y1	Cell	AT4G08950	EXO, EXORDIUM - OMAIN/s: Phosphate-induced protein 1
Y2	Cell	AT5G46430	Ribosomal protein L32e
Y3	Cell	AT3G17390	MAT4, METHIONINE ADENOSYLTRANSFERASE 4
Y4	Cell	AT4G05010	ATFBS3, F-BOX STRESS INDUCED 3, FBS3
Y5	Cell	AT2G41475	Embryo- specific protein 3, (AT53)
Y6	Cell	AT5G08180	Ribosomal protein L7Ae/L30e/S12e/Gadd45 family protein
Y7	Cell	AT5G46430	Ribosomal protein L32e
Y8	Cell	AT2G47550	Plant invertase/pectin methyltransferase inhibitor superfamily
Y9	Cell	AT4G36980	molecular_function unknown
Y11	Cell	AT1G41740	gypsy-like retrotransposon family
Y12	Cell	AT3G59900	ARGOS, AUXIN-REGULATED GENE INVOLVED IN ORGAN SIZE
Y13	Cell	AT5G28150	Plant protein of unknown function (DUF868)
Y14	Cell	AT5G08450	HDC1, HISTONE DEACETYLATION COMPLEX 1, RXT3-LIKE
Y15	Cell	AT1G41740	gypsy-like retrotransposon family
Y16	Cell	AT1G20920	RCF1, REGULATOR OF CBF GENE EXPRESSION 1
Y17	Cell	AT4G36980	molecular_function unknown
Y18	Cell	AT2G21850	Cysteine/Histidine-rich C1 domain family protein
Y19	Cell	AT1G20920	RCF1, REGULATOR OF CBF GENE EXPRESSION 1
Y20	Cell	AT5G28150	Plant protein of unknown function (DUF868)
Y21	Cell	AT5G19590	Protein of unknown function, DUF538
Y22	Cell	AT1G41740	gypsy-like retrotransposon family
Y23	Cell	AT1G20920	RCF1, REGULATOR OF CBF GENE EXPRESSION 1
Y24	Cell	AT1G20920	RCF1, REGULATOR OF CBF GENE EXPRESSION 1
Y25	Cell	AT2G42680	MULTIPROTEIN BRIDGING FACTOR 1A, ATMBF1A, MBF1A, MULTIPROTEIN BRIDGING FACTOR 1A
Y26	Cell	AT1G20920	RCF1, REGULATOR OF CBF GENE EXPRESSION 1
Y27	Cell	AT3G12500	ATHCHIB, B-CHI, BASIC CHITINASE, CHI-B, HCHIB, PATHOGENESIS-RELATED 3, PR-3, PR3
Y28	Cell	AT2G33370	Ribosomal protein L14p/L23e family protein
Y29	Cell	AT5G37740	Calcium-dependent lipid-binding (CaLB domain) family protein
Y30	Cell	AT5G48335	unknown protein
Y31	Cell	AT2G19570	AT-CDA1, CDA1, CYTIDINE DEAMINASE 1, DESZ
Y32	Cell	AT3G57320	unknown protein
Y33	Cell	AT4G13195	CLAVATA3/ESR-RELATED 44, CLE44
Y34	Cell	AT4G35830	ACO1, ACONITASE 1
Y35	Cell	AT1G70600	Ribosomal protein L18e/L15 superfamily protein
Y37	Cell	AT5G60980	Nuclear transport factor 2 (NTF2) family protein with RNA binding (RRM-RBD-RNP motifs) domain
Y38	Cell	AT1G20920	RCF1, REGULATOR OF CBF GENE EXPRESSION 1
Y39	Cell	AT2G19570	AT-CDA1, CDA1, CYTIDINE DEAMINASE 1, DESZ
Y40	Cell	AT5G47690	binding; FUNCTIONS IN: binding; INVOLVED IN: biological_process unknown
Y41	Cell	AT5G40850	UPM1, UROPHORPHYRIN METHYLASE 1
Y42	Cell	AT5G40850	UPM1, UROPHORPHYRIN METHYLASE 1
Y43	Cell	AT4G11110	SPA1-RELATED 2, SPA2
Y44	Cell	AT4G11420	ATEIF3A-1, ATTIF3A1, EIF3A, EIF3A-1, EUKARYOTIC TRANSLATION INITIATION FACTOR 3A, TIF3A1
Y45	Root	AT5G64570	ARABIDOPSIS THALIANA BETA-D-XYLOSIDASE 4, ATBXL4, BETA-D-XYLOSIDASE 4, XYL4
Y46	Root	AT2G30020	Encodes AP2C1. Belongs to the clade B of the PP2C-superfamily.
Y47	Root	AT4G36980	FUNCTIONS IN: molecular_function unknown
Y48	Root	AT1G64850	Calcium-binding EF hand family protein
Y49	Root	AT5G15090	ARABIDOPSIS THALIANA VOLTAGE DEPENDENT ANION CHANNEL 3, ATVDAC3, VDAC3,
Y50	Root	AT3G02040	ATGDPD1, GDPD1, GLYCEROPHOSPHODIESTER PHOSPHODIESTERASE 1, SENESCENCE-RELATED GENE 3, SRG
Y51	Root	AT4G31800	ARABIDOPSIS THALIANA WRKY DNA-BINDING PROTEIN 18, ATWRKY18, WRKY DNA-BINDING PROTEIN 18,
Y52	Root	AT5G47210	Hyaluronan / mRNA binding family
Y53	Root	AT2G02180	TOBAMOVIRUS MULTIPLICATION PROTEIN 3, TOM3
Y54	Root	AT3G02470	S-ADENOSYLMETHIONINE DECARBOXYLASE, SAMDC
Y55	Root	AT5G15090	ARABIDOPSIS THALIANA VOLTAGE DEPENDENT ANION CHANNEL 3, ATVDAC3, VDAC3,
Y56	Root	AT1G02500	ATSAM1, MAT1, METK1, S-ADENOSYLMETHIONINE SYNTHETASE 1, SAM-1, SAM1
Y57	Root	AT5G17690	ATLHP1, LHP1, LIKE HETEROCHROMATIN PROTEIN 1, TERMINAL FLOWER 2, TFL2
Y58	Root	AT1G44800	SIAR1, SILIQUES ARE RED 1, UMAMIT18, USUALLY MULTIPLE ACIDS MOVE IN AND OUT TRANSPORTERS 18
Y59	Root	AT2G43130	ARA-4, ARA4, ARABIDOPSIS RAB GTPASE HOMOLOG 5C, ATRAB11F, ATRABASC, RABASC
Y60	Root	AT2G30020	Encodes AP2C1. Belongs to the clade B of the PP2C-superfamily.
Y61	Root	AT2G02180	TOBAMOVIRUS MULTIPLICATION PROTEIN 3, TOM3
Y62	Root	AT2G02180	TOBAMOVIRUS MULTIPLICATION PROTEIN 3, TOM3
Y63	Root	AT2G01890	ATPAP8, PAP8, PURPLE ACID PHOSPHATASE 8
Y64	Root	AT1G05700	Leucine-rich repeat transmembrane protein kinase protein
Y65	Root	AT1G44800	SIAR1, SILIQUES ARE RED 1, UMAMIT18, USUALLY MULTIPLE ACIDS MOVE IN AND OUT TRANSPORTERS 18



Supplemental Figure 3 : Subcellular localization of YFP-Mh270. Stable transformed Arabidopsis plants were grown on MS media for one week. Fluorescence was observed using confocal microscopy with the appropriate filter set. YFP-270 localization in leaves (top) and roots (bottom) are presented.

References

- Abad, P., Gouzy, J., Aury, J.-M., Castagnone-Sereno, P., Danchin, E.G.J., Deleury, E., Perfus-Barbeoch, L., Anthouard, V., Artiguenave, F., Blok, V.C., et al. (2008). Genome sequence of the metazoan plant-parasitic nematode *Meloidogyne incognita*. *Nat. Biotechnol.* *26*, 909–915.
- Absmanner, B., Stadler, R., and Hammes, U.Z. (2013). Phloem development in nematode-induced feeding sites: the implications of auxin and cytokinin. *Front. Plant Sci.* *4*.
- Adrain, C., and Martin, S.J. (2001). The mitochondrial apoptosome: a killer unleashed by the cytochrome seas. *Trends Biochem. Sci.* *26*, 390–397.
- Arif, T., Vasilkovsky, L., Refaely, Y., Konson, A., and Shoshan-Barmatz, V. (2014). Silencing *VDAC1* Expression by siRNA Inhibits Cancer Cell Proliferation and Tumor Growth In Vivo. *Mol. Ther. — Nucleic Acids* *3*, e159.
- Asai, T., Tena, G., Plotnikova, J., Willmann, M.R., Chiu, W.-L., Gomez-Gomez, L., Boller, T., Ausubel, F.M., and Sheen, J. (2002). MAP kinase signalling cascade in Arabidopsis innate immunity. *Nature* *415*, 977–983.
- Barcala, M., García, A., Cabrera, J., Casson, S., Lindsey, K., Favery, B., García-Casado, G., Solano, R., Fenoll, C., and Escobar, C. (2010). Early transcriptomic events in microdissected Arabidopsis nematode-induced giant cells. *Plant J.* *61*, 698–712.
- Barker, K.R., Hussey, R.S., Krusberg, L.R., Bird, G.W., Dunn, R.A., Ferris, H., Ferris, V.R., Freckman, D.W., Gabriel, C.J., Grewal, P.S., et al. (1994). Plant and Soil Nematodes: Societal Impact and Focus for the Future. *J. Nematol.* *26*, 127–137.
- Baxter, A., Mittler, R., and Suzuki, N. (2013). ROS as key players in plant stress signalling. *J. Exp. Bot.* *ert375*.
- Bell, E., Creelman, R.A., and Mullet, J.E. (1995). A chloroplast lipoxygenase is required for wound-induced jasmonic acid accumulation in Arabidopsis. *Proc. Natl. Acad. Sci.* *92*, 8675–8679.
- Bellafiore, S., Shen, Z., Rosso, M.-N., Abad, P., Shih, P., and Briggs, S.P. (2008). Direct identification of the *Meloidogyne incognita* secretome reveals proteins with host cell reprogramming potential. *PLoS Pathog.* *4*, e1000192.
- Benz, R. (1994). Permeation of hydrophilic solutes through mitochondrial outer membranes: review on mitochondrial porins. *Biochim. Biophys. Acta BBA - Rev. Biomembr.* *1197*, 167–196.
- Bird, A.F. (1959). The Attractiveness of Roots To the Plant Parasitic Nematodes *Meloidogyne Javanica* and *M. Hapla*. *Nematologica* *4*, 322–335.
- de Boer, J.M., Yan, Y., Smant, G., Davis, E.L., and Baum, T.J. (1998). *In-situ* Hybridization to Messenger RNA in *Heterodera glycines*. *J. Nematol.* *30*, 309–312.
- Brenner, C., and Grimm, S. (2006). The permeability transition pore complex in cancer cell death. *Oncogene* *25*, 4744–4756.

- Brockmann, B., Smith, M.W., Zaraisky, A.G., Harrison, K., Okada, K., and Kamiya, Y. (2001). Subcellular localization and targeting of glucocorticoid receptor protein fusions expressed in transgenic *Arabidopsis thaliana*. *Plant Cell Physiol.* *42*, 942–951.
- Byrd, D.W., Kirkpatrick, T., and Barker, K.R. (1983). An Improved Technique for Clearing and Staining Plant Tissues for Detection of Nematodes. *J. Nematol.* *15*, 142–143.
- Carrie, C., and Small, I. (2013). A reevaluation of dual-targeting of proteins to mitochondria and chloroplasts. *Biochim. Biophys. Acta* *1833*, 253–259.
- Chauhan, J.S., Rao, A., and Raghava, G.P.S. (2013). In silico Platform for Prediction of N-, O- and C-Glycosites in Eukaryotic Protein Sequences. *PLoS ONE* *8*, e67008.
- Chen, X.-L., Shi, T., Yang, J., Shi, W., Gao, X., Chen, D., Xu, X., Xu, J.-R., Talbot, N.J., and Peng, Y.-L. (2014). N-glycosylation of effector proteins by an α -1,3-mannosyltransferase is required for the rice blast fungus to evade host innate immunity. *Plant Cell* *26*, 1360–1376.
- Chitwood, D.J., and Perry, R.N. (2009). Reproduction, Physiology and Biochemistry. In *Root-Knot Nematodes*, (CAB International), pp. 182–200.
- Choe, A., von Reuss, S.H., Kogan, D., Gasser, R.B., Platzer, E.G., Schroeder, F.C., and Sternberg, P.W. (2012). Ascaroside Signaling Is Widely Conserved among Nematodes. *Curr. Biol.* *22*, 772–780.
- Choi-Pheng, Y., and Birchfield, W. (1979). Resistance Host Studies and Reactions of Rice Cultivars to *Meloidogyne graminicola*. *Phytopathology* *497–499*.
- Ciuffetti, L.M., Manning, V.A., Pandelova, I., Betts, M.F., and Martinez, J.P. (2010). Host-selective toxins, Ptr ToxA and Ptr ToxB, as necrotrophic effectors in the *Pyrenophora tritici-repentis*–wheat interaction. *New Phytol.* *187*, 911–919.
- Clay, N.K., Adio, A.M., Denoux, C., Jander, G., and Ausubel, F.M. (2009). Glucosinolate Metabolites Required for an Arabidopsis Innate Immune Response. *Science* *323*, 95–101.
- Clough, S.J., and Bent, A.F. (1998). Floral dip: a simplified method for Agrobacterium-mediated transformation of *Arabidopsis thaliana*. *Plant J. Cell Mol. Biol.* *16*, 735–743.
- Cotton, J.A., Lilley, C.J., Jones, L.M., Kikuchi, T., Reid, A.J., Thorpe, P., Tsai, I.J., Beasley, H., Blok, V., Cock, P.J.A., et al. (2014). The genome and life-stage specific transcriptomes of *Globodera pallida* elucidate key aspects of plant parasitism by a cyst nematode. *Genome Biol.* *15*, R43.
- Cui, H., Tsuda, K., and Parker, J.E. (2015). Effector-Triggered Immunity: From Pathogen Perception to Robust Defense. *Annu. Rev. Plant Biol.* *66*, 487–511.
- Curtis, R.H.C. (2008). Plant-nematode interactions: environmental signals detected by the nematode's chemosensory organs control changes in the surface cuticle and behaviour. *Parasite Paris Fr.* *15*, 310–316.
- Dalzell, J.J., McMaster, S., Johnston, M.J., Kerr, R., Fleming, C.C., and Maule, A.G. (2009). Non-nematode-derived double-stranded RNAs induce profound phenotypic changes in *Meloidogyne incognita* and *Globodera pallida* infective juveniles. *Int. J. Parasitol.* *39*, 1503–1516.

- Danchin, E.G.J., Arguel, M.-J., Campan-Fournier, A., Perfus-Barbeoch, L., Magliano, M., Rosso, M.-N., Da Rocha, M., Da Silva, C., Nottet, N., Labadie, K., et al. (2013). Identification of Novel Target Genes for Safer and More Specific Control of Root-Knot Nematodes from a Pan-Genome Mining. *PLoS Pathog* 9, e1003745.
- DebRoy, S., Thilmony, R., Kwack, Y.-B., Nomura, K., and He, S.Y. (2004). A family of conserved bacterial effectors inhibits salicylic acid-mediated basal immunity and promotes disease necrosis in plants. *Proc. Natl. Acad. Sci. U. S. A.* 101, 9927–9932.
- Djamei, A., Schipper, K., Rabe, F., Ghosh, A., Vincon, V., Kahnt, J., Osorio, S., Tohge, T., Fernie, A.R., Feussner, I., et al. (2011). Metabolic priming by a secreted fungal effector. *Nature* 478, 395–398.
- Djian-Caporalino, C., Fazari, A., Arguel, M.J., Vernie, T., VandeCastele, C., Faure, I., Brunoud, G., Pijarowski, L., Palloix, A., Lefebvre, V., et al. (2007). Root-knot nematode (*Meloidogyne* spp.) Me resistance genes in pepper (*Capsicum annuum* L.) are clustered on the P9 chromosome. *TAG Theor. Appl. Genet. Theor. Angew. Genet.* 114, 473–486.
- Doyle, E.A., and Lambert, K.N. (2003). *Meloidogyne javanica* chorismate mutase 1 alters plant cell development. *Mol. Plant-Microbe Interact. MPMI* 16, 123–131.
- Elmore, J.M., Lin, Z.-J.D., and Coaker, G. (2011). Plant NB-LRR signaling: upstreams and downstreams. *Curr. Opin. Plant Biol.* 14, 365–371.
- Estelle, M.A., and Somerville, C. (1987). Auxin-resistant mutants of *Arabidopsis thaliana* with an altered morphology. *Mol. Gen. Genet. MGG* 206, 200–206.
- Eves-van den Akker, S., Lilley, C.J., Ault, J.R., Ashcroft, A.E., Jones, J.T., and Urwin, P.E. (2014a). The Feeding Tube of Cyst Nematodes: Characterisation of Protein Exclusion. *PLoS ONE* 9, e87289.
- Eves-van den Akker, S., Lilley, C.J., Jones, J.T., and Urwin, P.E. (2014b). Identification and Characterisation of a Hyper-Variably Apoplastic Effector Gene Family of the Potato Cyst Nematodes. *PLoS Pathog* 10, e1004391.
- Fabro, G., Steinbrenner, J., Coates, M., Ishaque, N., Baxter, L., Studholme, D.J., Körner, E., Allen, R.L., Piquerez, S.J.M., Rougon-Cardoso, A., et al. (2011). Multiple Candidate Effectors from the Oomycete Pathogen *Hyaloperonospora arabidopsidis* Suppress Host Plant Immunity. *PLoS Pathog* 7, e1002348.
- Fosu-Nyarko, J., Jones, M.G.K., and Wang, Z. (2009). Functional characterization of transcripts expressed in early-stage *Meloidogyne javanica*-induced giant cells isolated by laser microdissection. *Mol. Plant Pathol.* 10, 237–248.
- Freeman, B.C., and Beattie, G.A. (2008). An Overview of Plant Defenses against Pathogens and Herbivores. *Plant Health Instr.*
- Fudali, S.L., Wang, C., and Williamson, V.M. (2012). Ethylene Signaling Pathway Modulates Attractiveness of Host Roots to the Root-Knot Nematode *Meloidogyne hapla*. *Mol. Plant. Microbe Interact.* 26, 75–86.

- Fujimoto, T., Mizukubo, T., Abe, H., and Seo, S. (2015). Sclareol induces plant resistance to root-knot nematode partially through ethylene-dependent enhancement of lignin accumulation. *MPMI* 28, 398–407.
- Garg, G., and Ranganathan, S. (2012). Helminth secretome database (HSD): a collection of helminth excretory/secretory proteins predicted from expressed sequence tags (ESTs). *BMC Genomics* 13 Suppl 7, S8.
- Gheysen, G., and Mitchum, M.G. (2011). How nematodes manipulate plant development pathways for infection. *Curr. Opin. Plant Biol.* 14, 415–421.
- Gilchrist, D.G. (1998). Programmed cell death in plant disease: the purpose and promise of cellular suicide. *Annu. Rev. Phytopathol.* 36, 393–414.
- Gleason, C.A., Liu, Q.L., and Williamson, V.M. (2008). Silencing a candidate nematode effector gene corresponding to the tomato resistance gene Mi-1 leads to acquisition of virulence. *Mol. Plant-Microbe Interact. MPMI* 21, 576–585.
- Godbole, A., Varghese, J., Sarin, A., and Mathew, M.K. (2003). VDAC is a conserved element of death pathways in plant and animal systems. *Biochim. Biophys. Acta* 1642, 87–96.
- Goverse, A., and Smant, G. (2014). The Activation and Suppression of Plant Innate Immunity by Parasitic Nematodes. *Annu. Rev. Phytopathol.* 52, 243–265.
- Goverse, A., de Engler, J.A., Verhees, J., van der Krol, S., Helder, J.H., and Gheysen, G. (2000). Cell cycle activation by plant parasitic nematodes. *Plant Mol. Biol.* 43, 747–761.
- Gowen (1992). Chemical control of nematodes: efficiency and side-effects.
- Grunewald, W., Cannoot, B., Friml, J., and Gheysen, G. (2009). Parasitic Nematodes Modulate PIN-Mediated Auxin Transport to Facilitate Infection. *PLoS Pathog* 5, e1000266.
- Haegeman, A., Bauters, L., Kyndt, T., Rahman, M.M., and Gheysen, G. (2013). Identification of candidate effector genes in the transcriptome of the rice root knot nematode *Meloidogyne graminicola*. *Mol. Plant Pathol.* 14, 379–390.
- Hamilton, J.A., and Benson, M.D. (2001). Transthyretin: a review from a structural perspective. *Cell. Mol. Life Sci. CMLS* 58, 1491–1521.
- Hanahan, D. (1983). Studies on transformation of *Escherichia coli* with plasmids. *J. Mol. Biol.* 166, 557–580.
- Hartley, J.L., Temple, G.F., and Brasch, M.A. (2000). DNA cloning using in vitro site-specific recombination. *Genome Res.* 10, 1788–1795.
- Hemetsberger, C., Herrberger, C., Zechmann, B., Hillmer, M., and Doehlemann, G. (2012). The *Ustilago maydis* Effector Pep1 Suppresses Plant Immunity by Inhibition of Host Peroxidase Activity. *PLoS Pathog* 8, e1002684.
- Hewezi, T., Howe, P., Maier, T.R., Hussey, R.S., Mitchum, M.G., Davis, E.L., and Baum, T.J. (2008). Cellulose Binding Protein from the Parasitic Nematode *Heterodera schachtii* Interacts with Arabidopsis Pectin Methyltransferase: Cooperative Cell Wall Modification during Parasitism. *Plant Cell* 20, 3080–3093.

- Hobert, O. (2013). The neuronal genome of *Caenorhabditis elegans*. WormBook 1–106.
- Hoogenboom, B.W., Suda, K., Engel, A., and Fotiadis, D. (2007). The Supramolecular Assemblies of Voltage-dependent Anion Channels in the Native Membrane. *J. Mol. Biol.* 370, 246–255.
- Huang, G., Dong, R., Allen, R., Davis, E.L., Baum, T.J., and Hussey, R.S. (2006). A Root-Knot Nematode Secretory Peptide Functions as a Ligand for a Plant Transcription Factor. *Mol. Plant. Microbe Interact.* 19, 463–470.
- Iberkleid, I., Vieira, P., de Almeida Engler, J., Firester, K., Spiegel, Y., and Horowitz, S.B. (2013). Fatty acid- and retinol-binding protein, Mj-FAR-1 induces tomato host susceptibility to root-knot nematodes. *PLoS One* 8, e64586.
- Iberkleid, I., Sela, N., and Brown Miyara, S. (2015). *Meloidogyne javanica* fatty acid- and retinol-binding protein (Mj-FAR-1) regulates expression of lipid-, cell wall-, stress- and phenylpropanoid-related genes during nematode infection of tomato. *BMC Genomics* 16, 272.
- Jacob, J., Vanholme, B., Haegeman, A., and Gheysen, G. (2007). Four transthyretin-like genes of the migratory plant-parasitic nematode *Radopholus similis*: members of an extensive nematode-specific family. *Gene* 402, 9–19.
- Jacobs, S., Zechmann, B., Molitor, A., Trujillo, M., Petutschnig, E., Lipka, V., Kogel, K.-H., and Schaefer, P. (2011). Broad Spectrum Suppression of Innate Immunity Is Required for Colonization of *Arabidopsis thaliana* Roots by the Fungus *Piriformospora indica*. *Plant Physiol.* pp.111.176446.
- Janssen, G.J.W., Scholten, O.E., van Norel, A., and Hoogendoorn, C. (J) (1998). Selection of virulence in *Meloidogyne chitwoodi* to resistance in the wild potato *Solanum fendleri*. *Eur. J. Plant Pathol.* 104, 645–651.
- Jaouannet, M., Perfus-Barbeoch, L., Deleury, E., Magliano, M., Engler, G., Vieira, P., Danchin, E.G.J., Da Rocha, M., Coquillard, P., Abad, P., et al. (2012). A root-knot nematode-secreted protein is injected into giant cells and targeted to the nuclei. *New Phytol.* 194, 924–931.
- Jaouannet, M., Magliano, M., Arguel, M.J., Gourgues, M., Evangelisti, E., Abad, P., and Rosso, M.N. (2013). The root-knot nematode calreticulin Mi-CRT is a key effector in plant defense suppression. *Mol. Plant-Microbe Interact.* MPMI 26, 97–105.
- Jelenska, J., Yao, N., Vinatzer, B.A., Wright, C.M., Brodsky, J.L., and Greenberg, J.T. (2007). A J Domain Virulence Effector of *Pseudomonas syringae* Remodels Host Chloroplasts and Suppresses Defenses. *Curr. Biol.* 17, 499–508.
- J. Hallmann, S.K. (2007) Bekämpfungsstrategien für pflanzenparasitäre Nematoden im ökologischen Landbau Control strategies for plant parasitic nematodes in organic farming.
- Jones, J.D.G., and Dangl, J.L. (2006). The plant immune system. *Nature* 444, 323–329.
- Karczmarek, A., Overmars, H., Helder, J., and Govere, A. (2004). Feeding cell development by cyst and root-knot nematodes involves a similar early, local and transient activation of a specific auxin-inducible promoter element. *Mol. Plant Pathol.* 5, 343–346.

- Khoury, G.A., Baliban, R.C., and Floudas, C.A. (2011). Proteome-wide post-translational modification statistics: frequency analysis and curation of the swiss-prot database. *Sci. Rep. 1*.
- Kiemer, L., Bendtsen, J.D., and Blom, N. (2005). NetAcet: prediction of N-terminal acetylation sites. *Bioinforma. Oxf. Engl. 21*, 1269–1270.
- Krogh, A., Larsson, B., von Heijne, G., and Sonnhammer, E.L. (2001). Predicting transmembrane protein topology with a hidden Markov model: application to complete genomes. *J. Mol. Biol. 305*, 567–580.
- Kusano, T., Tateda, C., Berberich, T., and Takahashi, Y. (2009). Voltage-dependent anion channels: their roles in plant defense and cell death. *Plant Cell Rep. 28*, 1301–1308.
- Kyndt, T., Vieira, P., Gheysen, G., and Almeida-Engler, J. de (2013). Nematode feeding sites: unique organs in plant roots. *Planta 238*, 807–818.
- Landy, A. (1989). Dynamic, structural, and regulatory aspects of lambda site-specific recombination. *Annu. Rev. Biochem. 58*, 913–949.
- Lecoals, A.C., Rubio-Cabetas, M.J., Minot, J.C., Voisin, R., Bonnet, A., Salesses, G., Dirlwanger, E., and Esmenjaud, D. (1999). RAPD and SCAR markers linked to the *Mal* root-knot nematode resistance gene in Myrobalan plum (*Prunus cerasifera* Ehr.). *Theor. Appl. Genet. 99*, 328–335.
- Lee, S.M., Hoang, M.H.T., Han, H.J., Kim, H.S., Lee, K., Kim, K.E., Kim, D.H., Lee, S.Y., and Chung, W.S. (2009). Pathogen inducible voltage-dependent anion channel (*AtVDAC*) isoforms are localized to mitochondria membrane in *Arabidopsis*. *Mol. Cells 27*, 321–327.
- Lilley, C.J., Davies, L.J., and Urwin, P.E. (2012). RNA interference in plant parasitic nematodes: a summary of the current status. *Parasitology 139*, 630–640.
- Lin, B., Zhuo, K., Wu, P., Cui, R., Zhang, L.-H., and Liao, J. (2013). A novel effector protein, MJ-NULG1a, targeted to giant cell nuclei plays a role in *Meloidogyne javanica* parasitism. *Mol. Plant-Microbe Interact. MPMI 26*, 55–66.
- Lister, R., Carrie, C., Duncan, O., Ho, L.H.M., Howell, K.A., Murcha, M.W., and Whelan, J. (2007). Functional Definition of Outer Membrane Proteins Involved in Preprotein Import into Mitochondria. *Plant Cell 19*, 3739–3759.
- Liu, Q.L., and Williamson, V.M. (2006). Host-Specific Pathogenicity and Genome Differences between Inbred Strains of *Meloidogyne hapla*. *J. Nematol. 38*, 158–164.
- Livak, K.J., and Schmittgen, T.D. (2001). Analysis of relative gene expression data using real-time quantitative PCR and the 2^{(-Delta Delta C(T))} Method. *Methods San Diego Calif 25*, 402–408.
- Lozano-Torres, J.L., Wilbers, R.H.P., Warmerdam, S., Finkers-Tomczak, A., Diaz-Granados, A., van Schaik, C.C., Helder, J., Bakker, J., Goverse, A., Schots, A., et al. (2014). Apoplastic venom allergen-like proteins of cyst nematodes modulate the activation of basal plant innate immunity by cell surface receptors. *PLoS Pathog. 10*, e1004569.
- Mano, Y., and Nemoto, K. (2012). The pathway of auxin biosynthesis in plants. *Journal of Experimental Botany*.

- Manosalva, P., Manohar, M., von Reuss, S.H., Chen, S., Koch, A., Kaplan, F., Choe, A., Micikas, R.J., Wang, X., Kogel, K.-H., et al. (2015). Conserved nematode signalling molecules elicit plant defenses and pathogen resistance. *Nat. Commun.* 6.
- Mbeunkui, F., Scholl, E.H., Opperman, C.H., Goshe, M.B., and Bird, D.M. (2010). Proteomic and bioinformatic analysis of the root-knot nematode *Meloidogyne hapla*: the basis for plant parasitism. *J. Proteome Res.* 9, 5370–5381.
- Millet, Y.A., Danna, C.H., Clay, N.K., Songnuan, W., Simon, M.D., Werck-Reichhart, D., and Ausubel, F.M. (2010). Innate Immune Responses Activated in Arabidopsis Roots by Microbe-Associated Molecular Patterns. *Plant Cell* 22, 973–990.
- Mitchum, M.G., Wang, X., Wang, J., and Davis, E.L. (2012). Role of nematode peptides and other small molecules in plant parasitism. *Annu. Rev. Phytopathol.* 50, 175–195.
- Morgan, W., and Kamoun, S. (2007). RXLR effectors of plant pathogenic oomycetes. *Curr. Opin. Microbiol.* 10, 332–338.
- Nahar, K., Kyndt, T., Vleeschauwer, D.D., Höfte, M., and Gheysen, G. (2011). The Jasmonate Pathway Is a Key Player in Systemically Induced Defense against Root Knot Nematodes in Rice. *Plant Physiol.* 157, 305–316.
- Nam, K.H., and Li, J. (2004). The Arabidopsis Transthyretin-Like Protein Is a Potential Substrate of BRASSINOSTEROID-INSENSITIVE 1. *Plant Cell* 16, 2406–2417.
- Nicaise, V., Roux, M., and Zipfel, C. (2009). Recent Advances in PAMP-Triggered Immunity against Bacteria: Pattern Recognition Receptors Watch over and Raise the Alarm. *Plant Physiol.* 150, 1638–1647.
- Nickel, W. (2003). The mystery of nonclassical protein secretion. A current view on cargo proteins and potential export routes. *Eur. J. Biochem. FEBS* 270, 2109–2119.
- Nielsen, H., Engelbrecht, J., Brunak, S., and Heijne, G. von (1997). Identification of prokaryotic and eukaryotic signal peptides and prediction of their cleavage sites. *Protein Eng.* 10, 1–6.
- Niu, J., Jian, H., Xu, J., Chen, C., Guo, Q., Liu, Q., and Guo, Y. (2012). RNAi silencing of the *Meloidogyne incognita Rpn7* gene reduces nematode parasitic success. *Eur. J. Plant Pathol.* 134, 131–144.
- Olson, S.K., Bishop, J.R., Yates, J.R., Oegema, K., and Esko, J.D. (2006). Identification of novel chondroitin proteoglycans in *Caenorhabditis elegans*: embryonic cell division depends on CPG-1 and CPG-2. *J. Cell Biol.* 173, 985–994.
- Opperman, C.H., Bird, D.M., Williamson, V.M., Rokhsar, D.S., Burke, M., Cohn, J., Cromer, J., Diener, S., Gajan, J., Graham, S., et al. (2008). Sequence and genetic map of *Meloidogyne hapla*: A compact nematode genome for plant parasitism. *Proc. Natl. Acad. Sci.* 105, 14802–14807.
- Orion, D., Kritzman, G., Meyer, S.L.F., Erbe, E.F., and Chitwood, D.J. (2001). A Role of the Gelatinous Matrix in the Resistance of Root-Knot Nematode (*Meloidogyne spp.*) Eggs to Microorganisms. *Journal Nematol.* 33, 203–207.

- Ornat, C., Verdejo-Lucas, S., and Sorribas, F.J. (2001). A Population of *Meloidogyne javanica* in Spain Virulent to the *Mi* Resistance Gene in Tomato. A Population of *Meloidogyne javanica* in Spain Virulent to the *Mi* Resistance Gene in Tomato.
- Patel, N., Hamamouch, N., Li, C., Hewezi, T., Hussey, R.S., Baum, T.J., Mitchum, M.G., and Davis, E.L. (2010). A nematode effector protein similar to annexins in host plants. *J. Exp. Bot.* *61*, 235–248.
- Perry, R.N., Moens, M., and Starr, J.L. (2009). *Root-knot Nematodes* (CABI).
- Pessoa, J., Sárkány, Z., Ferreira-da-Silva, F., Martins, S., Almeida, M.R., Li, J., and Damas, A.M. (2010). Functional characterization of *Arabidopsis thaliana* transthyretin-like protein. *BMC Plant Biol.* *10*, 30.
- Petersen, T.N., Brunak, S., von Heijne, G., and Nielsen, H. (2011). SignalP 4.0: discriminating signal peptides from transmembrane regions. *Nat. Methods* *8*, 785–786.
- Petre, B., Lorrain, C., Saunders, D., Duplessis, S., and Kamoun, S. (2015). Rust Fungal Effectors Mimic Host Transit Peptides to Translocate into Chloroplasts. *bioRxiv* 019521.
- Postel, S., and Kemmerling, B. (2009). Plant systems for recognition of pathogen-associated molecular patterns. *Semin. Cell Dev. Biol.* *20*, 1025–1031.
- Postma, W.J., Slootweg, E.J., Rehman, S., Finkers-Tomczak, A., Tytgat, T.O.G., van Gelderen, K., Lozano-Torres, J.L., Roosien, J., Pomp, R., van Schaik, C., et al. (2012). The effector SPRYSEC-19 of *Globodera rostochiensis* suppresses CC-NB-LRR-mediated disease resistance in plants. *Plant Physiol.* *160*, 944–954.
- Prior, A., Jones, J.T., Blok, V.C., Beauchamp, J., McDermott, L., Cooper, A., and Kennedy, M.W. (2001). A surface-associated retinol- and fatty acid-binding protein (Gp-FAR-1) from the potato cyst nematode *Globodera pallida*: lipid binding activities, structural analysis and expression pattern. *Biochem. J.* *356*, 387–394.
- Ranf, S., Eschen-Lippold, L., Pecher, P., Lee, J., and Scheel, D. (2011). Interplay between calcium signalling and early signalling elements during defence responses to microbe- or damage-associated molecular patterns. *Plant J.* *68*, 100–113.
- Replogle, A., Wang, J., Bleckmann, A., Hussey, R.S., Baum, T.J., Sawa, S., Davis, E.L., Wang, X., Simon, R., and Mitchum, M.G. (2011). Nematode CLE signaling in *Arabidopsis* requires *CLAVATA2* and *CORYNE*. *Plant J.* *65*, 430–440.
- Rosso, M.-N., Vieira, P., de Almeida-Engler, J., and Castagnone-Sereno, P. (2011). Proteins secreted by root-knot nematodes accumulate in the extracellular compartment during root infection. *Plant Signal. Behav.* *6*, 1232–1234.
- Roze, E., Hanse, B., Mitreva, M., Vanholme, B., Bakker, J., and Smant, G. (2008). Mining the secretome of the root-knot nematode *Meloidogyne chitwoodi* for candidate parasitism genes. *Mol. Plant Pathol.* *9*, 1–10.
- Saverwyns, H., Visser, A., Van Durme, J., Power, D., Morgado, I., Kennedy, M.W., Knox, D.P., Schymkowitz, J., Rousseau, F., Gevaert, K., et al. (2008). Analysis of the transthyretin-like (TTL) gene family in *Ostertagia ostertagi*—comparison with other strongylid nematodes and *Caenorhabditis elegans*. *Int. J. Parasitol.* *38*, 1545–1556.

- Schwarzer, C., Barnikol-Watanabe, S., Thinner, F.P., and Hilschmann, N. (2002). Voltage-dependent anion-selective channel (VDAC) interacts with the dynein light chain Tctex1 and the heat-shock protein PBP74. *Int. J. Biochem. Cell Biol.* *34*, 1059–1070.
- Semblat, J.-P., Rosso, M.-N., Hussey, R.S., Abad, P., and Castagnone-Sereno, P. (2001). Molecular Cloning of a cDNA Encoding an Amphid-Secreted Putative Avirulence Protein from the Root-Knot Nematode *Meloidogyne incognita*. *Mol. Plant. Microbe Interact.* *14*, 72–79.
- Siddique, S., Matera, C., Radakovic, Z.S., Hasan, M.S., Gutbrod, P., Rozanska, E., Sobczak, M., Torres, M.A., and Grundler, F.M.W. (2014). Parasitic worms stimulate host NADPH oxidases to produce reactive oxygen species that limit plant cell death and promote infection. *Sci. Signal.* *7*, ra33.
- Sijmons, P.C., Grundler, F.M.W., von Mende, N., Burrows, P.R., and Wyss, U. (1991). *Arabidopsis thaliana* as a new model host for plant-parasitic nematodes. *Plant J.* *1*, 245–254.
- Snyder, D.W., Opperman, C.H., and Bird, D.M. (2006). A Method for Generating *Meloidogyne incognita* Males. *J. Nematol.* *38*, 192–194.
- Sohn, K.H., Lei, R., Nemri, A., and Jones, J.D.G. (2007). The downy mildew effector proteins ATR1 and ATR13 promote disease susceptibility in *Arabidopsis thaliana*. *Plant Cell* *19*, 4077–4090.
- Starr, J.L., Perry, R.N., and Moens, M. (2009). *Meloidogyne* Species - a Diverse Group of Novel and Important Plant Parasites. In *Root-Knot Nematodes*, (CAB International), pp. 1–17.
- Staskawicz, B.J., Mudgett, M.B., Dangl, J.L., and Galan, J.E. (2001). Common and Contrasting Themes of Plant and Animal Diseases. *Science* *292*, 2285–2289.
- Suh, J., and Hutter, H. (2012). A survey of putative secreted and transmembrane proteins encoded in the *C. elegans* genome. *BMC Genomics* *13*, 333.
- Tateda, C., Yamashita, K., Takahashi, F., Kusano, T., and Takahashi, Y. (2008). Plant voltage-dependent anion channels are involved in host defense against *Pseudomonas cichorii* and in Bax-induced cell death. *Plant Cell Rep.* *28*, 41–51.
- Terpe, K. (2003). Overview of tag protein fusions: from molecular and biochemical fundamentals to commercial systems. *Appl. Microbiol. Biotechnol.* *60*, 523–533.
- Tokmakov, A.A., Kurotani, A., Takagi, T., Toyama, M., Shirouzu, M., Fukami, Y., and Yokoyama, S. (2012). Multiple Post-translational Modifications Affect Heterologous Protein Synthesis. *J. Biol. Chem.* *287*, 27106–27116.
- Torres, M.A., Jones, J.D.G., and Dangl, J.L. (2006). Reactive Oxygen Species Signaling in Response to Pathogens. *Plant Physiol.* *141*, 373–378.
- Trudgill, D.L. (1997). Parthenogenetic root-knot nematodes (*Meloidogyne spp.*); how can these biotrophic endoparasites have such an enormous host range? *Plant Pathol.* *46*, 26–32.

- Trudgill, D.L., and Blok, V.C. (2001). APOMICTIC, POLYPHAGOUS ROOT-KNOT NEMATODES: Exceptionally Successful and Damaging Biotrophic Root Pathogens. *Annu. Rev. Phytopathol.* *39*, 53–77.
- Tuteja, N., and Mahajan, S. (2007). Calcium Signaling Network in Plants. *Plant Signal. Behav.* *2*, 79–85.
- Vidhyasekaran, P. (2013). PAMP Signals in Plant Innate Immunity: Signal Perception and Transduction (Springer Science & Business Media).
- Vieira, P., Danchin, E.G.J., Neveu, C., Crozat, C., Jaubert, S., Hussey, R.S., Engler, G., Abad, P., de Almeida-Engler, J., Castagnone-Sereno, P., et al. (2011). The plant apoplasm is an important recipient compartment for nematode secreted proteins. *J. Exp. Bot.* *62*, 1241–1253.
- Vos, P., Simons, G., Jesse, T., Wijbrandi, J., Heinen, L., Hogers, R., Frijters, A., Groenendijk, J., Diergaarde, P., Reijans, M., et al. (1998). The tomato *Mi-1* gene confers resistance to both root-knot nematodes and potato aphids. *Nat. Biotechnol.* *16*, 1365–1369.
- Wang, X., Allen, R., Ding, X., Goellner, M., Maier, T., de Boer, J.M., Baum, T.J., Hussey, R.S., and Davis, E.L. (2001). Signal Peptide-Selection of cDNA Cloned Directly from the Esophageal Gland Cells of the Soybean Cyst Nematode *Heterodera glycines*. *Mol. Plant. Microbe Interact.* *14*, 536–544.
- Wang, X., Li, W., Zhao, D., Liu, B., Shi, Y., Chen, B., Yang, H., Guo, P., Geng, X., Shang, Z., et al. (2010). *Caenorhabditis elegans* transthyretin-like protein TTR-52 mediates recognition of apoptotic cells by the CED-1 phagocyte receptor. *Nat. Cell Biol.* *12*, 655–664.
- Wildermuth, M.C., Dewdney, J., Wu, G., and Ausubel, F.M. (2001). Isochorismate synthase is required to synthesize salicylic acid for plant defence. *Nature* *414*, 562–565.
- Wojtaszek, P. (1997). Oxidative burst: an early plant response to pathogen infection. *Biochem. J.* *322*, 681–692.
- Wubben, M.J., Ganji, S., and Callahan, F.E. (2010). Identification and molecular characterization of a β -1,4-endoglucanase gene (*Rr-eng-1*) from *Rotylenchulus reniformis*. *J. Nematol.* *42*, 342–351.
- Xue, B., Hamamouch, N., Li, C., Huang, G., Hussey, R.S., Baum, T.J., and Davis, E.L. (2013). The *8D05* Parasitism Gene of *Meloidogyne incognita* Is Required for Successful Infection of Host Roots. *Phytopathology* *103*, 175–181.
- Yamamoto, Y., Yoshizawa, T., Kamio, S., Aoki, O., Kawamata, Y., Masushige, S., and Kato, S. (1997). Interactions of transthyretin (TTR) and retinol-binding protein (RBP) in the uptake of retinol by primary rat hepatocytes. *Exp. Cell Res.* *234*, 373–378.
- Yang, X.-Y., Chen, Z.-W., Xu, T., Qu, Z., Pan, X.-D., Qin, X.-H., Ren, D.-T., and Liu, G.-Q. (2011). Arabidopsis kinesin KP1 specifically interacts with VDAC3, a mitochondrial protein, and regulates respiration during seed germination at low temperature. *Plant Cell* *23*, 1093–1106.
- Zanotti, G., Cendron, L., Ramazzina, I., Folli, C., Percudani, R., and Berni, R. (2006). Structure of zebra fish HIUase: insights into evolution of an enzyme to a hormone transporter. *J. Mol. Biol.* *363*, 1–9.

Zhang, J., Shao, F., Li, Y., Cui, H., Chen, L., Li, H., Zou, Y., Long, C., Lan, L., Chai, J., et al. (2007). A *Pseudomonas syringae* effector inactivates MAPKs to suppress PAMP-induced immunity in plants. *Cell Host Microbe* 1, 175–185.

Zhang, M., Takano, T., Liu, S., and Zhang, X. (2015). Arabidopsis mitochondrial voltage-dependent anion channel 3 (AtVDAC3) protein interacts with thioredoxin m2. *FEBS Lett.* 589, 1207–1213.

Zipfel, C. (2008). Pattern-recognition receptors in plant innate immunity. *Curr. Opin. Immunol.* 20, 10–16.

Zipfel, C. (2014). Plant pattern-recognition receptors. *Trends Immunol.* 35, 345–351.

Acknowledgements

Firstly, I want to thank Cynthia Gleason for giving me the opportunity to do this work and support me during all ups and downs of my thesis. I also want to thank my lab members, Nathannon Leelarasamee, Jan Utermark, and Martin Muthreich for the nice lab atmosphere and the good team work.

Furthermore I want to mention the support of the colleagues in the departments of Prof. Gatz and Prof. Lipka which were always open for question and took their time if help was needed.

I also want to thank Christiane Gatz and Volker Lipka for being in my thesis committee and giving me feedback regarding my project. Additionally, I thank the members of my examination board namely, Jörg Stülke, Thomas Teichmann, and Ivo Feußner.

For personal support I would like to thank my family, friends and especially Gabriella who motivated me to do my Phd and encouraged me when it was necessary.

Vielen Dank ☺

Curriculum vitae

Personal information

Name:	Frederik Gunnar Polzin
Place of birth	Frankfurt am Main
Day of birth	22.08.1985
Nationality	German
E-Mail	f.polzin@titanz.de

University education

February 2012- present	Doctoral studies Georg-August-Universität Göttingen Department for Molecular Plant Sciences (Jun.Prof. Dr. Gleason)
March 2010-August 2011	Master of Science – Horticultural Science Hochschule Geisenheim/Hochschule RheinMain Plant and Food Research Institute Auckland, New Zealand Thesis title : Apple colour Final Grade: 1.7
September 2009- February 2010	Bachelor of Science – Horticultural Management Hochschule Geisenheim/Hochschule RheinMain Institut de recherche pour le développement Thesis title: <i>in vitro</i> cultivation and Cryopreservation of <i>Dioscorea spp.</i> Final Grade : 1.6

School education

September 1997- July 2005	Final secondary-school examinations with general qualification for university entrance (Abitur) Main-Taunus-Schule - Gymnasium Hofheim am Taunus Final grade : 2.7
September 1996-July 1997	Secondary-school Dreieich Schule (Gymnasium) Langen
September 1992- July 1996	Elementary school Ludwig-Erk-Schule Langen

Puplications:

Polzin F., Sylvestre I., Déchamp E., Ilbert., Pascal., Etienne H., Engelmann F. (2014). Effect of activated charcoal on multiplication of African yam (*Dioscorea cayenensis-rotundata*) nodal segments using a temporary immersion bioreactor (RITA®) In Vitro Cellular & Developmental Biology- Plant. Volume 50, Issue 2, p 210-216